MAPPING OF THE DETACHMENT FAULT IN KYTHERA ISLAND AND STUDY OF THE RELATED STRUCTURAL SHEAR SENSE INDICATORS

Abstract of a thesis presented to the Faculty of the University at Albany,

State University of New York

in partial fulfillment of the requirements

for the degree of

Master of Science

College of Arts & Sciences

Department of Earth and Atmospheric Sciences

Antonios Marsellos

2006

Abstract

The Island of Kythera is prominent horst structure in the southwestern part of the Hellenic subduction zone, which is governed by roll back of the African slab. The evolution of the plate boundary between Eurasia and Africa during the last 35 Ma is recorded in the geology of Kythera. Kythera Island is located at the southwest part of the Hellenic Arc, between two opposite indicated rotations, the clockwise rotation of west Aegean and Peloponnesus and the counterclockwise rotation of east Aegean and Crete. The latter location may host a differential rotation that strengthens the deformation to higher levels than this of vicinal areas, such of Peloponnesus and Crete Island.

The structure of Kythera is characterized by a pile of nappes derived from different paleogeographic zones. The upper unmetamorphosed units (pelagic limestones of Pindos lie on top of Tripolis neritic limestones) are separated from the lower metamorphosed unit of Phyllites-Quartzites and marbles lenses by an extensional detachment fault of Late Miocene age. The lower tectonic unit of Phyllites-Quartzites was overprinted by high-pressure/low-temperature blueschist phase metamorphism after the middle Miocene. At the contrary, the higher tectonic limestone units were affected only by recrystallization.

The detachment fault indicates exhumation of the HP-LT metamorphic units by extension. The exhumation of the high-pressure rocks was accompanied by NEE-SWW extensional graben model, which is related to the observed NEE-SWW mylonitic dislocation creep. Later brittle-ductile faulting provoked S/C? fabric of NNW-SSE orientation and top-to-the southeast displacement that occur mostly at the northeastern coast of Kythera, while at the northwestern coast of Kythera occur S/C fabric of NNE-

SSW orientation and top-to-the southwest displacement. The latter implies a NE-SW gradient shear that maximizes through northeastern direction pointing to Cyclades area. Furthermore, a tectonic model of syncompressional uplift and vertical buoyancy of the subducted crustal underplating caused the rapid exhumation and denudation of the metamorphic PQU in Kythera Island. The precise date for the onset of extension, possibly controlled by the roll-back of the subsiding African lithosphere, remains at this point a discussion.

Kinematic and structural data from both unmetamorphosed and metamorphosed nappes of the MMC of Kythera Island have enabled to determine a first approximation to structural evolution of the region and to present a plate tectonic scenario for the southwest lowest rigidity part of the Hellenic arc. Mapping and GIS thematic maps were constructed in order to clarified the spatial distribution of the shear-sense kinematic indicators that determine the architecture of the detachment that occurs underneath the PQU. Landsat image interpretation determined the orientation of a broad antiform structure of the PQU assuming that infiltration and lineation are collaborating. DEM analysis of the Kythera Landscape revealed Riedel fractures of a kilometer-scale that infer extensional dextral shear of W-E direction.

MAPPING OF THE DETACHMENT FAULT IN KYTHERA ISLAND AND STUDY OF THE RELATED STRUCTURAL SHEAR SENSE INDICATORS

A thesis presented to the Faculty of the University at Albany,

State University of New York

in partial fulfillment of the requirements

for the degree of

Master of Science

College of Arts & Sciences

Department of Earth and Atmospheric Sciences

Antonios Marsellos

2006

Acknowledgements

This Thesis is by far the most significant scientific accomplishment in my life and it would he impossible to have done it without some people who supported me and believed in me. Foremost, I thank my research advisor, Professor W.S. F. Kidd, for suggesting that I do my graduate research in Kythera Island, the Island of my parents' home, my grandparents' home and my best place of vacations and spiritual inspirations. This is the Island of love, of Venus (the goddess of Greek mythology), this is the region where the Antikythera mechanism was found in the bottom of the sea. This Island hosts a lot of secrets, where I did my best on to decipher of its tectonic mysteries.

I also want to thank my advisor Bill Kidd for his time and patience in reviewing my thesis. Not only do I appreciate all of his suggestions on this research, in tectonics and remote sensing, as well as all of those hours of optical microscope examination of my samples, but also for his experience in microtectonics and interpretation of shear sense kinematic indicators. He was always giving me suggestions for research directions. He encouraged me to think through all the scales, since geology is applicable to microworld, as well as to macro-world.

I am also grateful to Prof. John Arnason for providing useful information about unknown minerals in my rock samples, as well as about blucschist metamorphism mineralogical phenomena, and for reading the thesis.

This thesis has benefited from discussions with Prof. Adam Schoonmaker, who read my thesis and helped me to interpret complicated shear sense kinematic indicators. Also, I can't forget the times even that he was away from the Campus he still advised me where to search.

I also thank Prof. Kyriakopoulos of the National & Kapodistrian University of Athens (UOA), Greece, who was my advisor during my undergraduate thesis and has continued to work with me on for petrological and mineralogical advice. Also, I thank him for urging me to continue my geological studies overseas and to interact with other scientific faculty in Earth sciences.

My best regards I want to give to Prof. Pepy Vassilopoulou, who teaches remote sensing and GIS in the National & Kapodistrian University of Athens (UOA), and advised me on GIS issues.

I am also very grateful to Chul Lim and Jamie Macdonald who had an impact to this work, especially in advice in optical microscope examination of my samples.

I also have a lot of friends nearby Albany who made it much easier to get through hard winters and holidays. I thank Mrs. Maroula Liapis, to be more than a friend here in the USA, to support me with more than I could imagine, the most beautiful house, her best "spanakopita" (pie of spinach and feta cheese), the best golf company. I admire her great friends Nancy, Tony and Alice, John and Guen, Robin and Mat, that they helped me, especially in the beginning, where anybody needs more than a "push" to stand on his feet. Maroula is such a great person, who happened to have the best Greek Restaurant "Pegasus", located in Coxsackie, NY. I cannot forget Maroulas sons, Thanassi and Ntino, who make me feel their home as my home.

To my fiance, and future wife Katerina, for continuous support and love, these moments, these years of graduate studies were passed like an exciting dream. She made me think that time consuming on studying or working is meaningful when we are together. I also have to say that she was my best partner at the field trips in Kythera Island, she brings me luck to find significant outcrops, and even that she does not like

spiders and especially the snakes! She was inspiring me by her most simple questions on geology of Kythera and leading me, without knowing, to a better understanding. I have to say that she was also studying for her PhD preliminary exams in the Dept. of Mathematics & Statistics in the 4x4 vehicle, thanks to the vehicle's air-condition!

None of this tremendous fieldwork to Kythera Island would have been possible without my Australian-Kytherean aunt Botitsa, who gave us more than hospitality and the best Kytherean food, at her beautiful house. "Sa afchureesto" which means in Greek, something a lot more than "thank you!".

Lastly, I would like to thank those whose spiritual support is even more important. I thank my parents and all of my grandparents and Greek friends for their support. None of this would have been possible without my family's love. You are so important to me. Above all, I cannot express my full love to my sociologist brother, who believes that I am a crazy geologist.

Table of Contents

List of Figures

Introduction

Greece lies at the southern end of the Balkan Peninsula. The Hellenide orogen forms part of the Alpine-Himalaya belt that formed by the destruction of Tethys. The present Hellenic subduction zone and South Aegean island arc (Fig. 1) mark the subduction of the African beneath the Eurasian plate. The accurate location of the recent Hellenic arc is 34-39°N, 19-28°E). The Hellenic arc consists of the interaction of two plates. The East Mediterranean lithosphere, which is the front part of African plate,

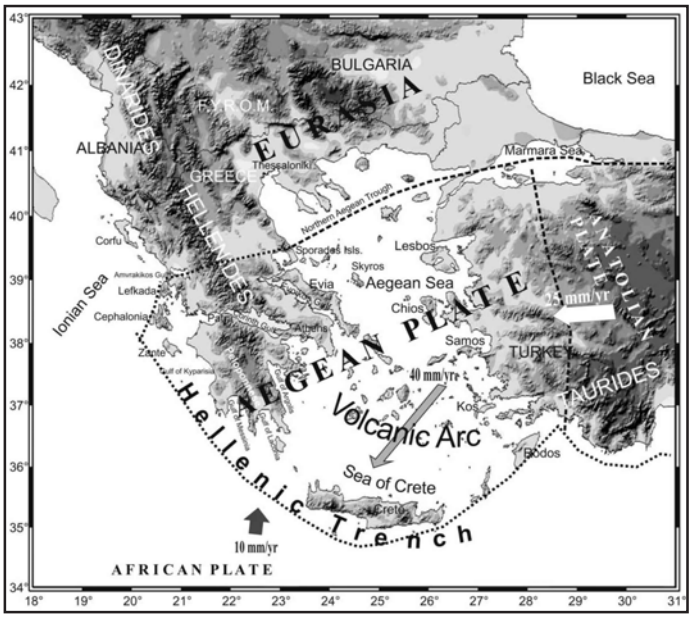

Figure 1: Location map of the Aegean Sea and the surrounding lands. The dashed line indicates the boundaries of the Aegean plate and the arrows indicate the motion of the plates relative to Eurasia. (Anastasia Kiratzi et al., 2003)

and the Aegean plate which is the front part of European plate. The Hellenic arc is an ocean-continent interaction (Papazachos, B.C., 2000), while some recently studies (Aya Shimizu et al, 2004) reveal the Aegean arc as continent-continent collision or some parts of the arc (fig. 2), such as the south (central) and the western part of the arc (D.J.W. Piper, C. Perissoratis, 2003). The latter conclusion, of the forenamed authors, arises from the observation of the N-S faults and further fundamental tectonic

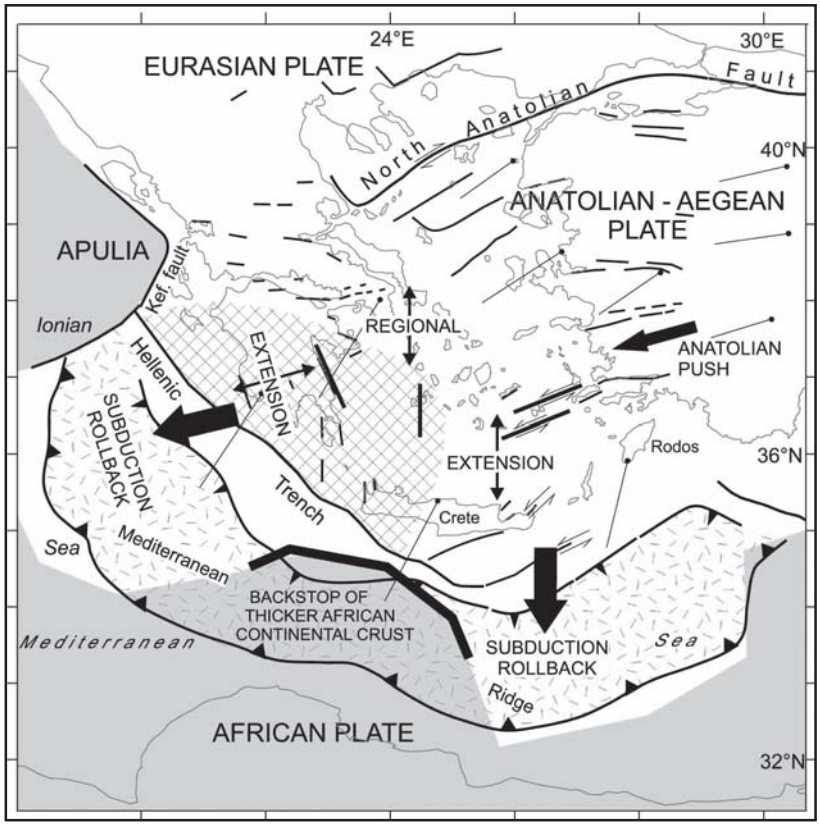

Figure 2: Schematic tectonic interpretation of the South Aegean arc. Data sources are from Huguen et al. (2001), while grey area is an indication of inferred distribution of relatively thicker African plate continental crust, implying continental collision of the African plate with the Hellenide orogenic belt at the south-western part of the arc, from D.J.W. Piper, C. Perissoratis, (2003).

changes in the past two million years in the western part of the arc, which are similar to those on land in the south Peloponnesus.

The interaction between the African Plate and Eurasian Plate occurs on a curved surface. This surface is located in the depth of 20-100km at the whole Hellenic arc range. This is a part of the Wadati-Benioff zone. Coupling, between the subducted oceanic crust and the overriding of the Aegean lithospheric plate, takes place on this surface.

According to the description of Wadati-Beniof zone from B.C. Papazachos (2000), close to Kythera Island, the Wadati–Benioff zone starts at a depth of 20 km under the convex (outer) side of the sedimentary part of the arc (Ionian Islands - western

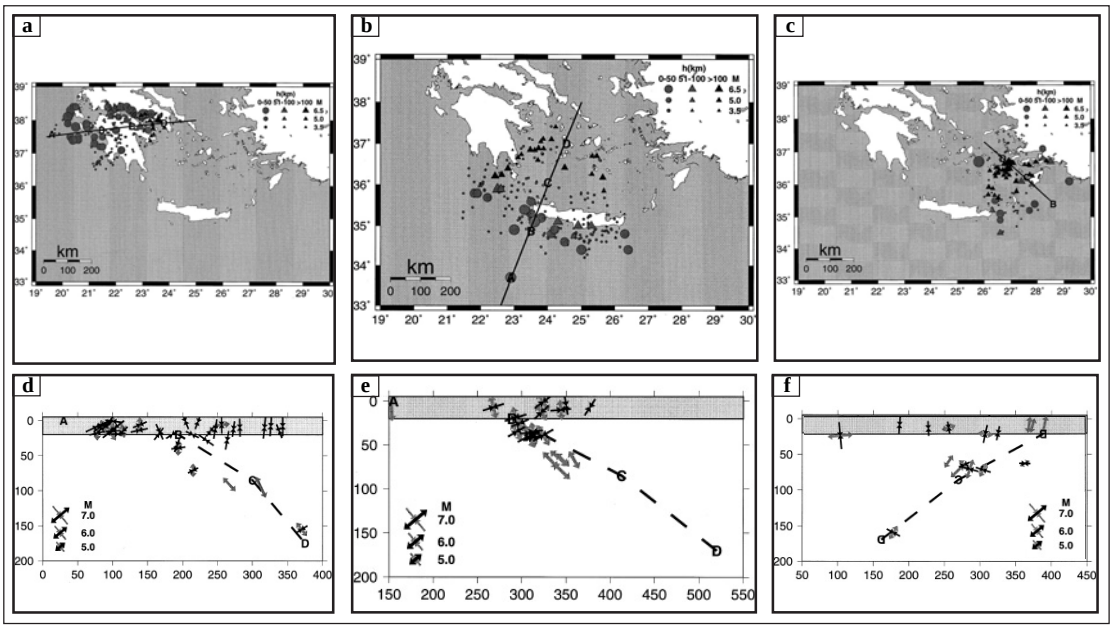

Figure 3 : (a-c) Shallow and deep branch show the 30 and 45 degrees respectively. Sketch sections through the Ionian Islands (western part), western Crete (central part) and Rhodes (eastern part). (d-f): Stress field along the same cross-sections (a-c) presented. Extension can be seen easily that occur parallel to the dipping of the Wadati-Benioff zone in all cross-sections at depth of more than 50-60km (from Papazachos, 2000).

Peloponnese–west and south of Kythera–south of Crete–southeast of Rhodes) and dips towards the back-arc area where it reaches a depth of 150 km under the volcanic arc in the southern Aegean. Some earthquakes are located even deeper, up to a focal depth of about 180 km. This Wadati–Benioff zone can be separated into two branches, one shallow of 20 km to 100 km, with a dip angle of about 30˚ and one deep from 100 km to 180 km, with a dip angle of about 45˚. The existing scattering of the intermediate depth seismicity does not allow the determination of these dip angles with high accuracy (less than 5–10˚). Although the systematic increase of the dip angle in the cross-section (Fig. 3d-3f) suggest that this is a robust feature of the subducted slab. From seismic-tomography of NNE-SSW transect of Greece (fig. 4), Transect VII, (Spakman, 1993), can easily be seen the forenamed bending of the slab. Moreover, the bending of the subducted slab implies a trench retreat or otherwise named as slab

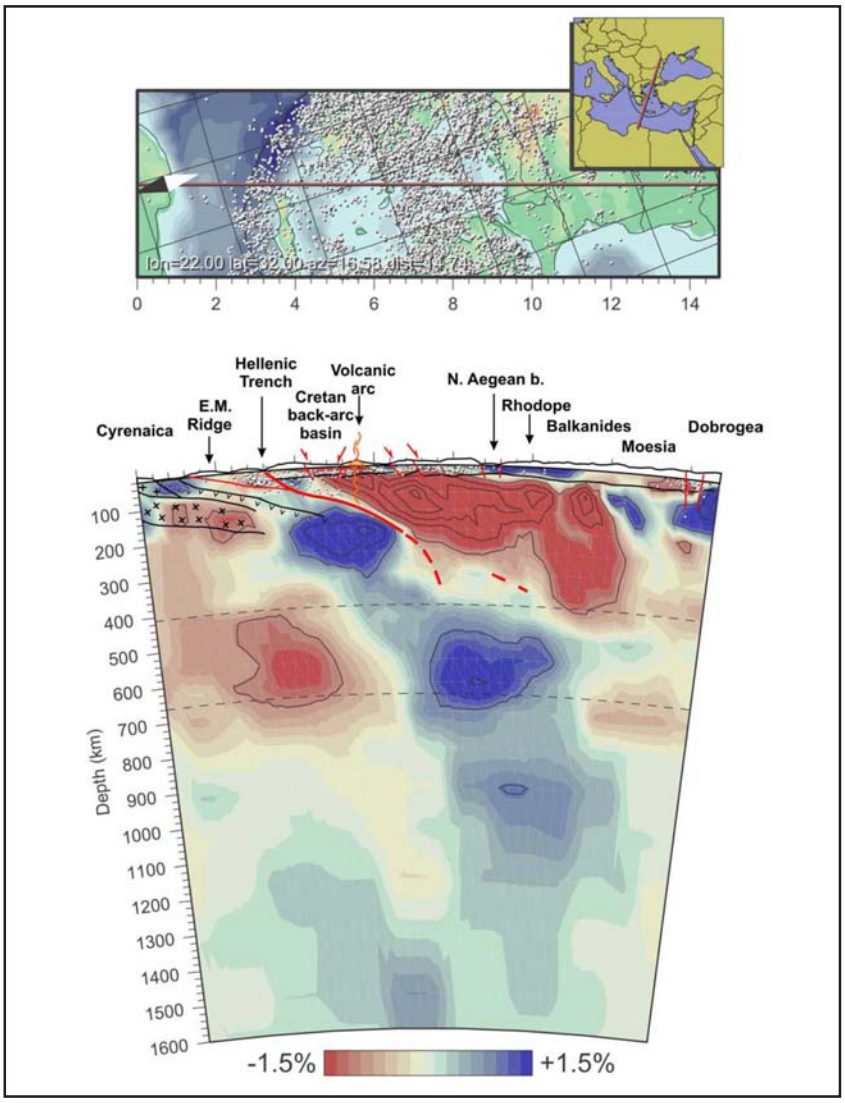

***Figure 4**:* Seismic-tomography of NNE-SSW of Greece, Transect VII, (Spakman, 1993).

roll-back. The latter characteristic of this subduction is the mainly cause of the predominantly extension of the overiding plate of the outer island arc since the late Miocene (Royden, 1993; J.H. ten Veen & P. Th. Meijer, 1998; Meulenkamp et al., 1988; J.H. ten Veen & G. Postma, 1999; Papazachos, 2000; Piper et al., 2002).

There are strong deep earthquakes (h>100km) in the fore-arc area of the southwestern part of Hellenic arc (west of Cythera) which indicate that oceanic crust is destroyed in this part of the Hellenic trench due to roll-back of the descending lithospheric slab (Papazachos, B.C., 2000). The latter was confirmed from the recent earth-

quake of 6.9 magnitude (thrust fault) at 5km western of Kythera Island and 70km deep. Slab pull on the subducted plate causes a southward retreat (roll-back) of the subduction zone. In addition, decreased rates of convergence between Africa and Eurasia in the Oligocene (Savostin et al. 1986) resulted in roll-back of the subducting plate boundary (Royden 1993). This action generates extension in the Aegean Sea and the movement of Crete (central part of Hellenic arc) to the south (Le Pichon, 1982; Meulenkamp et al., 1988). Recently studies with GPS, proved that within recent five years southwestern Greece has moved to the southwest by an average rate of 30 mm/yr, increasing from 10 mm/yr at the island of Lefkada, in the center of the Ionian islands, to nearly 40 mm/yr along the southwest part of the Peloponnesus (close to Kythera Island) and to 35 mm/yr on the islands of Crete and Gavdhos (M. Cocard, 1999), implying that the maximum extension manifests at the area close to Kythera Island.

History of Hellenic arc

The first orogen of Hellenides is the paleoalpine which takes place between Malm-early Cretaceous. In the late Paleozoic, the supercontinents of Laurasia and Gondwana converged and collided along the Hercynian or Varscide orogeny of Europe (Rey et al. 1997). Greece lies at the western end of the Paleotethyan Ocean between the two supercontinents and experienced Hercynian deformation. Greece consists of microcontinental blocks. The microcontinental blocks of Greece appear to be fragments of Gondwana. Permian to Triassic rifting of the northern margin of Gondwana resulted in the opening of the eastern Mediterranean Neotethys ocean. At least three oceanic basins are represented in Greece and the one is open hitherto (fig. 5). The

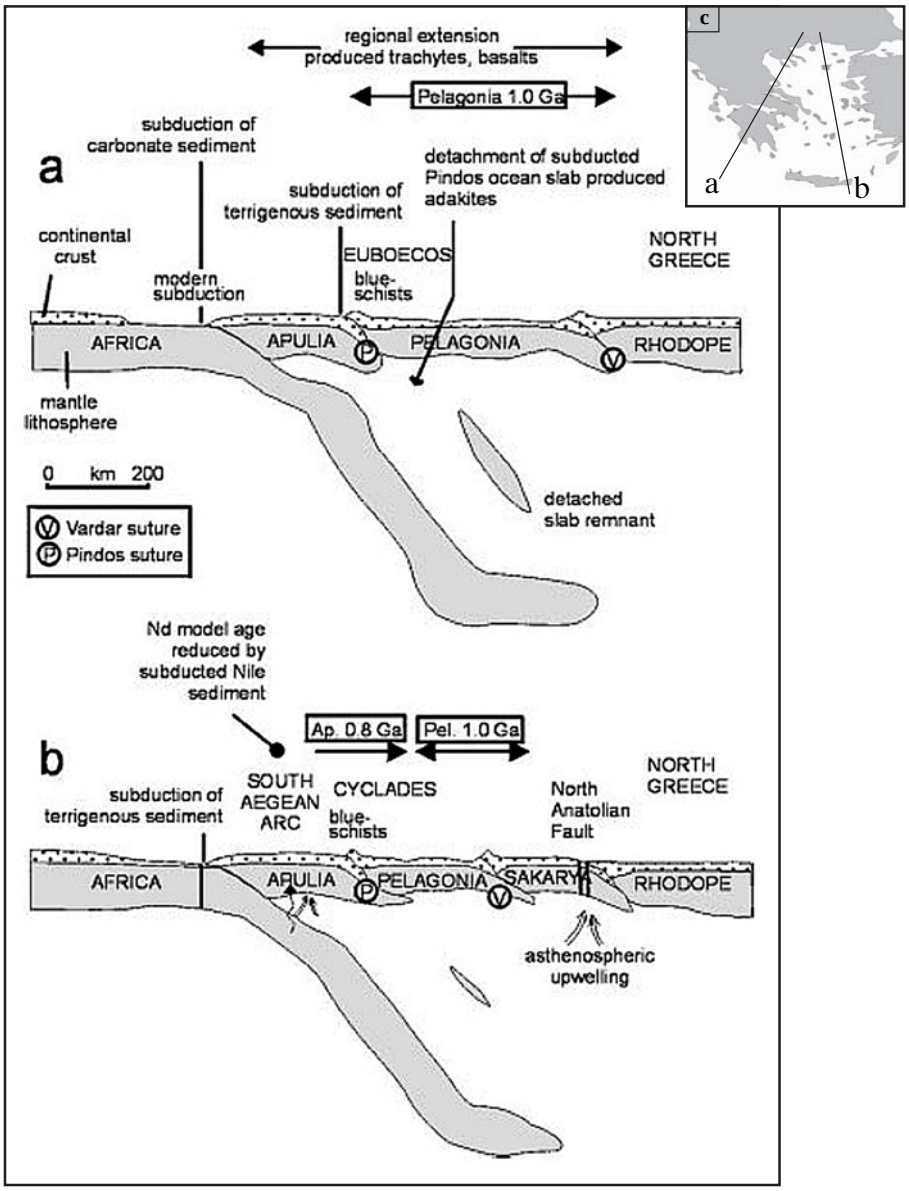

***Figure 5**:* Tectonic cartoon (from Pe-Piper, 2001) illustrating inferred Late Cenozoic plate configurations. Sections (a,b) are approximately S to N (see inset figure c).

two, Pindos suture and Vardar suture, were closed mostly in the late Cretaceous, after the emplacement of ophiolites. The third oceanic basin started to close when the collisional orogenic uplift began in the Early Cretaceous, and mainly Late Eocene. In the early Cretaceous, the orogenic uplift stopped and marked by the Cenomanian transgression of the sea, until the next uplift, which arrived in the Late Eocene.

After a crustal thickening episode at the fore-arc area, the extension occurred shortly, which culminated in the Late Eocene (Blake et al., 1981; Bonneau & Kienast,

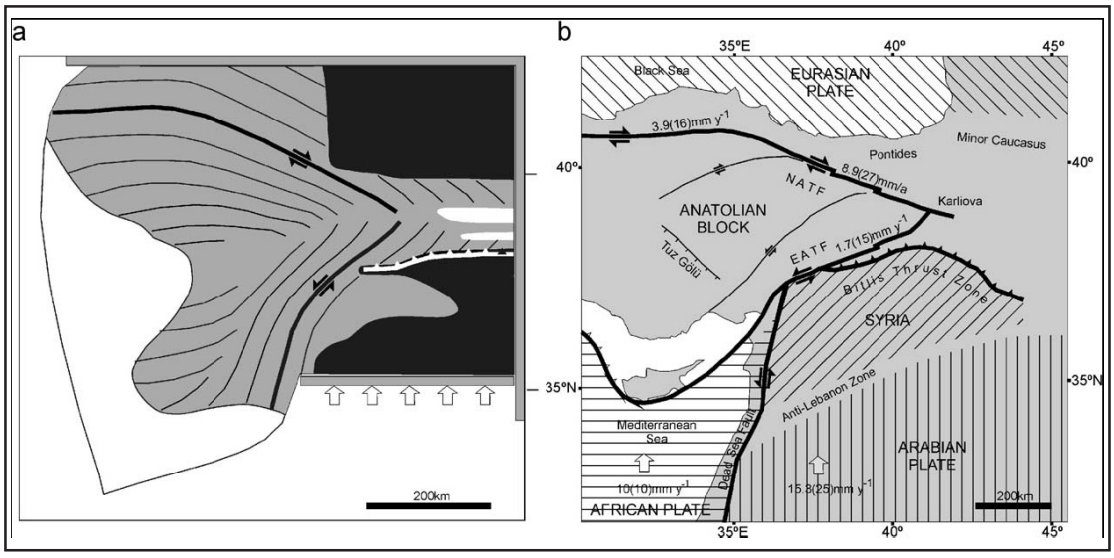

Figure 6: Plate tectonic sketch map of the collision zone between Arabia and Eurasia leading to westward escape of Anatolia (modified from Seyferth & Henk, 2003; after Dewey et al., 1986). Displacement rates are given with respect to Eurasia: averaged values for the last 9 Ma (Dewey et al., 1986; Sengor, 1979) and in brackets present-day slip rates (Kiratzi, 1993; Oral et al., 1995; Reilinger et al., 1997).

1982). Extensional collapse of the South Greece took place at the early Miocene, while subduction of the eastern Mediterranean remnant of Neotethys continued from the South (Pe-Piper et al, 2002).

In the upper Miocene, the westward tectonic escape of Turkey followed (fig. 6). This tectonic episode was attributed to the northern movement of Arabian plate that resulted to Arabian-Eurasian collision zone in eastern Turkey (fig. 7). The forenamed westward tectonic escape of Turkey controls the kinematics of modern deformation in Greece (McKenzie, 1970; Le Pichon et al., 1993). This results in some convergence between NW Greece and Apulia (Taymaz et al. 1991) and rollback of the South Aegean subduction zone (Royden 1993). As an additional result, of the tectonic escape of the Turkey microplate was the acceleration of the compression in the area of Crete Island. The change in deformation style from strike-slip in the Aegean Sea to mainly normal faulting in mainland Greece is related to the collision of northern Greece and

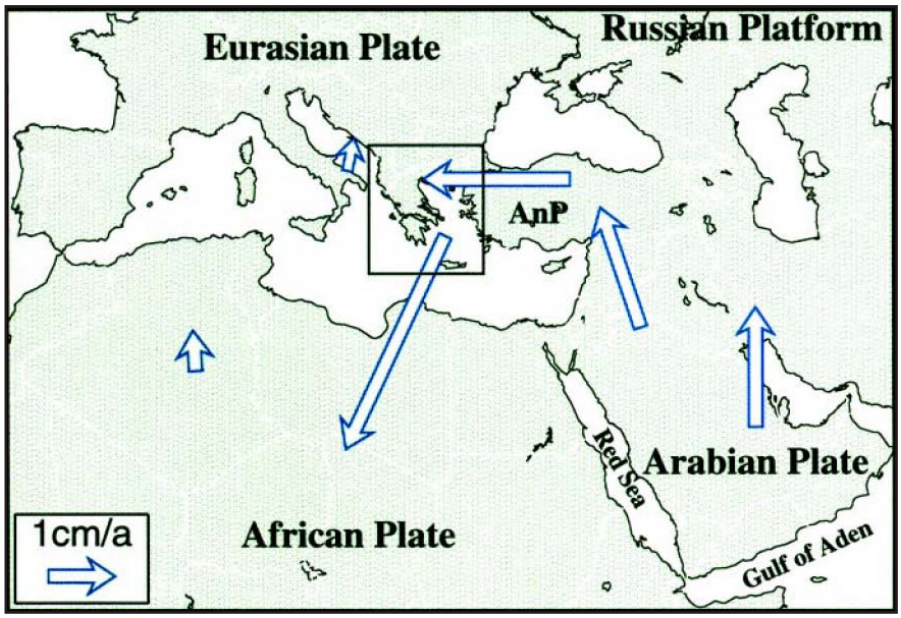

Figure 7: Summarized geodynamic framework around the Mediterranean Sea together with the major plates involved in the collision process. Superimposed on the ccw rotation of the African plate is a pronounced right-lateral motion of the Aegean/Anatolian plate towards the WSW. The large arrows describe the average motion of the African and Arabian plates as well as of the Anatolian and Aegean microplates, relative to the Eurasian plate (Cocard et al., 1999).

Albania with Apulia, so that western Greece cannot rotate rapidly enough to take up the western motion of Turkey. This results in E-W shortening and N-S extension. Furthermore, the N-S extension took place at the South Aegean as a result of the compensation of the southern Aegean margin's motion, while it was migrating easily over the South Aegean subduction zone.

Cenozoic evolution of the Hellenic arc – Major tectonic rotations

Kissel & Laj (1988), detected clockwise rotations in several sites of tertiary formations in the Aegean domain. They are in agreement with the hypothesis that the Lower Miocene arc was almost rectilinear with an E-W trend (fig. 8a) and that its cuvature has been acquired tectonically in 2 major rotation phases, whereas rotations on the Turkish side of the Aegean are less uniform, being both clockwise and anticlockwise. Furthermore, they refer that during the Middle Miocene a first phase of

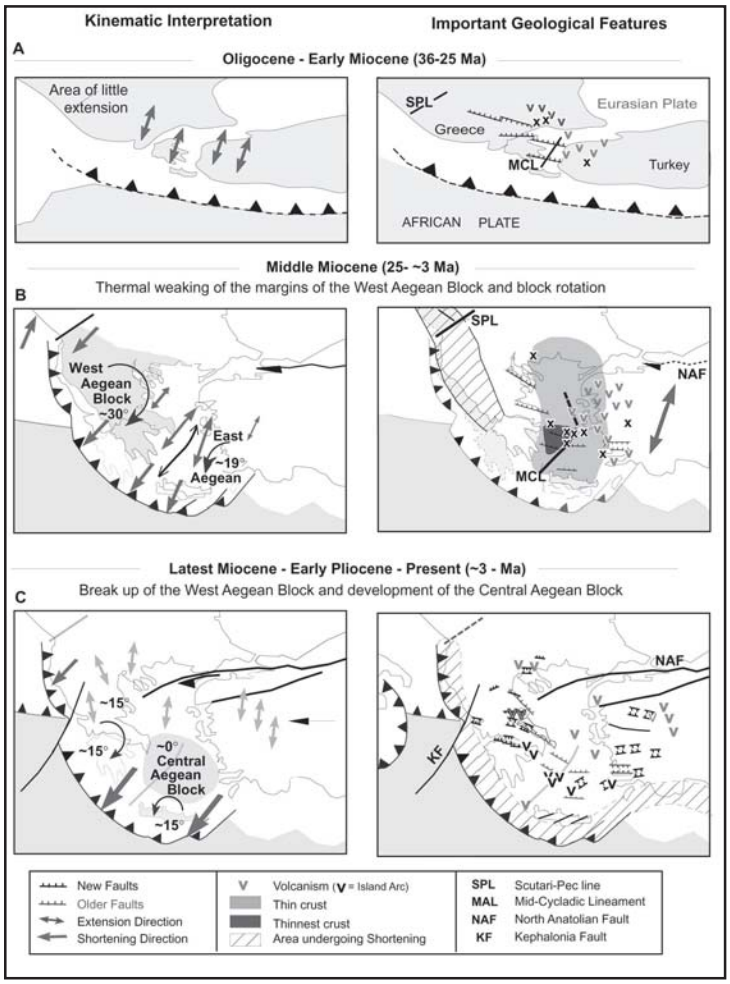

***Figure** 8:* Chrono-Kinematic interpretation and important geological features at the Aegean. (From Walcott & White 1998).

deformation is characterized by cw (clockwise) and ccw (counter clockwise) rotations in the W (Epirus) and E (SE Anatolia), respectively. The second rotation phase occur in the last 5Ma, after the propagation of the NAF, about a pole situated in the South Adriatic Sea affected only the NW part.

In addition, Kissel and Laj, (1988) suggested that the rotations in the Aegean region resulted in the development of the Hellenic arc and its southward migration above the Hellenic trench. From the other hand, Taymaz et al., (1991), suggested that the westward motion of Turkey, the resistance to this motion in the northern part of Greece and in Albania, and the presence of the Hellenic subduction zone that acts as a free

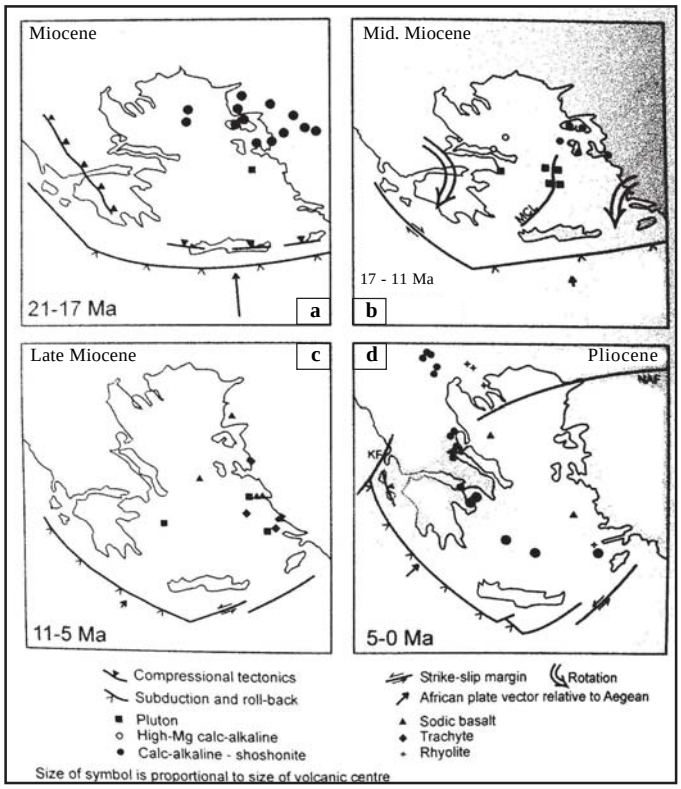

***Figure 9**:* (a,b,c,d): Evolution of the curvature of the Aegean arc during the Cenozoic, based on paleomagnetic data from Piper 2002 "Igneous rocks in Greece". (modified from Kissel & Laj, 1988 and Walcott & White, 1998). KF = Kefallinia fault; MCL = Mid-Cycladic lineament, NAF = North Anatolian Fault.)

boundary, govern the overall southward flow of the Aegean crust. The same authors depicted a series of NW-SE-trending crustal segments ('slats') in the western part of the Aegean, and NE-SW-trending slats in its eastern part. In this model, the deformation in the Aegean involved opposite sense of rotations of these crustal segments and was accompanied by roughly N-S extension.

Existing kinematic models (Le Pichon and Angelier, 1981; Angelier et al., 1982; Taymaz et al.,1991; Westaway, 1991) which attempt to account for the geodynamic development of the Aegean imply that major tectonic rotations must have played an important role during the late Cenozoic evolution of the Hellenic arc. An important example of the high extension was caused by rotation of Cyclades Islands. Specifically, it was estimated that post-l2-Ma vertical-axis rotation increased the N-S dimension of

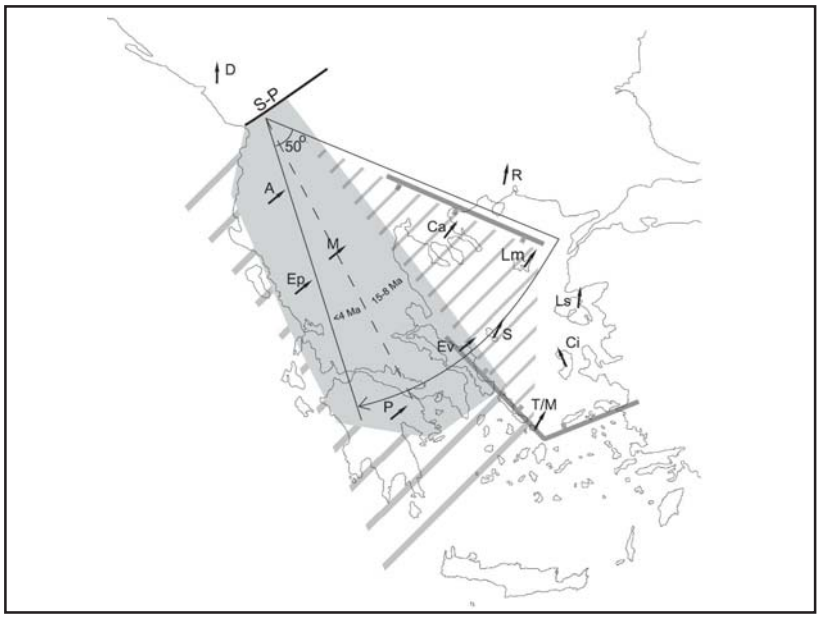

***Figure 10**:* Schematic map that indicates the inferred rotation of 50°cw by Hinsberger et al., (2005). The shaded area is inferred to rotate 50°cw, while hatched area presents the the finite post-Oligocene rotation of 30°-40°cw . The widely hatched area does not contain middle Miocene sediments but it is inferred from structural observations that it belonged to the 50°cw rotating domain. A=Albanides; Ca=Chalkidiki peninsula; Ci=Chios; D=Dinarides; Ep=Epirus; Ev=Evia; Lm=Limnos; Ls=Lesvos; M=Mesohellenic basin; P=Peloponnesos; R=Rhodope; S=Skyros; S-P=Scutari-Pec transform; T/M= Tinos and Myconos.

the Cyclades by ca**.** 31% (e.g. 25 km) (Dov. Avigad et al., 1998).

Block rotation affected the Cyclades (back-arc basin of Hellenic arc) when crustal thickness was restored to normal and its gravitational potential relatively reduced. Thus, vertical-axis rotations were probably induced by the westward extrusion of Turkey and/or the southward retreat (roll-back) of the subduction zone south of Crete, both acting on the periphery of the Aegean domain (Avigad et al., 1998). Block rotations in the Cenozoic (fig. 8) inferred from paleomagnetic data (Walcott & White 1998) range from 25° to 50° in much of western Greece, to near zero in Crete, Rhodes and Thrace, to 15° to 30° ccw in the eastern Aegean and western Anatolia.

From post-Middle Miocene tectonic evolution clues of the Aegean region revealed Neogene clockwise rotations on vertical axes, of up to 50° (fig. 10), in the western side

of the Aegean (Hinsberger et al., 2005). Zero rotations were detected on Crete (fig. 9) according to Kissel & Laj (1988), while C.E. Duermeijer et al. (1998) observed some rotations in Crete. According to latter author, the amount of ccw rotation varies from 10^o to 20^o in Crete, but in central Crete appears up to approximately 40^o. In addition, they indicate post-rotational WNW-ESE extension, or NNE-SSW compression. On the Turkish side, both clock wise and anticlock-wise tectonic rotations were detected, while according to Walcot & White (1998) observations of the palaeomagnetic declinations vary at the Aegean, referring a less coherently behavor of the eastern Aegean than this of the western Aegean, on a large scale (fig. 9). Yet, data on block rotations in the central part of the Aegean Sea, in the area of the Cyclades that bridges Mainland Greece with Turkey, was not available until Morris and Anderson (1996) revealed opposite-sense, vertical-axis rotations of significant magnitudes on Naxos and Mykonos (Central Aegean). The latter authors suggested that Mykonos belongs to a NW-striking block that rotated 22^o clockwise, while Naxos, which shows 30^o anticlockwise rotation, is tied to a NE-striking crustal segment perhaps connected to the Turkish side of the Aegean Sea.

Palaeomagnetic study of Avigad et al. (1998) revealed 23^o vertical-axis clockwise rotation of the 12-Ma-old dike swarm on Tinos. Post-10 Ma clockwise rotations were also detected on Mykonos (Morris & Anderson, 1996), as well as, in Evia (Kissel & Laj, 1998). These results support the general outlines of the model proposed by Taymaz et al. (1991), and strengthen the possibility that Mykonos and Tinos lie on a NW-SE-striking crustal segment that stretches as far north as central Evia and rotated clockwise.

Throughout the Miocene (fig. 8a, 8b, 9b), a discrete West Aegean crustal block

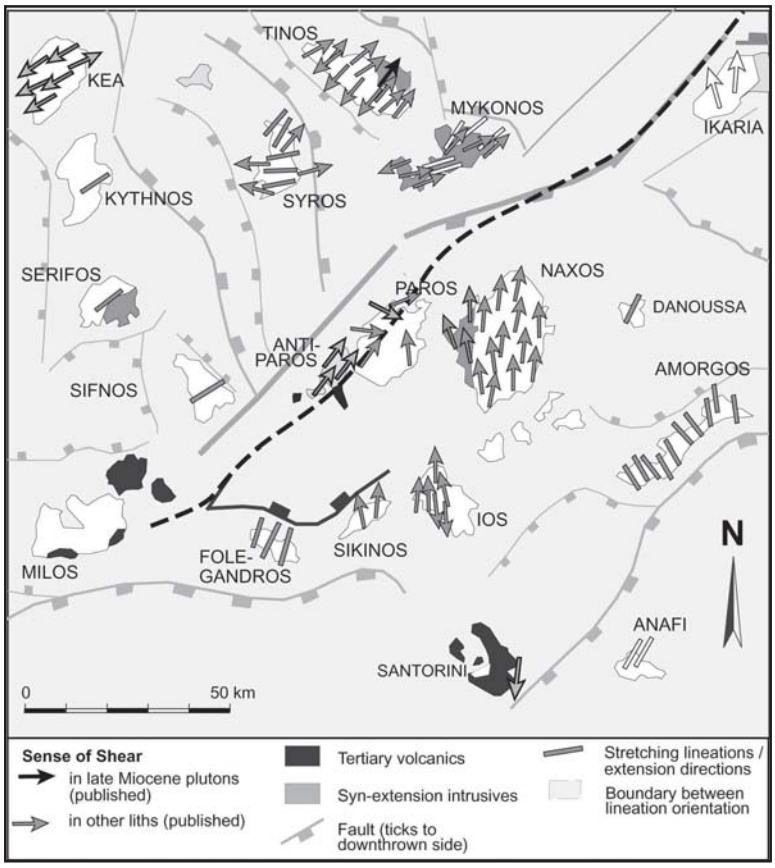

Figure 11: Structural map of the central Aegean region showing MCL (MidCycladic Lineament), the distribution of ductile shear and the stretching lineations directions (from Walcott & White 1998). Black arrows on Kea, Tinos, Santorini, Antiparos are from Walcott & White, 1998; lighter arrows represent data from Gautier, 1995; Sowa, 1985; Faure et al., 1991.

ROTATION		**Relative rotation**	***Reference***
West Aegean	**East Aegean**		
(clockwise)	**(anticlockwise)**		
25° (0 to 12 Ma)		25° (0 to 12 Ma)	Kissel and Laj (1988)
25° (> 12 Ma)	30° (> 12 Ma)	55° (> 12 Ma)	
25° (0 to 5 Ma)	0° (0 to 12 Ma)	25° (0 to 12 Ma)	Kissel et al. (1986)
30° (12 to 30 Ma)			Morris and Anderson (1996)
22° (0 to 12 Ma)	33° (0 to 12 Ma)	55° (0 to 12 Ma)	
NWM: 10-15° (0 to 3 Ma)	SM: ´15 Ma	´30° (0 to ´3 Ma)	Walcott & White (1998)
30° (3 to 25 Ma)	19°(3 to 25 Ma)	49° (´3 to ´25 Ma)	
**NWM: northwest margin of Central Aegean Block*			
** SM: southern margin of Central Aegean Block*			

Table 1: Rotations of West and East Aegean regions.

rotated 30° clockwise, with the Mid-Cycladic Lineament marking the junction with the eastern Aegean-Anatolian block (Kissel & Laj, 1988; Walcott & White, 1998). Le Pichon et al., (1995) suggest that a major change in the kinematics of central and

western Aegean occurred in the Pliocene. Morris and Anderson (1996) report a major NE-SW of trending fault in the northern Cyclades and interpreted to mark the boundary between the eastern and western Aegean (fig 11). The apparent sharpness of the Mid-Cycladic Lineament (MCL), on a regional scale, is one of the more striking aspects of the West Aegean Block, according to Walcott & White (1998), who suggest that the margin comprises a discrete shear zone. Relative motion between these two blocks ended in the Latest Miocene - Early Pliocene, when the North Anatolian Fault propagated into the Aegean Sea (fig 8c, 9d), (Walcott & White, 1998; Piper et al., 2002). In addition, Walcott & White, (1998) report that the MCL boundary between zones of opposing rotation is a sharp, linear feature, not a gradational feature, and it does not coincide with a fault in Cyclades, in contrast to Morris and Anderson (1996). Moreover, the Mid-Cycladic Lineament diverges from this fault in the southern Cyclades and crosses Paros Island itself (fig. 11), implying that the previously observed fault may represent, in part, a younger structure than accommodating rotation of the West Aegean Block.

Published estimates of the amount of finite rotation of the west Aegean relative to the east Aegean vary widely (Table 1). Morris and Anderson (1996) found that the southeast Cycladic region underwent 50% more (1.5 times) rotation than the NW Cycladic region (part of the WAB=Western Aegean Block) whereas Kissel et al. (1986) suggest that only the west Aegean rotated of about 25^{o} clockwise at the same time span (fig. 12). The question is “how much absolute rotation did each side undergo before and after the cessation of activity across theMCL?” To answer this question, Walcott & White, (1998), compare the orientation of lineations (fig. 13) from those areas and conclude that the northwestern Cyclades region appears to have rotated

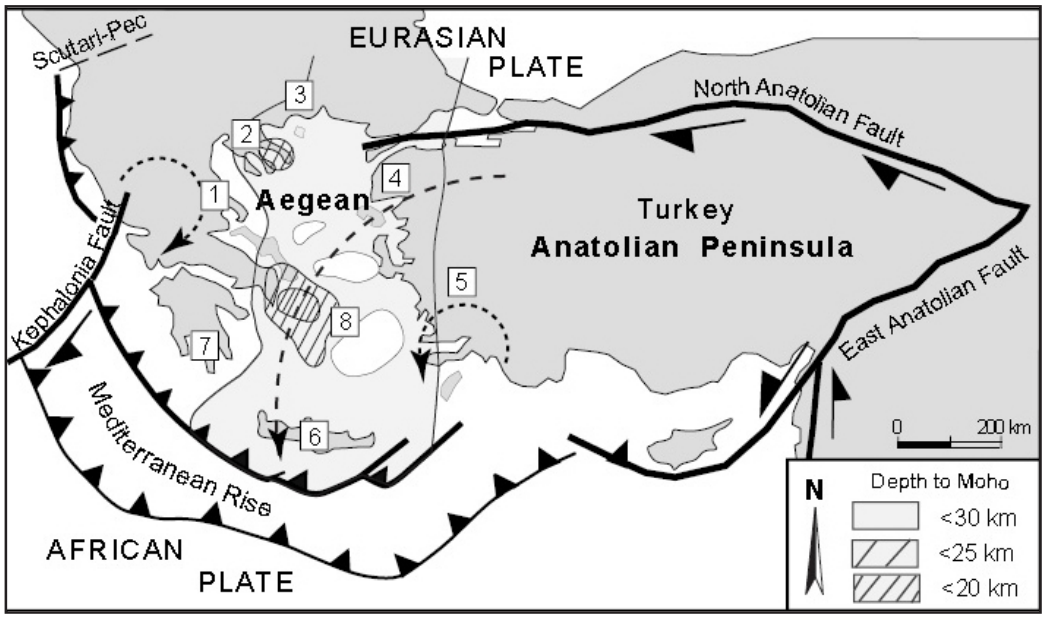

Figure 12: Schematic tectonic map of rotations according to Walcott & White, (1998). Deformed basement of Tertiary age exposed within and around the area of relatively thin crust of the Aegean. Deformed basement of Tertiary age exposed within and around the area of relatively thin crust of the Aegean. *1 = northern Pelagonian Zone; 2 = Chalkidiki; 3 = Rhodope; 4 = NW Turkey; 5 = Menderes Massif; 6 = Crete; 7 = Peloponnesos; 8 = Attico-Cycladic belt*. Also shown are the palaeomagnetically determined senses of rotation (shown as small dashes) associated with regional SSW-directed extension (Kissel et al., 1986, 1987). The line with larger dashes follows the trace of a small circle published by Jolivet et al. (1994) to describe anticlockwise motion of Turkey. Crustal thicknesses from Tsokas and Hansen (1997).

twice as much as the southeast Cyclades region. The latter evidence may imply that extension at Aegean migrates southern, indicating highest extension, at the southwestern part of the arc (Kythera - Antikythera strait), at the last 5 Ma (Late Pliocene).

The latest calculation is based on the assumption that there has been no block rotation of the central Cycladic region since cessation of activity across the MCL in Latest Miocene-Early Pliocene, when NAF propaged to the North Aegean. In addition, the latest estimation is based on the comparison between available palaeomagnetic data of declinations and lineations. The angle that derives from the indicated above comparison is 23^{o}, orientating the lineations approximately 023^{o} relative to palaeonorth when rotation started to occur. Vertical-axis block rotation, commonly associ-

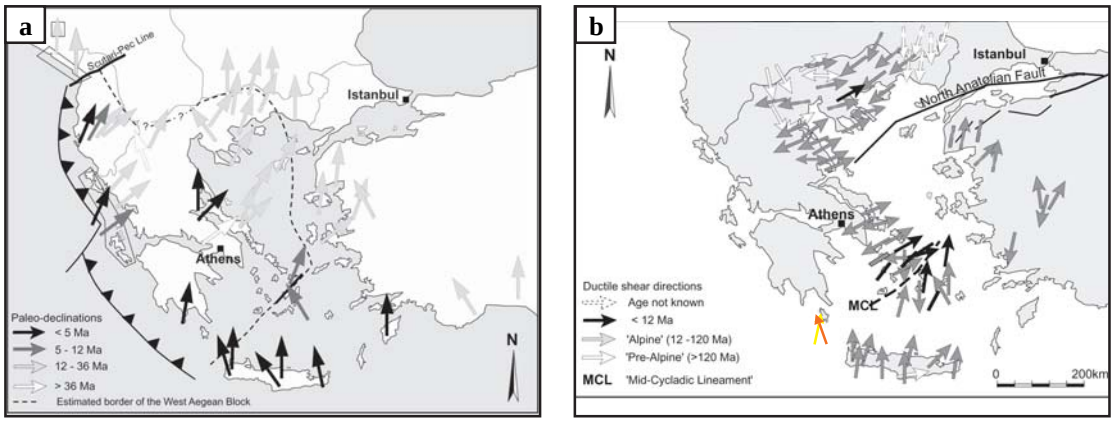

***Figure 13**:* a. Summary of Cenozoic paleomagnetic declination from Walcott & White 1998 for the Cenozoic rocks in Greece (modified). The map shows that the Scutari-Pec Line in the NW Aegean and a similar structure in the southern Aegean mark the boundaries of an area of predominantly clockwise rotation from an area of anti-clockwise rotation (West Turkey). b. Directions of ductile shear and stretching lineations within Aegean basement (from Walcott&White, 1998, after other published references of ages). The yellow and red arrows are the streching lineation on Kythera Island, below the detachment fault that measured in current research on Kythera Island.

ated with wrench-faulting, is an important deformation style of the Aegean continental crust. Vertical-axis block rotation is a two-dimensional crustal deformation mechanism that preserves area and crustal thickness, but modifies the length and width of the domain boundary (Ron et al., 1984). McKenzie and Jackson (1986) suggested a different mode of block rotation in which the length of the domain boundary is kept constant. In this case, the faults bounding each of the rotating blocks show oblique-slip with a component of extension perpendicular to the strike of the crustal blocks. The axis of rotation is thus inclined, and a tilting component is involved. Because no tilting was found on Tinos (Northern Cyclades, central Aegean), the axis of clockwise rotation was considered by Pe-Piper (2002) as a purely vertical one. Therefore, the mode of block rotation preserves area, but modifies the length of the domain boundaries, which may be related to the construction of the Mid-Cycladic Lineament .

Cenozoic evolution of the Hellenic arc – Major tectonic extensions

Neogene crustal extension in the Aegean area has been generally interpreted as

a result of escape tectonics, with the Anatolia – Aegean microplate "squeezed" westwards between the Arabian indentor and Eurasia (Jackson 1994; Pe-Piper, 2002). Collision of Anatolia with Eurasia in the Miocene resulted in crustal thickening of eastern Anatolia and subsequent westward gravitational collapse leading to the escape of Anatolia and the development of the North Anatolian Fault, which has progressively propagated westward in the past 10 Myr, reaching the north Aegean at about 5 Ma (Armijo et al. 1999). Since Pliocene time, the south region of Aegean experienced an extension (C. Fasoulas, 1999).

The igneous activity appears to have migrated southward through the Cenozoic: from north Greece and Bulgaria (Eocene-Oligocene volcanism and plutonism), through the north Aegean islands (widespread early Miocene volcanism) and the Cyclades (Miocene I-type plutonism) to the modern South Aegean Arc (Pliocene-Quaternary). These rocks are representing a volcanic arc that migrates southwards as a result of the rapid post-middle Miocene extension of the Aegean Sea (e.g. Fytikas et al. 1984). In contrast, according to Van Hinsbergen et al. (2004) he assumes that it is unlikely that extension of the Aegean lithosphere led to melting of the underlying mantle. However, he is accordant to the idea that the extension probably played a significant role in the timing of the onset of Pliocene volcanic activity in the Aegean. The position of the volcanic centers is probably the result of the depth of the subducted slab below the Aegean and the formation of a network of extensional faults in the overriding Aegean lithosphere.

Decreased rates of convergence between Africa and Eurasia in the Oligocene (Savostin et al., 1986) resulted in roll-back of the subducting plate boundary (Royden, 1993) and extension of the Aegean. Extensional collapse probably began in the Rhodope

orogen (Burg et al., 1990) and continued later as a result of the elevation of the Hellenide orogen.

The N-S dimension of the Cyclades (i.e. the distance between Tinos and Santorini; fig. 11) is at present 100 km long. According to Avigad et al. (1998) calculations, it was implied that about 25 km of this length are due to post-12-Ma vertical-axis block rotation, while no major crustal thinning is required to have accompanied this phase of N-S elongation in the western Cyclades.

The origin of extension involved on low-angle normal faults (D. Avigad et al., 1998). At the Cyclades area, according to D. Avigad et al. (1998), various types of deformation styles may lead to crustal extension, but one of the most typical modes of upper-crust continental extension involves normal faulting and tilting of blocks in a domino-style geometry. An important corollary of the planar geometry associated with domino-style is that both, the faults and the blocks they bound, rotate about a horizontal axis. The absence of such tilting on Tinos (Cyclades - Central Aegean) implies that post-12 Ma crustal thinning in this area was minor.

Sonder & England (1989) and Taymaz et al. (1991) have found good agreement between earthquake motions and models involving simple extension of the lithosphere in the Aegean area. In addition, the stretching parameter for the post-mid Miocene Aegean has higher values than those that were estimated for the Oligocene of northern Greece (e.g., Sonder & England 1989).

Structural evidence shows that plutons of the Cyclades and North Greece were emplaced during active extension and formation of core complexes (Boronkay & Doutsos 1994, Dinter et al. 1995).

Today, the Aegean Sea and the surrounding land areas are one of the most rap-

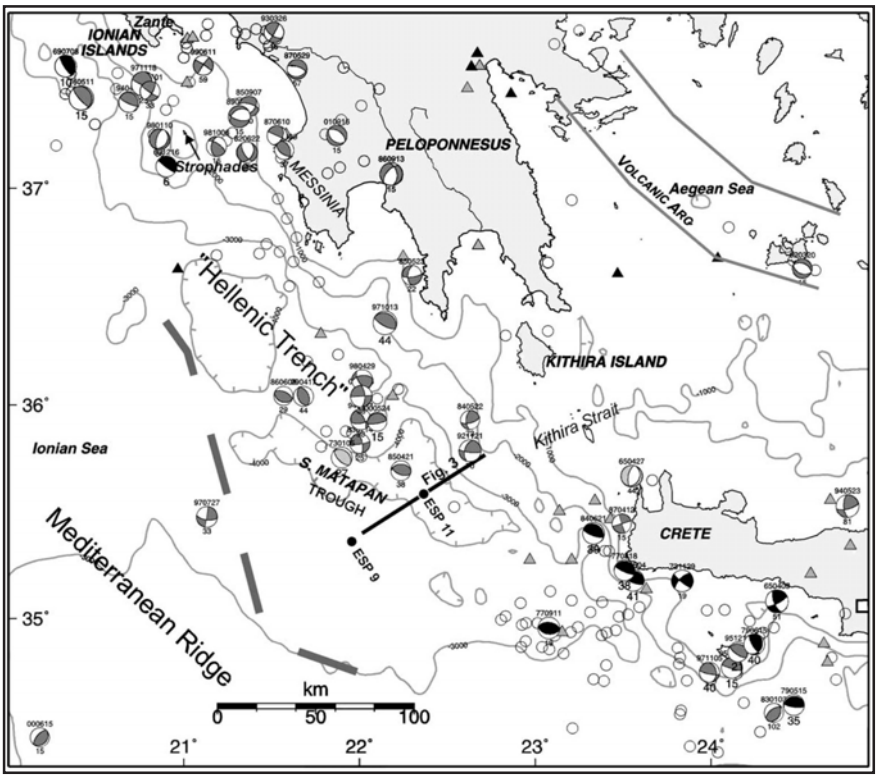

***Figure 14**: Map of the SW Aegean region. Epicenters of all earthquakes with M>=4.8 (from Engdahl et al.,1998; are plotted, as circles for depth less than 50 km, gray triangles for 50-70km depth, and black triangles deeper. Earthquake focal mechanisms are labeled with centroid depths from the Harvard CMT catalog, and are located at the epicenters of Engdahl et al., 1998. Dark gray shading indicates Harvard CMT solutions, light gray shading indicates solutions by Papazachos et al., 2000; and black shading indicates solutions by Taymaz et al., 1990; around Crete and by Baker et al., 1997; in the Ionian Islands.(From Laigle et al., 2004)*

idly extending areas of continental crust in the world, with the southern Aegean moving at about 35 mm/yr relative to Eurasia (Jackson, 1994).

Rotation in Kythera Island

Lyberis et al., (1982) suggested that as Crete has not undergone significant rotation since the Late Miocene (Laj et al., 1982), the clockwise rotation of Peloponnesus may imply some equivalent counterclockwise rotation in the Kythira-Antikythira segment. However, palaeomagnetic studies were perfomed on the Miocene and Pliocene at Kythera island indicating anticlockwise rotations, although the error is large and therefore this result may only be considered as indicative, at Kapsali area (Southern

part of Kythera Island) the Miocene sediments determine (by NRM, natural remanent magnitization) a very reliable 8° degree anticlockwise rotation indication, while there is a mean declination of 100.7° (AMS, anisotropy of the magnetic susceptibility), implying a NNW-SSE extension in a time span of Miocene-middle Pliocene (Duermeijer et al., 2000). Steenbrink (2001) refers to a mean counterclockwise rotation of 5° degrees and declination of 355.2° in middle Pliocene sediments in Kythera Island. Older studies from Meulenkamp et al. (1977) reveal both counter clockwise and clockwise rotations in Tortonian sediments of Kythera Island. Specifically, the values are 3° (ccw) and 5° (cw) degrees of rotation and 356.7° and 4.7° declination, respectively.

Recently studies of Hinsbergen et al. (2005) reveal both counterclockwise (ccw) and clockwise (cw) rotations in Lower Pliocene sediments of Kythera Island. Specifically, two sample localities result to cw of 5° and declination of 5.4°, and the other sample results to ccw of 9° degrees with declination of 350.9°.

Extension at the area of Kythera Island

The accurate location of the Kythera Island is (N36.39304 –N36.12570, E22.88853 –E23.12208). Within the southwestern Hellenic outer arc, Peloponnesus and Crete are connected by a 100km long NNW-SSE ridge (fig. 14), where have found good earthquake motions and models that reveal extension of the lithosphere in the Southwestern Aegean area. At the axis of this submarine high, mostdepths are shallower than 150m; two islands, Kythira and Antikythira, and numerous islets are present. This narrow segment of the Hellenic arc is bounded by major scarps on both sides, and it separates the 3000-5000 m deep Hellenic trench to the west from the 1000-2000 m deep Cretan Sea basin to the east. After accurate bathymetric data obtained using a

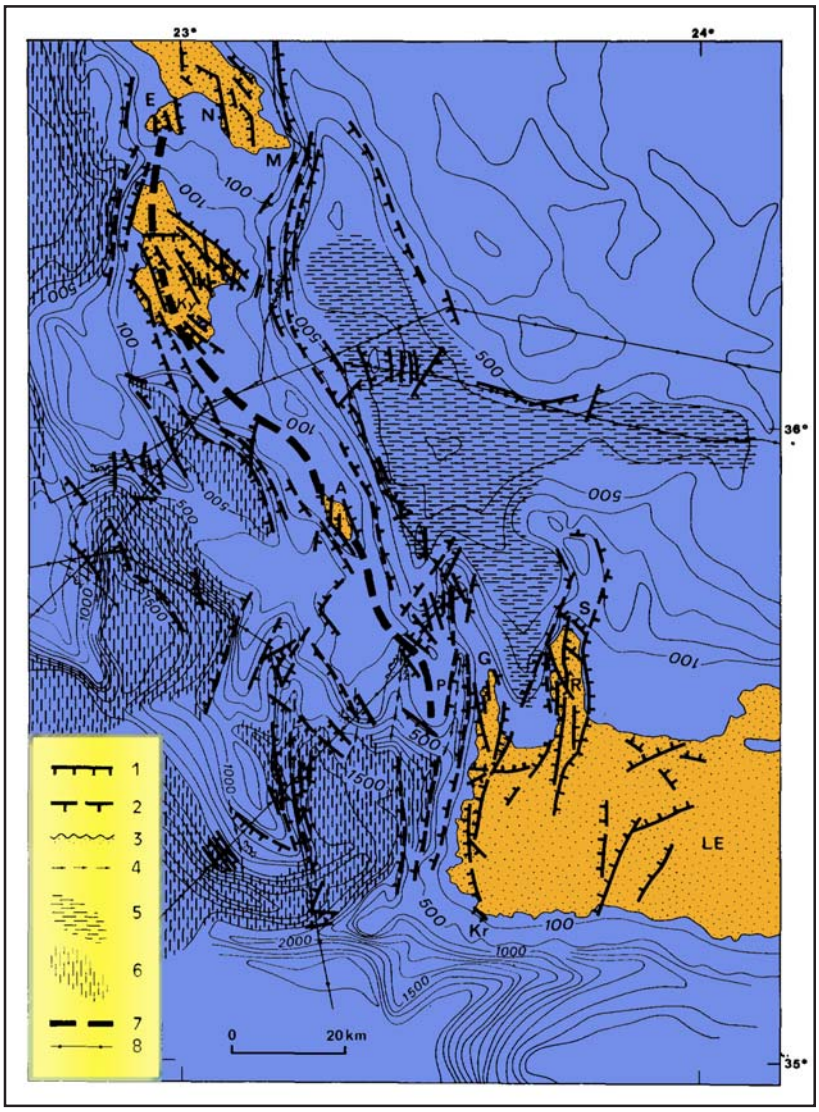

Figure 15: Neotectonic structure of the Kythira strait area. E, Elafonissos; N, Neapolis; M, Cape Maleas; Ky, Kythira; A, Antikythira;P, Pontikonissi; G, Cape Gramvoussa; R, Rhodopou peninsula; S, Cape Spatha; Kr, Cape Krios; LE, Lefka Ori. 1, normal fault scarp; 2, probable normal fault scarp;3, erosional morphologies; 4, submarine canyon; 5,deep Cretan Sea Basin; 6, deep sedimentary bsins of the Hellenic margin; 7, morphological axis of the Kythira-Antikythira ridge; 8, ship-track lines. Submarine contours in fathoms (after Defense Mapping Agency, Hydrographic Center, Washington).

multi-beam echo sounder on submarine fault scarps (fig. 15, fig.16c), the results of studies on land lead to a new interpretation of the neotectonic deformation of this segment of the Hellenic arc (Heat Cruise of R/V Jean Charcot, 1978). The field analysis took place on Late Cenozoic faults which has been carried out in the southwest Hellenic arc, on the islands of Kythira and Antikythira, by Lyberis et al. (1982). According

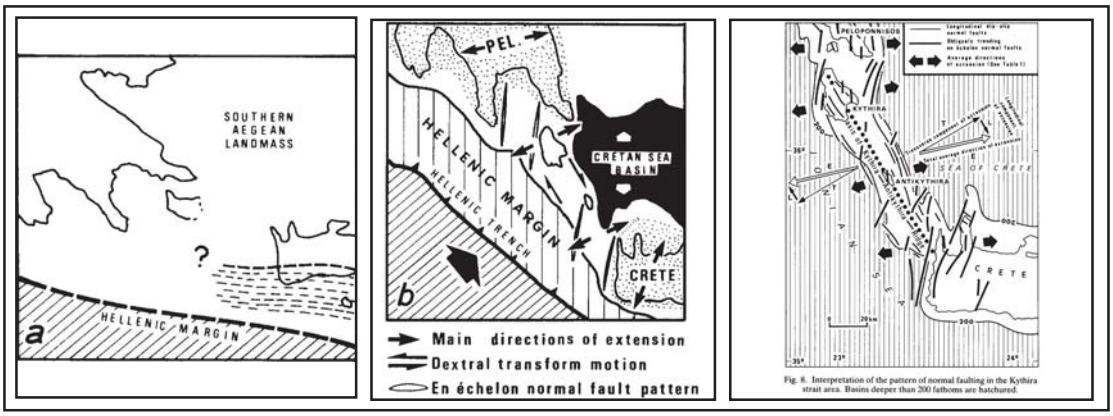

***Figure 16**:* (a-b)Horizontal deformation of the southwestern Hellenic arc. (a) Beginning of Hellenic subduction associated with Aegean expansion, approximately 13-12 Ma ago (Late Serravallian-Early Tortonian). The dashed pattern designates the area where marine Late Serravalian deposits are identified. (b) Present day. Major blocks of the arc dotted. Wide black arrow: motion of Africa relative to Aegea. Pel, Peloponnesus. (c) Interpretation of the pattern of normal faulting in the Kythira strait area. Basins deeper than 200 fathoms are hatchured. (from Lyberis et al., 1982).

to Lyberis et al. (1982), the submersion of the strait Kythera-Antikythera is a consequence of extension related to normal faulting, while this extension rate is being faster than in adjacent segments of the arc. The existence of oblique en echelon normal faults indicates that dextral deformation of NW-SE plays a role within the Kythira strait (fig. 16b). The whole pattern of fault systems in southeast Peloponnesus is consistent with the clockwise rotation that has been independently proposed and verified by palaeomagnetic studies. Moreover, the same authors implied that the Kythira strait provides an example of a complex transform-extensional deformation and rotation between two major segments of external arc.

The most precise information for dating faulting events has been obtained on Kythira island where both the Upper Miocene sediments and the Pliocene are represented (Christodoulou, 1965; Freyberg, 1967; Theodoropoulos, 1973). In the main NW-SE graben of central Kythira, the marine Pliocene sediments overlie Upper Miocene deposits which have been slightly tilted and covered by the Pindos nappe. In

contrast, on both sides of the graben, the same uncomformable Upper Miocene sediments overlie the Mesozoic-Palaeogene sediments and flysch of the Tripolis nappe (Theodoropoulos, 1973). Thus, according to Lyberis et al. (1982), the NW-SE graben was created prior to the Pliocene transgression. Synsedimentary faults within these grabens, as well as the tilting of Late Miocene strata prior to Pliocene deposition, suggest that the tectonic activity started in the Late Miocene. This tectonic activity has continued from the Late Miocene until today, since scarps of the same orientation occur at the graben margins (Kokkalas et al., 2001).

Synsedimentary structures in the graben show that faulting continued during the Pliocene. Finally, numerous normal faults cut the whole of the Pliocene series in Kythira as well as in order regions of the Aegean arc (Angelier, 1979; Mercier et al., 1979). Synchronous N-S normal faults and NW-SE that generally cut each other affect the Pliocene (Lyberis et al., 1982), as well as near Kythira Island (Blanc & Blanc-Vernet, 1968). Normal faults also affect the Pleistocene marine deposits of Tyrrhenian age that are exposed on the coast between Neapolis (Southeastern Peloponnesus - northern of Kythera Island) and Cape Maleas (Theodoropoulos, 1973). Finally, marine and land data of fault patterns and mechanisms (fig. 17) are in good agreement in the area of the Kythera strait (Lyberis et al., 1982). Thus, taking into account both the geometry of the fault pattern and the chronology that has been established on Kythira, by Lyberis et al. (1982), one must conclude that the development of the ridge between Peloponnesus and Crete had begun prior to the Pliocene transgression and has continued since then (Angelier et al., 1976).

Stratigraphic studies on Crete of uplfited subsided fault blocks from Drooger & Meulenkamp (1973) imply that the disruption of the Southern Aegean land mass into

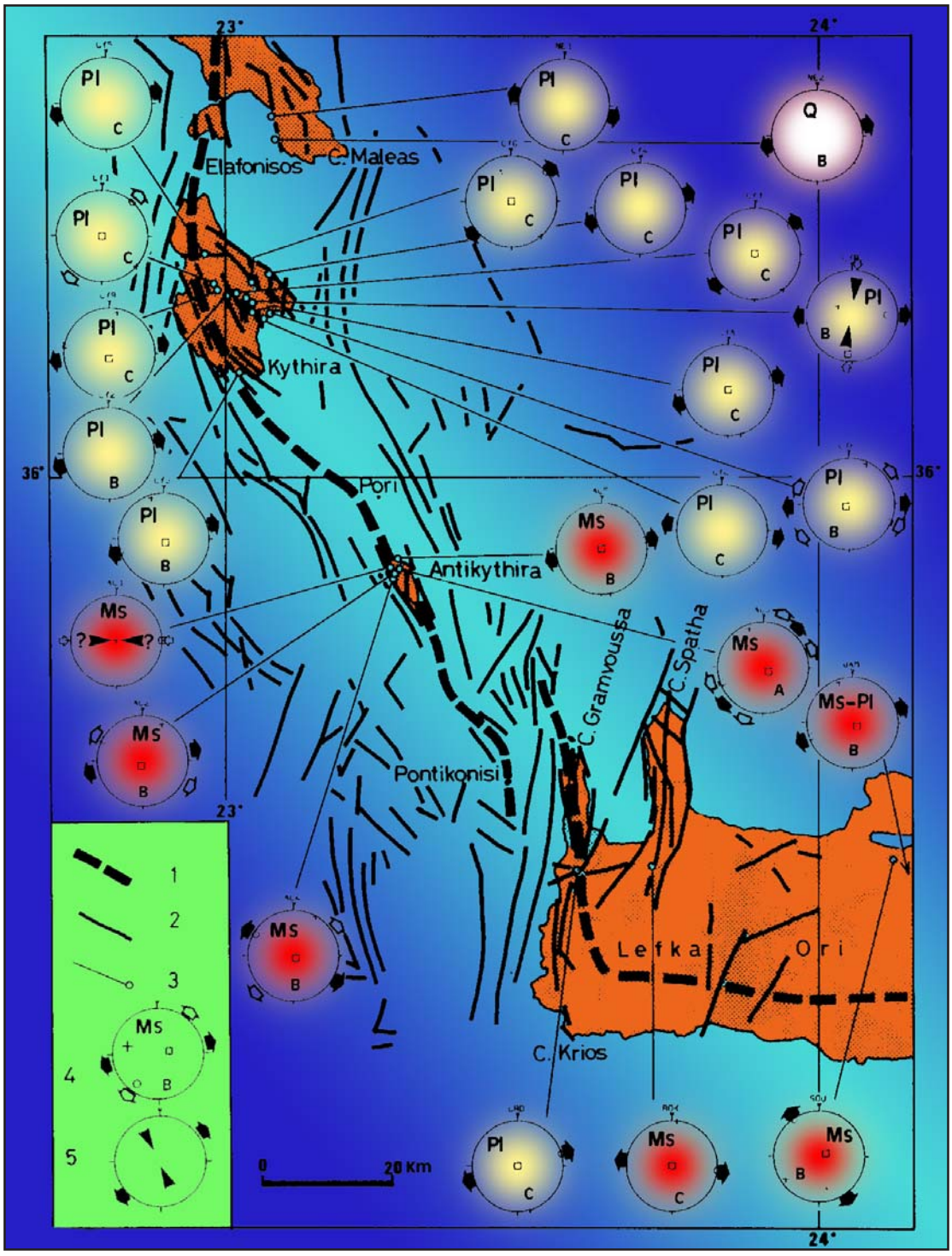

Figure 17: Fault-population mechanisms reconstructed after field analysis in the Kythira strait area. 1. morphological axis of the arc; 2. main fault lines; 3. sites of fault population measurements; 4. main results obtained in one site. Directions of generalised extension given by black arrows, open arrows refer to directions of extension related to particular families of faults. Poles show the principal stress axes (σ1 as squares, σ2 as crosses, σ3 as open circles). The quality of each determination is recorded as A (excellent), B (acceptable) or C (poor). The age of the youngest faulted sediments is indicated by Ms (Late Miocene, in red color), P1 (Pliocene, in yellow color) or Q (Quaternary, in white color), 5. conjugate strike-slip mechanism (direction of compression as centripetal arrows), from Lyberis et al. (1982).

a mosaic of uplifted and subsided fault blocks began during the Late Serravallian, at the close of the Middle Miocene. Consequently, we agree to hypothesis that the fault pattern depicted (fig. 15) also began during this period, approximately 13-12 Ma ago.

Geodynamic context of Kythera

The seismic tomography along Transect VII (fig. 4) shows a well pronounced subduction zone, which can be followed for several hundreds of km below the Aegean Sea (Spakman et al. 1988). This subduction zone is largely over-extending the maximum length of subducted slab during the modern (last) stage of subduction of the Ionian oceanic lithosphere, which was initiated after the Late Miocene. The tomographic section indicates the cumulative result of a long-lasting subduction process, which includes continental fragments of a few hundreds of km in width. A difference in the angle of the subduction zone from gentle to steeper dips, in a roughly trend of N-S of the Cretan basin is also observed from Papazachos (2000) by studying the localized focal earthquakes. The seismic Benioff zone, however, stops at about 150-200 km depth, approximately below the modern Aegean volcanic arc. The seismic tomography (fig. 4) is in agreement with the Middle-Late Cenozoic tectonic history of the Aegean, characterized by a continuous northward polarity of subduction under the European margin.

The Aegean arc is the visible part of a large accretionary complex. The island of Kythera is almost the center of the Hellenic arc, as well as, it undergoes tensional stress. Normal faults rework a stack of nappes built during the Oligocene and Early Miocene at the expense of platform limestones and pelites. NE-SW extension and top-to-the-eastern, -southeastern and -southwestern shear on detachment planes are recorded in Kythera island, where shear sense indicators and lineations are discussed

by the current research.

In most cases, detachments are first recognized because they bring into close contact a non-metamorphosed upper plate and a lower plate metamorphosed to various grades, with always a pressure and temperature gap in between, separated by a major extensional shear zone. The detachments first described by Platt (1986), in Alpine mountain belts can be characterized not only by metamorphic omissions but also by clear structural and metamorphic characteristics. In all the examples studied by Platt (1986), the existence of large-scale detachements during the formation of the accretionary complex leads to the exhumation of HP-LT metamorphic rocks, which is shown in the structures of the metamorphic nappe of Kythera Island.

The exhumation of high-pressure and low-temperature (HP – LT) metamorphic rocks of Kythera Island was controlled by the active flat-lying detachment during the build-up of the mountain belt of the Hellenic arc. This syn-orogenic extension of the metamorphic nappe of Kythera island was controlled also by extensional shear zones, which are reported on the current research.

Jolivet et al. (1998) was considered Crete island to be at an immature stage of mountain building because only the upper part of sedimentary cover was involved in the construction of the accretionary complex, and no thrusts involving the entire upper crust have yet formed. Because Kythera belongs to the same tectonic context as Crete, then we could agree, in some points, with Jolivet et al. (1998) that Crete, as well as, Kythera could be considered to be at an immature stage of mountain building because only the upper part of the sedimentary cover was involved in the construction of the accretionary complex, and no thrusts involving the entire upper crust have yet formed. Because of the similar lithologic unit synthesis and tectonic setting of Crete and Kythera,

we could conclude to the same assumption of Jolivet et al. (1998).

The predominant role of extensional tectonics related to Late Cenozoic normal faulting of this studied area of the Hellenic arc is a major characteristic that may resolves the main question of the induced subsidence of Kythera Island compare to Peloponnesus and Crete Island. The low altitude (fig. 18) of Kythera Island relative to other arc segments (e.g. Peloponnesus, Crete) could be explained by interpreting the Moho-depth map of Makris (1977) which suggests that the crust is thinner beneath Kythira and Antikythira than beneath Crete and Peloponnesus. It is thus very likely that the whole of the Kythira strait has undergone more extension than the adjucent segments of the arc (Lyberis et al., 1982). Furthermore, the results of the studies of Lyberis et al. (1982) imply a particular role that the Kythira-Antikythera segment of the outer arc plays between the larger less deformed blocks of Peloponnesus and Crete. The latter hypothesis of this evolution is related to the progressive bending of the arc, which is demonstrated by the absence of rotation of Crete compared to the 25°-30° rotation of Peloponnesus; the greatest part of the bending being absorbed in the Kythira-Antikythera strait.

Detachment Fault in Kythera Island and Metamorphic evidence of PQU at the outer island arc and Kythera Island

The geology of Kythera is characterized by the superimposition of several nappes. From base to top they are: (1) the questionable Mani nappe (the semi-metamorphic marbles), (2)The phyllite-quartzite unit (PQU) or otherwise named as Arna unit; (3) the Tripoli nappe, unmetamorphosed limestones, mostly dolomites; (4) the Pindos nappe, pelagic isoclinal and recumbent folds of limestones and radiolarites. Finally, tertiary and quaternary sediments are lie on the previous nappes in mostly cases as an

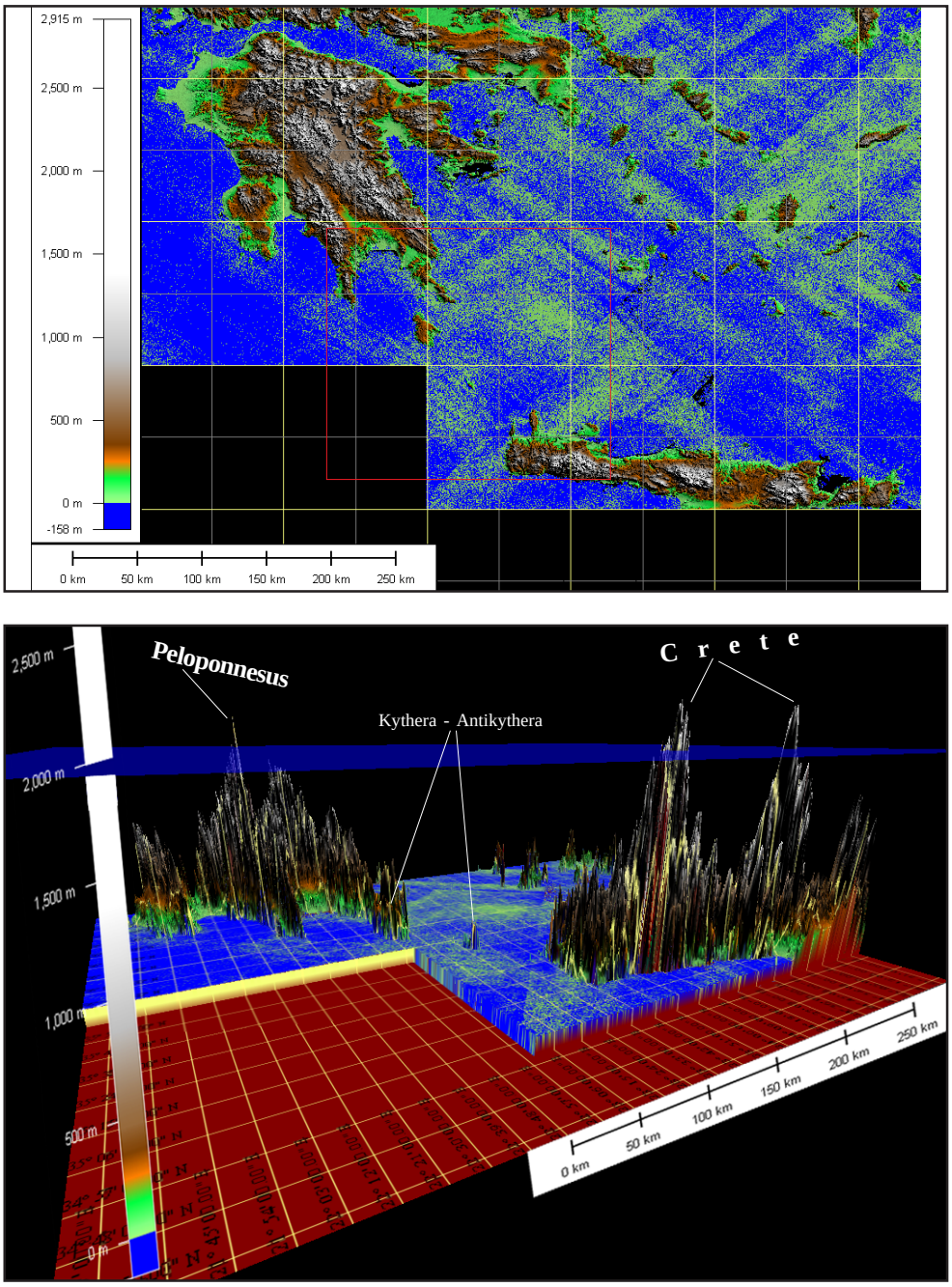

Figure 18: 3D representation of the highest elevations of the Southerneastern part of the Hellenic Arc. Blue planar surface on the top of the Digital Elevation Model represents the 2000 m elevation. Vertical exaggeration of 50 was necessary in order to simplify the results for better visualization.

angular unconformity.

In most marble or recrystalized limestones occurences, the detachment fault was considered to situated between the PQU and the carbonate platforms. This is based on the assumption that marbles occur mostly as lenses among the PQU, as well as, the recrystallized limestones are part of the Tripolis unit basement.

Conditions of P- T- t at the PQU of the outer Island arc

The P-T paths of metamorphic rocks in the Hellenide orogen at the outer arc are characterized by near isothermal decompression (Avigad 1993). According to Jolivet et al. (1998), during extension, HP-LT parageneses were exhumed and preserved. In general, rocks situated in the uppermost parts of the PQ nappes show better preserved HP–LT parageneses than those below. P–T conditions were estimated to 8 kbar (Ida nappe, HP-LT metapelites, carpholite in metabauxites) of north eastern Crete, 12 kbar (PQ decompression path with slower cooling) in central Crete and up to 16–17 kbar (PQ decompression path with fast cooling) in western Crete for temperatures ranging between 300 and 400°C, using the P–T grid described above (Jolivet et al., 1998).

According to Theye & Seidel (1991) studies of regional differenes in the mineralogical compositions of the PQU of the external Hellenides, it was indicated that a gradation in P-T conditions of metamorphism from Eastern Crete via Western Crete to Peloponnesus exists. Specifically, the estimated P-T of Eastern and Central Crete, are about 300°C-350°C, 8-10kbar, of Western Crete, is about 400±50°C, 10±3kbar. Peloponnesus is of higher grade than on Crete. It was estimated a minimum pressure of about 10kbar at 450°C. Furthermore, the examination of the higher grades metapelites from the PQU, Theye & Seidel (1991) were yielded to an estimation of 450°C ± 30°C, 17±4kbar for the Peloponnesus prograde PQ metasediments. Hence, according to the latter authors the prograde metamorphic evolution of Crete and Peloponnesus may be connected towards higher grade with the eclogite facies.

According to zircon dating and quartz microstructures studies of Brix et al. (2002) at Crete, there is a pattern of increasing trend of metamorphic temperatures from low

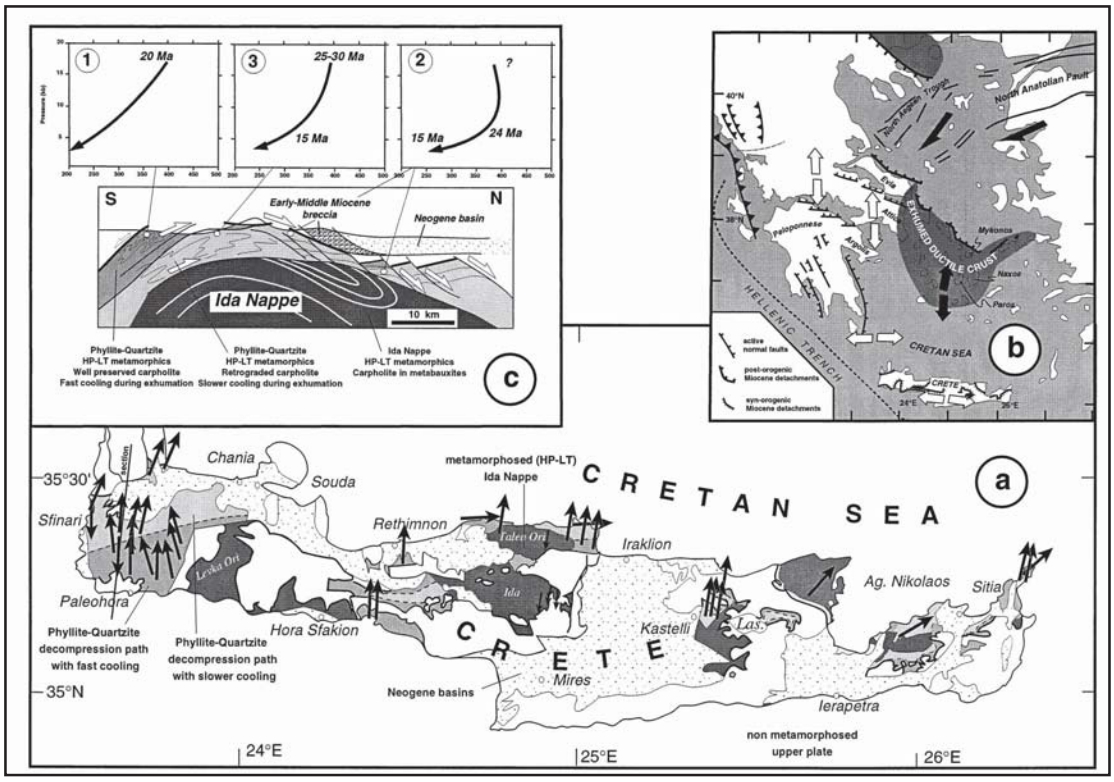

Figure 19: (a) Schematic map of the island of Crete showing the distribution of metamorphic rocks and the two types of P-T paths below the major detachment. Arrows represent the trend of stretching lineation and sense of shear. (b) General tectonic context of Crete in the Aegean Sea. (c) Cross-section through western Crete showing the distribution of metamorphic rocks and their various *P* and *T* paths (Jolivet et al., 1998).

to low-medium grade of metamophoses of PQU from Eastern Crete to Western Crete. The latter is associated with a decreasing stress trending and more effective recovery and recrystallization from Eastern to Western Crete. Specifically, it was determined an age of 145-414Ma of Eastern Crete metamorphic PQU, while at Western Crete an age of 17-22Ma was revealed. The P-T conditions that were estimated were 300±50 ^{o}C, 0.8GPa (sudoite and Fe-Mg-carpholite in eastern Crete points to a minimum of 0.7 GPa conditions in order to be formed) and 400±50 ^{o}C, 1.0GPa (determined by the presence of aragonite in marbles and the assemblage omphacite-quartz-low albite in metavolcanites), respectively for Eastern and Western Crete. The same authors (Brix et al., 2002) explain the ±50^{o}C as a result of the time at near peak temperatures of 4±2 Ma during Oligo/Miocene metamorphism of the PQ tectonic evolution (Thomson

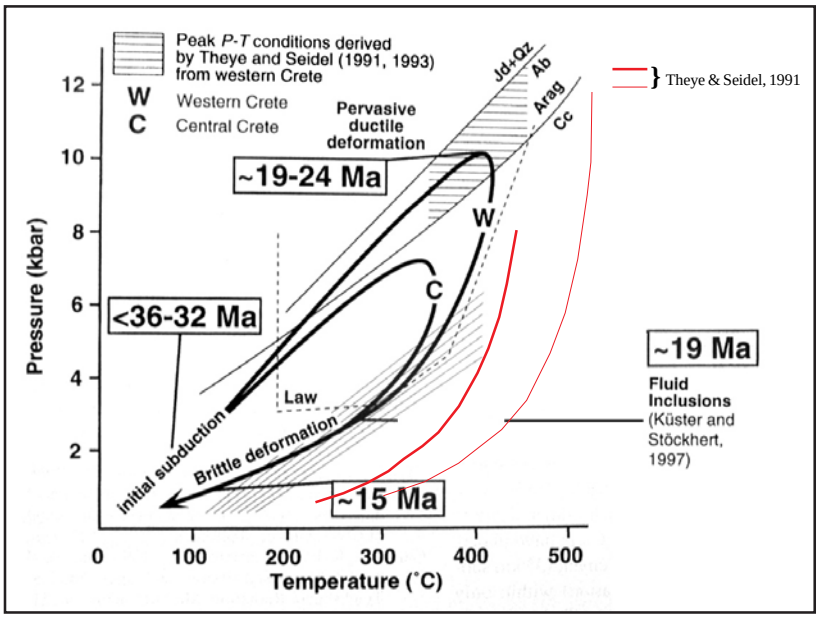

Figure 20: Fault breccias close to contact of Jurassic limestones of Tripolis.

et al., 1999). However, it should be note that the classification of the Permian rocks as PQU at Eastern Crete is suspect and questionable according to disagreement the lower age of zircon dating than the stratigraphic age of fossils.

In detail, Thomson et al. (1999) using fission-track dating, he estimates the metamorphism of PQU that took place in Western Crete between 24-19Ma, and rapid exhumation to <10km and <300°C at a minimum rate of 4km/m.y. and completed before 19Ma. The determinations of the above references indicate a pattern of migration of metamorphism and faster exhumation from Eastern Crete to Peloponnesus through Western Crete and Kythera Island.

The base of the Tripolis unit nappe probably did not experience more than 4–5 kbar and thus a gap of at least 10 kbar exists across the thrust between unmetamorphosed and metamorphic PQU. Rocks from the best preserved HP units do not show replacement of carpholite by chloritoid and have well preserved aragonite and lawsonite. While at Eastern Crete formation of chloritoid in metapelites is not observed (Brix et al., 2002). The proposed P–T path of Crete from Jolivet et al. (1998)

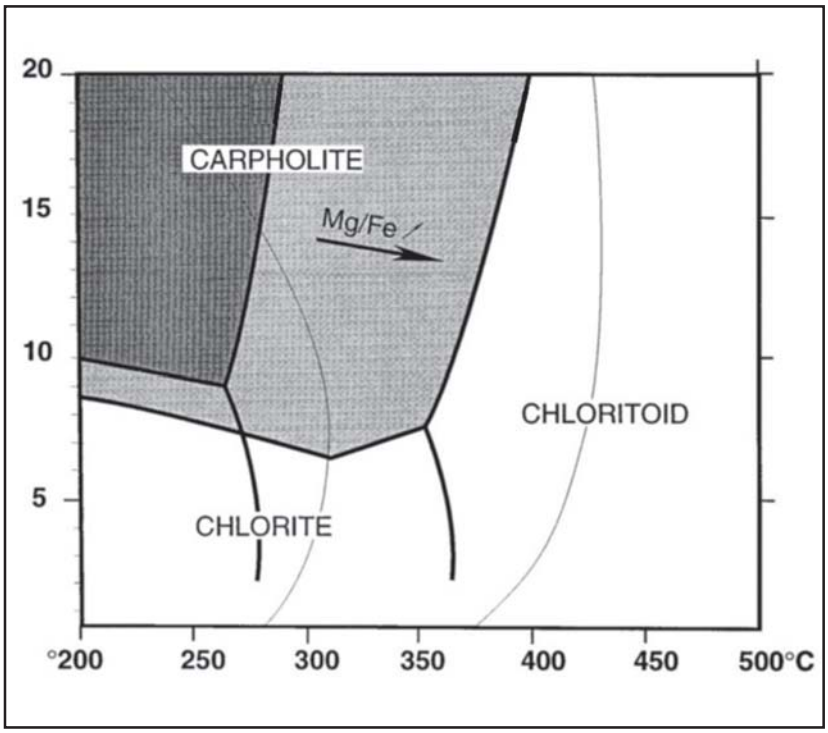

Figure 21: Simplified grid showing the displacement of reactions involving Fe-Mg carpholite with the variation of the Mg/Fe ratio (from Jolivet et al., 1998).

involves significant cooling during early decompression. Rocks situated deeper in the nappe show partial replacement of carpholite by chloritoid and a complete destabilization of aragonite implying higher temperature (fig. 21). The calculated P–T path involves an early isothermal decompression. Most of the nappe pile was exhumed quickly, while enough to maintain a constant temperature, without exchanging heat with neighbouring units, and the uppermost part was further cooled by the upper plate.

Characteristics of Detachment fault

After a brief comparison between two examples of detachment faults of Jolivet et al (1998), they concluded to the suggestion that kinematic boundary conditions may contribute to the geometry of detachments and especially control the polarity of extension, either toward the external or internal zones. The extensional domain present in the back-arc basin north of Crete is absent in the central Alps which are more characterized by large crustal-scale thrusts and backthrusts. Extension in Crete and

the Aegean Sea is a consequence of the retreat of the subducting oceanic lithosphere (Le Pichon, 1981) since the Oligocene or the Late Eocene, while in the central Alps underthrusting of the European continental crust has constructed a thick accretionary complex that collapses toward the external zones. According to Jolivet et al. (1998), an overall contractional context leads to "forward detachments", while the extensional context and migration of the subduction one leads to backward detachments.

The extensional domain present in the back-arc basin north of Crete and the Aegean Sea is a consequence of the retreat of the subducting oceanic lithosphere since the Oligocene or the Late Eocene. In contrast, similar collision tectonic setting like in the central Alps, where underthrusting of the European continental crust has constructed a thick accretionary complex that collapses toward the external zones. Considering the above indicated determination of the backward detachment from Jolivet et al., (1998), the detachment fault that occurs in Kythera Island extensional context could be characterized as backward detachment, too.

Crustal thickening, by imbrication of thrust slices, was active in the central Aegean Cycladic region, in the Eocene (Bonneau, 1982), while Kythera Island appears to be active, at least, up to Late Miocene. The latter evidence derives from the Late Miocene or Pliocene angular unconformity, where Late Miocene or Pliocene sediments lie on the folded imbricated Cretaceous limestones of Pindos, and appears at the outcrop of Likodimos beach area. The forenamed alleged determination of crustal thickening is in aggrement with the assumption of Duermeijer, (1998), that crustal thickening was active in the most external zones (Crete) until some time during the (late) Middle Miocene. The extension in the Aegean region occured shortly in Middle (Late) Miocene (Bonneau, 1982), after a crustal thickening episode which culminated in the

Late Eocene (Blake et al., 1981; Bonneau and Kienast, 1982). In addition, according to Jolivet 1998, metamorphic nappes of Crete Island are included in the external tectono-metamorphic signature of large-scale extensional detachments in high-pressure belts of the South Aegean arc. Futhermore, we could include that Kythera backward detachment fault is a result of the same, indicated above tectono-metamorphic signature of western Crete , and intensive post or syn-orogenic block-faulting of horsts and grabens mosaic.

Analyses of numerous slickenside lineations, stretching lineations, shear bands, symmetric and asymmetric structures have enabled us to reconstruct the orientations of shear sense kinematics. The methods used have already been presented and described in detail by (...). Finally, all the kinematic indicators were plotted in a GIS map in order to correlate the shear sense versus the mapped detachment fault.

Scope of the investigations

The aim of this research is to get information about kinematics of the detachment fault and the tectonic setting of the exposed PQU at the southwestern part of the Hellenic Arc.

The following problems and questions are addressed:

To what extent is the tectonic evolution of the island of Kythera recorded in the metamorphic occurrences as well as in the related limestones to detachment fault.

Is their formation related to a period of compressional tectonics or to an extensional stage leading to the exhumation of the HP-LT metamorphic rocks?

What is the possible protolith of the PQU before its metamorphism? Is the mylonite a fault rock product derived of PQU?

In what grade and scale has the deformation and shear affect the geological formations in Kythera Island?

How satellite imagery and elevation data could be useful to interpret geological features of shear sense kinematics?

Could the inferred antiform that comprise the MMC of Kythera Island be confirmed by satellite imagery?

During the field studies detailed geological mapping and sampling was carried out. The mapping took place on a GIS (ARCGIS9) platform associated with GPS and elevation data. The elevation data were derived from topographical contour lines of 1:5.000 scale as well as from SRTM (Shuttle Radar Terrain model) of 1 arc resolution. The latter data were combined with image interpretation of Landsat 7 ETM imagery. The satellite images were orthorectified and carried out from an image pro-

cessing software, such of ERMAPPER for atmospheric correction and image enhancement. The results of the field observations, structural studies and interpreted shear sense indicators from several road-cut locations across the detachment are pictured in the geological map in a variety of thematic maps. In addition, comparative studies were carried out, using Landsat imagery and field data in order to prove, whether infiltration of water match the direction of lineations and the inferred broad antiform of the exposed PQU.

FIELD MAPPING ON NORTH PART OF KYTHERA ISLAND

Field observations and references of mapped lithological units on the mapped area of Kythera Island.

PHYLLITES - QUARTZITES UNIT (PQU)

Carboniferous to Triassic metasedimentary rocks beneath the Tripolis unit of the Peloponnesus are known as the Phyllite Series or the Phyllite-Quartzite unit. In Peloponnesus area, Thiebault & Triboulet (1984) and Bassias & Triboulet (1994) distinguished three nappes in the Phyllite Series overlying the parautochthonous Ionian zone Plattenkalk series.

The lower nappe ("Princinpal Crystalline System" of Ktenas 1924) consists of metasedimentary rocks with a protolith of Paleozoic to Triassic rocks and probably Oligocene Ionian metaflysch. It experienced blueschist metamorphism and the peak metamorphic conditions were estimated as 400^{o}C and 10 kbar (Theye 1988, Bassias & Triboulet 1994). The middle nappe (Faros-Lakkomata nappe of Thiebault 1982) consists of phyllite, metaconglomerate, quartzites and limestone/marble, dated as Carboniferous, Permian and Triassic, together with minor metavolcanic rocks. The upper nappe (Tyros nappe of Thiebault 1982) lacks penetrative deformation. It comprises shales, pyroclastic and volcanic rocks: the term "Tyros Beds" has been widely applied to this unit. The rocks of both the middle and upper nappes are locally conformably overlain by Triassic limestone, that pass up into the Tripolitsa limestone (Thiebault 1982).

At Kythera area, the PQU appears at the northern area of the island, below the detachment fault. Renz (1955) assumes that the metamorphic rocks of Kythera Island are part of the bedrock of Central Peloponnesus and Crete. Christodoulou (1967)

refers that these rocks include also eruptive rocks, mainly volcanic rocks. At the geological map of Petrochilos (1966) has been noted a diabase appearance inside to schists of Karavas and Gerakari area, while Theodoropoulos (1973) reports those forenamed rocks as quartz with rich of iron oxides. Also, Theodoropoulos (1973) refers different types of metamorphic shales, such as shales rich of quartz, sericite, clay and iron oxides, or white micas rich of actinolite, muscovite, quartz and iron oxides, or white micas rich of sericite, quartz oxides and iron oxides. Theodoropoulos (1975) certifies the presence of an altered peridotite, which is consisted of serpentine and magnetite at the Agia Pelagia area. The same author assumes a neopalaezoic age of the metamorphic rocks. This assumption comes from the correlation of the Kythera metamorphic rocks with these of Peloponnesus area. Also, he thinks, that these were made after an epizone metamorphic phase and sometimes mesozone metamorphic phase.

According to Leonhard (1899), mica schists comprise the oldest lithologic unit of Kythera Island. Northeastern of Potamos area, mica schists appear with big K-Feldspars and small particles of quartz, which show an eye schema. Sericited phyllites and quartz schists occur at the Gerakari area. Moschovite-mica shales of black color appear that was caused by carbon mixing at the northern area of the Dedianika, while lens of marbles occur in the schistosity of the those schists.

TRIPOLIS UNIT

The Tripoli's carbonate sediments appear at the two big mountain chain of the island. The first is at the northestern part and the second at the western part of the island. The first starts from the Agia Pelagia area in a southern direction to the south side of the island (Avlemonas area). The second covers the western part of the island

and consists of the Mermigari, Mirtidia, Agia Elesa and Castle of Choras mountains.

The Tripolis unit lies disconformably on the crystalline bedrock. It is devided by two parts. The lower part consists of open-color dolomites, which occurs at the northern areas of the island, while the upper part consists of fine grained limestones in black color, because of Bitumen's presence (Leonhard, 1899).

Renz (1940, 1955) is accordant to the unconformity of Tripoli's Limestones on top of the crystalline bedrock. Furthermore, he supports the idea that they belong to the sedimentary succession of the main basement of Peloponessus.

At the geological map of Petrochilos (1966, IGME ed. Scale 1:50.000) reports the total column as follows: a.Triassic-Mid. Jurassic limestones and dolomites without fossils, b.Kimmeridian (Late Jurassic) limestones with Cladocoropsis, c.Cretaceous limestones with roudists, Miliolidae, Textulariidae,d.Eocene limestones with Nummulites, Alveolines.

According to Theodoropoulos (1973) the lower parts of the Tripoli's stratigraphic column appear between the areas Agia Pelagia and Plataia Ammos. Furthermore, Danamos (1992) observed that Tripoli's early's Jurassic limestones appear to have overthrust the Arna unit. These limestones are very pure of fossils. Also volcanoclastic sediments (Tyros formation) appear as the lower part of Tripoli unit, at the southwestern part of the island which are the base of the stratigraphic column of Tripoli unit. The forenamed clastic sediments as well as the flysch consist of clastic sediments. The rest of the stratigraphic column of Tripoli unit is comprised of limestones of neritic setting.

The presence of Discorbidae fossil, which is a good index of showing a shallow sea-water environment, and other lamellibranchia in the Tripoli's early Paleocene

limestones define an organic activity in shallow depths of lagoonaire setting (Danamos, 1992). The same author assumed that the carbonate phases of the Tripoli unit are the same with these of Peloponnesus. The same author accepted the dating which was made by Thiebault (1982) and Fleury (1980). The results were upper Jurassic, early Cretaceous by Thiebault (1982) and Palaocene, Eocene by Fleury (1980).

At Kythera Island, three basic lithological series represent the stratigraphic column of Tripolis unit. A clastic series of sediments, named as "Tyros Beds", the carbonate platform of Upper Jurassic-Upper Eocene dolomites and the Tripolis Flysch of psammite and pelitic sediments. It has to be noted that the succession from "Tyros Beds" to the Jurassic carbonate series of Tripolis has not found in Kythera (Danamos 1992), but only in Peloponnesus (named as "Tyros Beds") and at the central-eastern area of Crete Island (named as "Ravdoucha"). At the mapped area and specially close to the main detachment fault of Kythera Island, only the two upper series of Tripolis unit occur.

The "Tyros Beds" occur at Myrtidia area (western area of Kythera Island) and appear as very low grade of metamorphic rocks. The latter is supported from the observation of chlorite, sericite, quartz (Danamos, 1992). The latter dating implies that the metamorphose was alpine. Thiebault (1982) describes the very low grade metamorphose as a result of Prehnite - Pumpellyite metamorphic face, while he infers this formation as the basement of Tripolis unit.

Jurassic – Cretaceous of Tripolis Unit

The early Cretaceous stratigraphic layers appear (Aptian-Alvian) at the Agia Pelagia area, which are the upper stratigraphic horizons of the limestones of Tripolis

unit. The forenamed limestones comprises of dolomitic and recrystallized limestones, which contain Salpingoporella dinarica radoicic and Praechrysalidina infracretacea luperto-sinni (Danamos, 1992). The lower stratigraphic horizons of the Tripoli limestones appear at the area of Plataia Ammos, where they consists of black dolomitic or recrystalized limestones and dolomites, which contain lamellibranchia fragments (Clypeina jyrassica FAVRE). The estimation of the limestone horizon's thickness of both of the forenamed locations of Tripoli limestones was impossible. Mainly, they consist of isolated carbonated masses, and not a sedimentary preserved succession. The abundance of the algae in the Jurassic-Cretaceous limestones of Tripoli unit denotes the shallow sea depth of the platform where the sun radiation supply adequate conditions for the algae growth.

Dercourt (1964) describe a series of Tripoli unit upper Jurassic-early Cretaceous limestones rich of fine grained limestones of 600m thickness, which contain trematophores and algae, at the area of Feneou (Crete). Dercourt (1964) believed that this dense presence of algae characterizes the stable shallow depth of the sea at all the duration of sedimentation as well as the active subsidence of Tripoli platform.

Zager (1972) notes the presence of algae Dasycladaceae in upper Jurassic limestones of Tripoli unit, while early Cretaceous dolomites are above the forenamed upper Jurassic laminated limestones.

Karakitsios (1979) reports the presence of upper Jurassic-early Cretaceous limestones with Clypeina jurassica, Kurnubia palastiniensis and coproliths at the North-Central Crete as well as the early Cretaceous with Pseudotextulariella sephontainei. The same author reports the presence of carbonated breccia at the upper Jurassic, Alvian, upper Cretaceous and Paleocene limestone horizons of Tripoli unit. Further

more he supports the idea that the presence of the forenamed breccia was caused by independently tectonic episodes, that took place on different places on the Triploli platform. In addition, he assumes that these tectonic episodes are related to palaoalpine orogen.

Many authors (Fleury & Bernier, 1980; Karotsieris, 1981; Thiebault, 1982; Alexopoulos, 1990) supports the idea that the platform of Tripoli unit started to become shallower depth (lagoonaire) after the early Paleocene . The platform started to raise, at the Paleocene, while it returns to a subtidal setting with some exceptions that appear in Peloponnesus. It is obviously that the Tripoli platform started to sink and accept its flysch (Eocene) and the deposition of the first pelites.

Fitrolakis (1980) notes that the buoyancy of the Tripoli platform created a paleosurface where after the tectonic impact, a lot of bauxitogenesis phenomena derived. Danamos (1992) could not find any appearance of these phenomena in the early Eocene Tripoli limestone horizons and neither the current research found.

Danamos (1992) believes that the carbonated shallow series, which appear in Kythera island, are part of Tripoli unit and not of Gavrovo unit.. The sedimentary phases of Tripoli unit in Kythera area appear dark-colored and less rich of fossils than these of Gavrovo. Fleury (1980) observed the appearance of the first pelites of Tripoli flysch to be present in the upper Eocene, in contrast to Gavrovo where the beginning of its flysch had been placed at the early oligocene.

Flysch of Tripolis unit (Upper Eocene)

The Eocene appears at the north side of the mapping area of the Kythera Island at the cape Spathi, (also at the center of the island – Skliri – and at the south side of the Kythera Island, according to Danamos, 1992). The Eocene limestones of Tripoli unit

are the last carbonate layer before the deposition of its flysch.

In Kythera island, Leonhard (1899) describes the appearance of the Tripoli's flysch at the southeastern area of Kythera island, where it succeeds the Eocene limestones. Theodoropoulos (1973) says that Tripoli's flysch in Kythera island appears in small range areas such as at the southern area of the mapped detachment fault at the north part of the Kythera Island, near at Araioi and at the street Aroniadika-Dokana. Moreover, Danamos (1992) observed that the appearance of Tripoli's flysch occurs more often at the southern place of Kythera island (Chora, Kseroniamata, Lourantianika areas) and lesser at the center part of the island (Dokana-Araioi area), as well as at the northern part of the island (Aroniadiadika area).

The thickness of the Tripoli's flysch fluxuates. It appears to vary in different places in Peloponnesus and in Crete for many researchers from less of 200m to 1000m (Mariolakos 1975, Lekkas 1978, Katsikatsos 1980, Danamos 1992).

The transition of Eocene limestones of Tripolis to its flysch appears as tectonic contact at most areas of Kythera Island. However, at Aroniadika area there is a succession from the Eocene limestones of Tripolis to the Upper Eocene Flysch of Tripolis (Danamos, 1992; Theodoropoulos, 1973).

PINDOS UNIT

The unit of Pindos comprises a large tectonic nappe, which spreads in Continental Greece, Peloponnesus, Crete and Dodecanese islands (Rhodes), (Cayeux, 1903; Negris, 1906; Ktenas, 1908; Philippson, 1930; Blumenthal, 1933; Renz, 1940; 1955; Aubouin, 1959; Celet, 1962; Dercourt, 1964).

The Pindos Group is defined as all the sedimentary successions of the Pindos unit

within the north-western Peloponnesus area and is divided into five formations, full details of which are given by Degnan (1992), because of the scope of our research, they were not described here. The sedimentary successions of Pindos unit comprise deep-water carbonate, siliciclastic and siliceous rocks, ranging in age from Late Triassic to Eocene. The Pindos Group is deformed into a series of imbricate thrust and isoclinal folded sheets that were finally emplaced over the Gavrovo-Tripolitza carbonate platform to the west in early Tertiary time (Degnan & Robertson 1997).

According to the last forenamed authors, these rocks accumulated along the western margin of a small Neotethyan oceanic basin (i.e. Pindos ocean), separating the continental blocks of Adria (Apulia) and Pelagonia. The oldest sediments comprise disrupted siliciclastic turbidites, largely derived from a metamorphic source to the west and deposited on young oceanic basement. From the Late Triassic to latest Maastrichtian (Late Cretaceous), variable thicknesses of hemipelagic carbonate and proximal carbonate debris flows accumulated in westerly areas, while mainly hemipelagic carbonate and calciturbidite were deposited further east. This pattern was interrupted by an extended period of siliceous, radiolarian-dominated sedimentation during the Aalenian to Tithonian (Middle-Late Jurassic). From the composition of dominantly carbonate deposition, supplied from the Gavrovo-Tripolitza carbonate platform to the west, ocean resulted in deep-sea sedimentary lithologies being detached from their oceanic igneous basement as an accretionary prism and emplaced westwards onto the adjacent carbonate platform, ending up as a series of thin-skinned thrust sheets.

The lithological unit of Pindos is represented by all its stratigraphic horizons according to Fleury (1980). The palaeogeographic area of Pindos was mainly a deep

sedimentation setting for its total pre-orogenetic history. Althought, there are some benthic foraminifera fossils, which they are the only index fossils in some sedimentary layers (Danamos, 1992). The source of the allocthonous fossils is the vicinal shallow depth platforms through the turbidites, where in our situation, Tripolis unit was the closest.

In Kythera Island, it covers the 1/3 of the Island area and it occurs among the two mountain chain of Tripoli unit. Generally, the Pindos unit occurs with the Triassic clastic sediments, the Jurassic cherts, the upper cretaceous squamiform limestones and the Paleocene Flysch. These occur also in the current research mapped area , that is close, below or above the main detachement fault.

Petrochilos (1966) note that the sedimentary succession of Pindos unit follows as: a.Upper Jurassic green, redish schist-irestones, b.Thin-breccia with irestone and limestone fragments and sometimes limestone segments, c.Cretaceous thin-bedded limestones and marly limestones.

Theodoropoulos (1973) assumes that the redish limestones of cenomanian are the oldest sediments of Pindos unit on the island. According to the same author the stratigraphy of Pindos follows as: a.Cenomanian redish limestones, b.Radiolarites, c.Redish pelites, d.Marly flysch, e.Maastrichtian limestones. In contrast to Tsoflias (1977), he reports the occurance of Triassic sediments at the area of Perati river, close to Logothetianika village (center part of Kythera Island).

Triassic clastic sediments of Pindos unit

Danamos (1992) supports the idea that the clastic Triassic of Pindos unit which occur on Kythera island is similar with these of Peloponnesus. Furthermore, he classified the psammite-pelitic clastic sediments to Triassic (Carnian) as “clastic Triassic”.

A number of lines of evidence indicate that the sedimentary basin of Pindos was of oceanic character (Smith et al., 1975; 1979; Jones, 1990; Robertson et al., 1991; Degnan, 1992; Robertson, 1994).Pindos unit occur at Peloponnesus and Crete Island area, but in different stratigraphic thicknesses and nomeclature. Ethia series is the Pindos unit that occurs at Crete Island. Although the similarities between Crete and Kythera, the presence of diabase-dolerites of Ethias series (Pindos unit) was not observed in any characteristic of Pindos unit on Kythera Island.

Clastic psamite and pelitic sediments were observed at the north area of Likodimos beach (west side of the map), as well as, at Agia Pelagia area, where it was difficult at both locations to date this formation. However, Danamos (1992), Danamos & Zambetaki-Lekka (1989) and Tsoflias (1977) describe the clastic sediment mapped area at North area of Likodimos beach as Clastic Triassic sediments of Pindos. They describe the clastic triassic sediments of Pindos as psammitic and pelitic sediments. In addition, at Southwestern Peloponnesus (Ithomi), there are some occurrences where it has been noticed that the clastic Triassic of Pindos was tectonically wedge between the Tripoli unit and Pindos unit (Negris, 1908; Ktenas, 1908).

From a first approximation, the forenamed formation seems as a flysch. It consists of psammites, pelites and some layers of limestones, conodonts and halobies (Danamos & Zampetaki-Lekka, 1989). It occurs tectonically between the Upper Jurassic Cherts of Pindos and the metamorphic nappe. Because of its succession to the upper Jurassic cherts, any hypothesis of defining this formation as a flysch is discarded. The thickness was difficult to be observed, because of its location, while Danamos (1992) assumes a thickness of 50m approximately .

In addition, Danamos & Zambetaki-Lekka (1989) studied the superposed lime-

stones of Tripolis, which lie against the clastic triassic of Pindos at the mapped area of Likodimou, and according to capture fossils was dated as Paleocene Limestone of Tripolis. The latter limestones are tectonic wedge between the below metamorphic nappe and the above Cretaceous limestones of Pindos.

Upper Jurassic cherts of Pindos

The black intermittent cherts that occur at the Jurassic cherts layers of Pindos unit, as suggested by Fleury (1980), appears to represent a regionally significant time marker of increased siliceous productivity. The black colour could reflect an originally relatively high organic carbon content, as indicated by studies elsewhere in the Pindos Unit (Neumann et al., 1996). During deposition of the member, the proportion of terrigenous sediment entering the Pindos basin increased dramatically, eventually swamping carbonate deposition. Assuming the black chert is a time horizon, terrigenous sediment was not deposited coevally.

Pindos Flysch

The Pindos Flysch formation is dominanted by alternating relatively pale coloured sandstones and siltstones, with mudstone and subordinate pink marls, which is accordant to the observations of Degnan & Robertson, (1998). The Flysch Pindos formation occurs in Kythera Island, implying that it had taken place close to the subduction zone, at the trench at that time of orogenesis. The latter was further strengthen by the correspondance of some characteristics of turbidites that were observed in between the Pindos flysch formation. Furthermore, the nature of the clastic material which comprises the flysch (quartz, feldspars) denotes its continental origin.

Pindos unit in Kythera occurs intensely thrust imbricated, however at the eastern part of our mapped area (Agia Pelagia), the observation of the passages between the

formations was difficult. Basically, the Pindos unit is deformed into a series of imbricate thrust sheets that were finally emplaced over the Tripoli unit carbonate platform. Structural mapping show that their emplacement was achieved by piggy-back thrusting.

The dating of the Pindos unit's sediments was based on the fossils dating techniques of J.J. Fleyry (1980), while the upper cretaceous limestones of Pindos unit was based on the zonation method dating of Globotruncana which was proposed by Sigal (1977) and Fleury (1980). Petrochilos (1966) denotes at his map (IGME ed. map) that the flysch formations that occur on the Kythera island belong to Tripoli unit, while Christodoulou (1967) reports that belongs to either Pindos or Tripoli unit. Moreover, Theodoropoulos (1973), observed that the Flysch of Pindos, that consists of altered psammites, pelites and marls, is clarified enough to be distinguished from the Flysch of Tripoli.

Detailed structural characteristics and field mapping

Introduction

This map (fig. 22) shows the geology of the northern part of Kythera Island, just a few miles south-east of Peloponnesus and north-west of Crete Island, and including part of the south-western part of the South Aegean Arc. A sedimentary series of Jurassic – Quaternary age lies on a basement of Palaezoic rocks (slates, phyllites, quartzites, schists, gneisses). The latter reveal evidence of folding, extension and shear events. The oldest rocks are of Carboniferous-early Triassic Phyllite-Quartzite Unit (PQU) meta-sandstones, meta-pelites and Plattenkalk (?) fine-grained, light coloured quartzites, marbles, gypsum and recrystallized limestones. They appear phyllitic structure, schistosity, crenulation cleavage, foliation, banding, mylonitization, typically develop as a result of recrystallization and high deformation of sedimentary or igneous or other unknown parent rocks during HP-LT metamorphism. They are generally composed of very fine to fine-grained minerals and can be defined by compositional banding, by a preferred planar orientation of platy or prismatic minerals, such as micas are, or elongate quartz or feldspar crystals into quartzites. The compositional banding occurs mostly at a scale of some mm to some cm, while they are discontinued by a lot of fractures. Most of the latter structures can be mapped across some meters (1-3m) to discontinuous localities that pinch out, and are able to be observed, within individual outcrops, hand specimens, or thin sections. Furthermore, the high strain environment of ductile shear zones confirmed the detachment fault presence, where the mylonitic occurrences were hosted, and appear mostly at the southeastern area of Potamos.

The mapped area is also composed of Jurassic, Cretaceous and Eocene limestones. The limestones occur on the perimeter of the metamorphic rocks outcrop. The

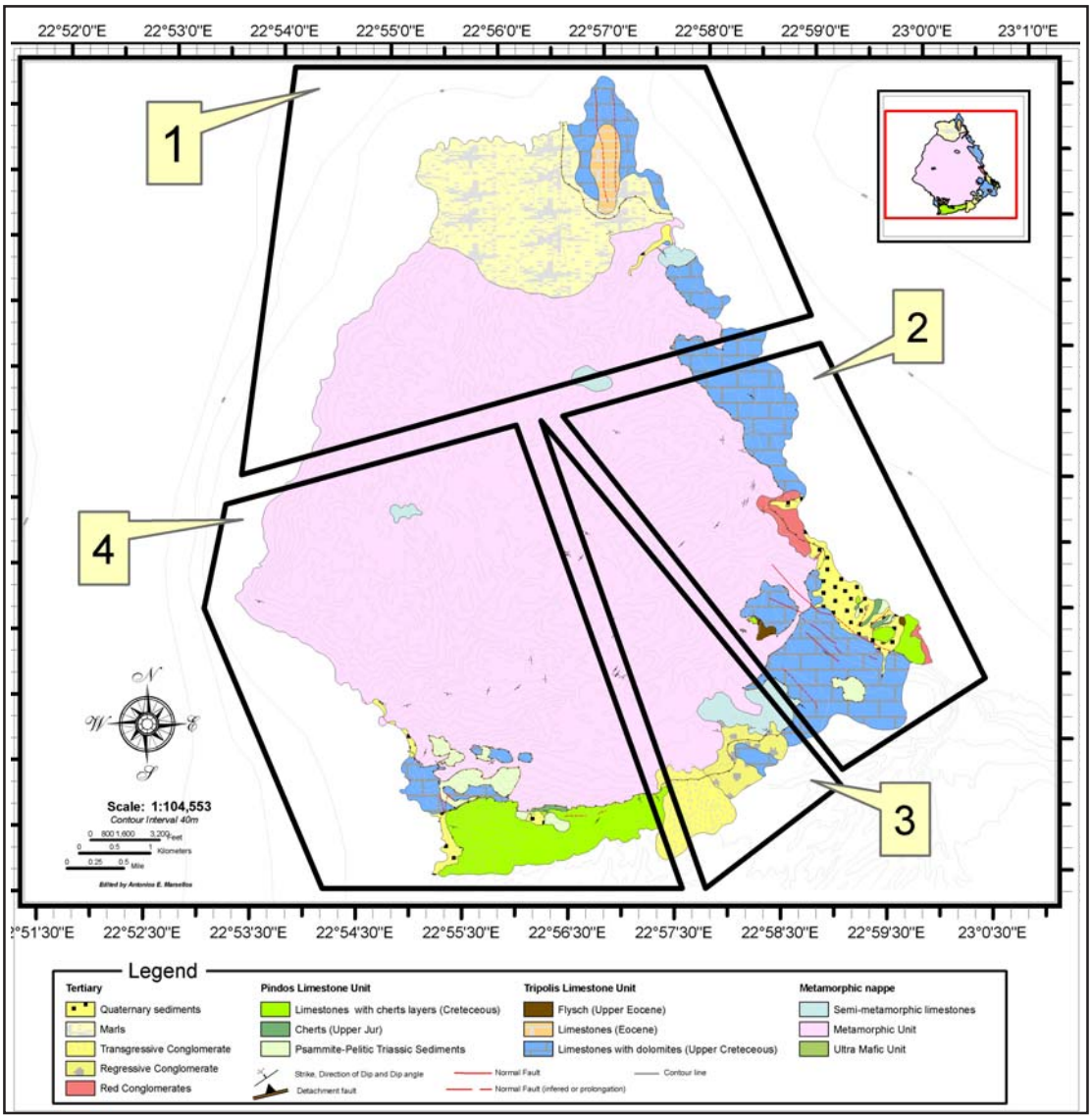

Figure 22: *Mapped area divided in 4 smaller areas, Fanari, Agia Pelagia, Potamos and Likodimou-Ligia, respectively.*

perimeter of the metamorphic and limestone occurrences comprises the detachment fault. The limestone region is of NW-SE trending normal fault scarps. The southeastern region of the map area appears with more alternating escarpments and low-level hills, which have resulted from more rapid erosion and normal faults, while the southwestern region of the map area appears steeper with less alternating escarpments and lowlying hills. Under normal faulting and a tectonic setting of uplift exhumation, it would be unusual to find thrust faults or wrench movements as these would be results of reverse or transform faults. The neogene and tertiary sediments appear mostly at

the northern and southern mapped area. These consist of quaternary and neogene sediments, marls, regressive and transgressive conglomerates.

The metamorphic nappe forms in a broad antiform of a NW-SE trending hinge trace line (Danamos, 1992). If we consider the topography of the metamorphic occurence, then we could broad estimate that the latter antiform has a gently dipping southeast limb and a steep northwest limb. A set of folds, distributed on both the metamorphic and limestone mapped areas, was observed and derives the presence of a fold belt constitution, which is a common feature of orogenic zones. Long normal faults appear mostly at the southern area of both of the antiform's limbs, where is closer to detachment fault. In the mapped area, it was observed that the normal faulting is mostly of NW-SE and NE-SW trending. There is no wrench movement on the faults as it does not appear of any kind of a linear displacement at the outcrops. In opposite, a graben model is more applicable to name the tectono-stratigraphic evolution of the limestone units' location as Danamos &Papanikolaou (1990) have already proposed. This is the result of the disposition that caused by the normal faults of the rapid uplift, which intensely occur at the near areas of the island's coasts. Furthermore, the area between the faults appears as a fault-trough. The latter observation is strengthened by the correspondance of the above Pindos unit (overthrusted unit of Tripolis limestone unit) at lower elevation locations of 100-200m than of the below 400-500m of Tripoli's unit limestones.

The thicknesses of the limestones and the metamorphic nappe are very difficult to be estimated either from outcrops or either from stratum contours. This derives from the observation of the Cretaceous limestones of Tripoli's thickness, which alters from the occurrence of more than of 150m at Kaki Lagada to 15m at Agia Pelagia at

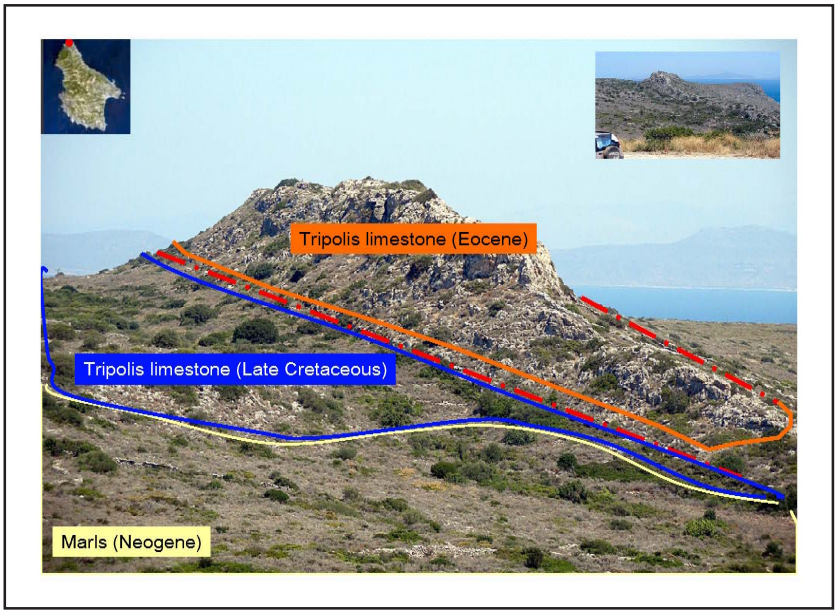

Figure 23: Cretaceous to Eocene succession of Tripolis limestones.

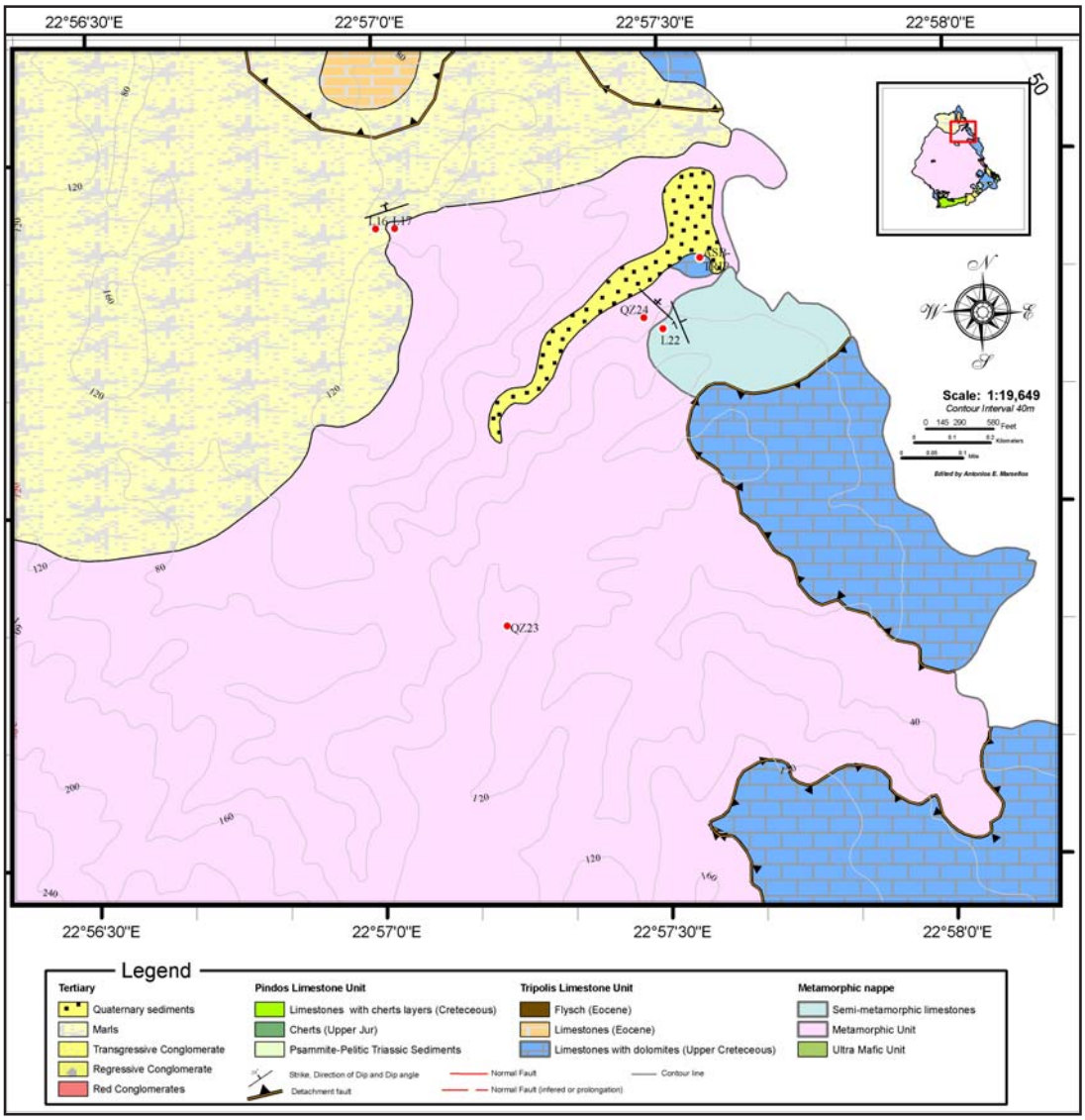

Figure 24: The Northeastern mapped area of the detachment fault, close are Karavas, Plataia ammos villages.

Figure 25*:* Fault breccia texture close to contact of Jurassic limestones of Tripolis.

a NW-SE trending. The latter distance between these two locations is no more than 2km. Broadly estimating, we could calculate that the detachment fault dips at an angle of approximately more than 4.3 degrees, [tan(150/2000) = 4.3 degrees]. The latter implies a very broad estimation of the detachment fault as a low-angle normal fault.

A detailed description of the 1,2,3,4 (fig. 22) mapped locations of the North part of Kythera Island are explained below.

1. Fanari area (northeastern area of the map)

No bauxite horizons in Kythera Island

The Cretaceous limestone rocks of Tripolis are covered by Eocene strata at the north (fig. 23,24). Two N-S trending faults appear at the Eocene limestones of Tripoli and die out in the older limestone of Tripolis (upper Cretaceous). It has been noted from a lot of authors that there are bauxites in between the Eocene limestone layers of Tripolis unit, in Peloponnesus (Kiskyras, 1958; Dercourt, 1964; Tataris, 1964; Tataris&Maragoudakis, 1965; Karotsieris, 1978,1981; Bernier&Fleury, 1980; Fleury,

1980; Thiebault, 1982; Bassias, 1984) or in Crete (Fytrolakis, 1980). In Kythera Island, they were not observed in any studied outcrop in Kythera Island, as well as, it was observed that there was no flysch deposition on top of the Eocene limestones of Tripolis. In addition, Danamos (1992) mention that there is no bauxites in an outcrop of the South area of Kythera Island, where early Eocene limestones of Tripolis occur. The absence of bauxites could be explained as a result of a slow exhumation of the metamorphic occurrences at the Eocene, while there was a very rapid uplift at the Eocene of Peloponnesus area (Taygetos). Consequently, the deposition of Eocene limestone of Tripolis at Kythera, took place far away from any orogenic episode, in comparison of Peloponnesus occurrences of Tripolis Eocene limestones, which is still under doubt. From the other hand, the absence of the upper Eocene flysch of Tripolis at the top of the Eocene limestones of Tripolis at fanari area could be explained as a consequence of high erosion and displacement caused by graben forces. However, the latter Tripolis limestones that occur at Peloponnesus, appear with bauxite formations among the Eocene limestone layers, as a result of the rapid uplift of the Eocene limestones of Tripolis at Peloponnesus area (Mariolakos, I., 1975).

Fault Breccia

The neogene sediments cover the detachment fault (fig. 23,24) and comprise the neogene disconformity. The latter consists of white to yellowish marls and sands but very compacted. In some places, specifically close to contact of Cretaceous limestones of Tripolis, come into sight of sandy limestones (?). Close to the contact of Jurassic limestones of Tripolis and neogene sediments, fault breccias were found (fig. 25). These consist of angular fragments of limestones in a finer pink to reddish grained matrix of crushed material. The field observation determine that the cataclastic rocks are marked

by unsorted clasts without any preferred orientation. The presence of fault rocks close to this area may indicate that the detachment fault is indeed below the fault breccias, and furthermore closer to the contact between the deposition of Neogene marls and Jurassic limestones of Tripolis than closer to the contact between the metamorphic occurrences and the neogene disconformity. For the above reason the inferred detachment fault was depicted at the map, closer to the contact of Neogene marls and Cretaceous limestones of Tripolis. However, it should be note that this is still questionable.

Plataia ammos- Tension gashes of vertical and horizontal indicate dextral shear sense - Top-to-the East displacement and possible right lateral transform fault

At the coast of Plataia Ammos, a horizontal outcrop of the Tripolis limestones unit hosts swarms of tension gashes (fig. 27a). This outcrop provides both vertical and horizontal sides for observations. It is located exactly above the detachment and some meters upward of the contact with the Metamorphic unit. En echelon vein arrays exhibit a diversity of morphological and geometric characteristics that reveal further kinematics evidence. At both horizontal and vertical sides of this outcrop appear some poorly organized veins and some that we can organize them to conjugate divergent or convergent arrays. A convergent conjugate vein array system is one in which the trends of veins converge when followed into the blocks of rock which contain the inferred principal shortening strain axis. In contrast in divergent conjugate vein array systems the trends of the veins diverge when followed into the blocks of rock which contain the inferred principal shortening strain axis (Smith, 1996).

It was noticed that the tension gashes show a gradual change in morphology from planar to sigmoidal. The Kinematics of vein openings are in agreement with the "Durney

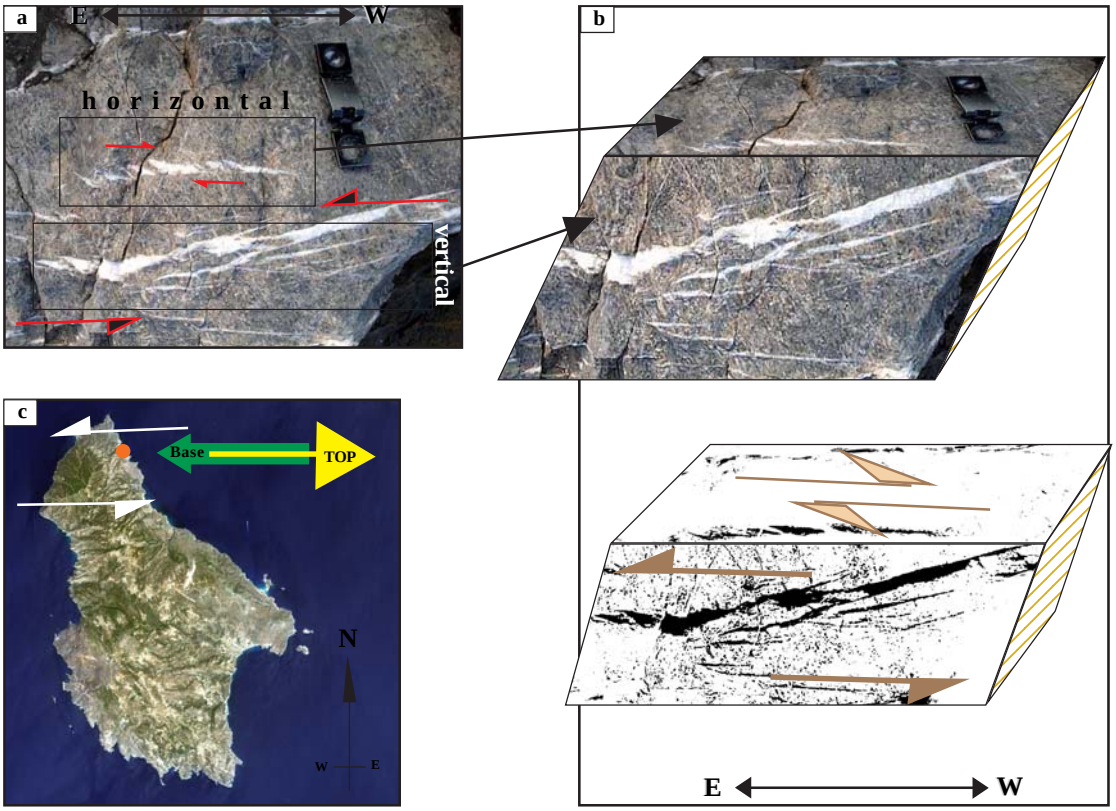

Figure 26: Three dimensional morphology of veins from a vertical and horizontal side of the same spot of the outcrop at Plataia Ammos area.

- Ramsay" model of en enchelon vein development. This model emphasizes the role of concurrent fracture propagation and shear displacement on arrays in producing sigmoidal veins. Furthermore, this process produces an increase in the size of veins as they change from straight to sigmoidal (Durney & Ramsay, 1973). On the outcrops of (fig. 27c, red rectangle of 45 degrees) , it appears that there is an offset of the sigmoidal veins. The veins are distorted by a later deformation, which was not accompanied by concurrent extensional fracturing. The en echelon break-down veins were built up due to displacement of competent and incompetent material. The latter could be explaining also as a higher contrast between these two materials. Furthermore, it reveals a right-lateral transform fault of almost E-W trending.

Vein size, vein spacing and vein position relative to the array centre line vary. This was caused as a result of different rock bridge aspect ratios which lead to the

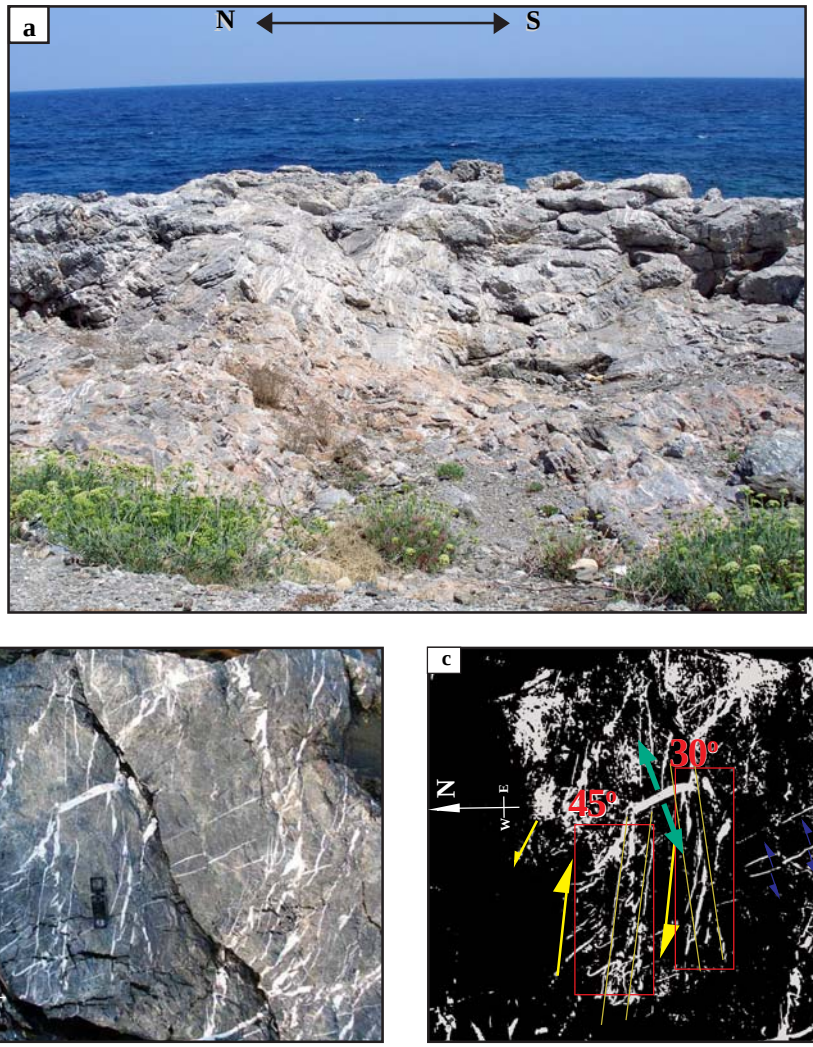

Figure 27: a. Horizontal side of the outcrop of the Tripolis limestone unit that hosts swarms of tension gashes, (b-c) one of the horizontal sides of the outcrop that hosts tension gashes which reveal a dextral shear sense, at the same location in Plataia Ammos area(a).

diversity of vein shapes observed in fig. 26a of horizontal side (Smith, 1996). The three-dimensional morphology of veins as indicated by the figure 26b, infers that the sigmoidal shape of the veins is primarily due to the rotation of bridges of rock between veins in the manner described by Nicholson & Ejiofor (1987). The latter could be also observed at the figure 27b. In detail, the vein arrays (fig. 26a, 27b, 28a) appear vein shapes grading from straight to sigmoidal and rock bridges maintaining orthogonal thickness and rotational symmetry.

The geometry of the conjugate vein arrays of figure 28a-b should be further ex-

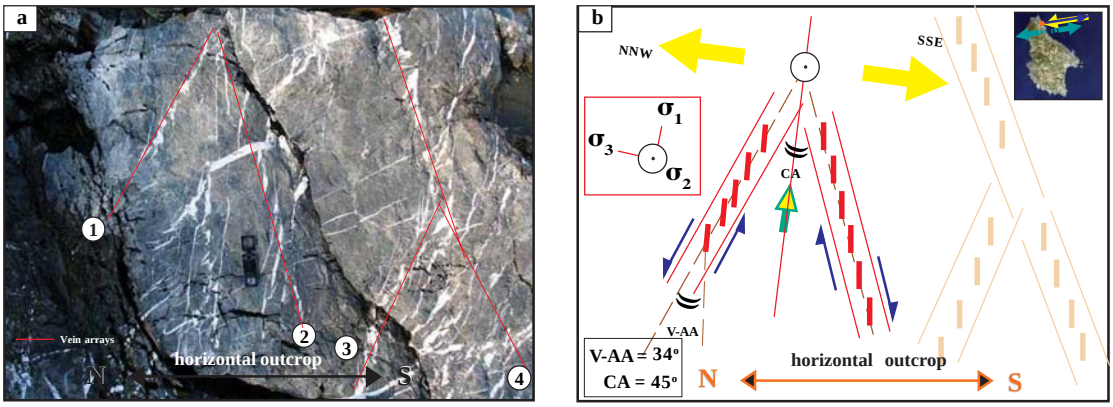

Figure 28: Horizontal side of the outcrop of Plataia Ammos area. a. The geometry of the conjugate vein arrays reveal strain and shear that were undertaken, b. The three principal axes of strain.

plained in order to understand strain and shear that were undertaken. The three principal strain axes are approximated by the two bisectors of the vein arrays and the intersection line of the arrays. The bisector lying within blocks which move toward each other is interpreted as the principal shortening direction; the bisector lying within blocks which move away from each other is interpreted as the principal extension direction, and the line of intersection of the arrays is interpreted as the intermediate strain axis.

According to Smith (1995), a significant parameter is the acute angle which veins make with their host array. In this approach, veins at 45o to the array have been attributed to extensional fracturing, veins at 15o (fig. 27c) have been attributed to synthetic shear fracturing and those in between have been ascribed to a hybrid of those fracture mechanisms (Hancock 1972; 1973; 1985; Engelder, 1987).

According to Smith (1996), the geometric continuum of conjugate vein array systems can be defined in terms of the relationship of the angle between conjugate vein arrays (conjugate angle, CA in fig. 28b) and the orientation of veins relative to their host arrays (vein-array angle, V-AA in fig. 28b). In this outcrop, according to Smith (1996) classification of conjugate vein array types, it appears as "bisector-parallel sys-

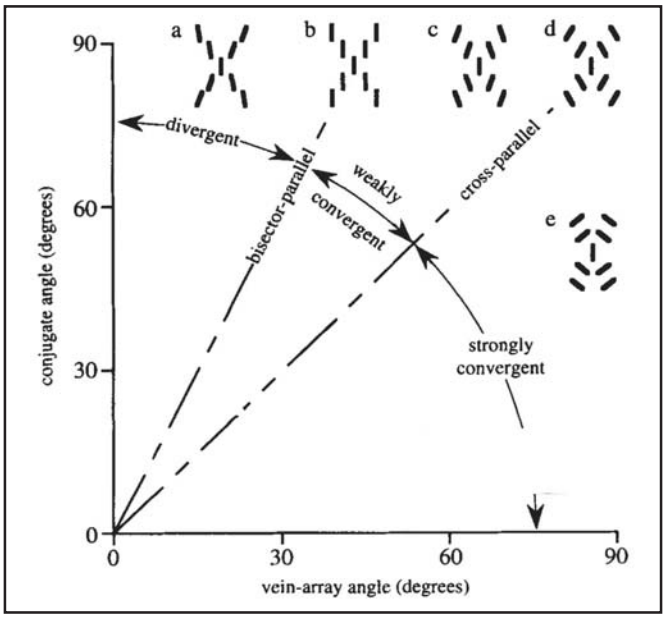

Figure 29: Classification of conjugate-angle (CA) versus vein-array angle (VAA) for conjugate vein array systems from Smith (1996).

tems", which is the boundary between convergent and divergent types (fig. 29). In addition, it has to be noted that Roering (1968) and Beach (1975) concluded that in bisector-parallel systems, veins initiated as extension fractures.

These veins are the result of brittle faulting usually accompanied by dilatation, shearing and solution associated with calcite precipitation. These parallel arrays of en enchelon calcite veins have an orientation of mostly E-W. The tales of the en enchelon veins are exposed on a horizontal surface showing an NW-SE trending, implying a dextral shear sense, while the vertical surface of the same outcrop infers a top-to-the east displacement. Finally, the combine dextral shear kinematics on both horizontal and vertical surface of the same outcrop may imply a kind of a clockwise rotation (fig. 30a-b).

In figures 28a-b, the conjugate vein arrays define a divergent conjugate vein array system, where the trends of the veins are parallel when followed into the blocks of rock which contain the inferred principal shortening strain axis (fig. 28b). Both Roering (1968) and Beach (1975) concluded that in bisector-parallel systems, veins initiated

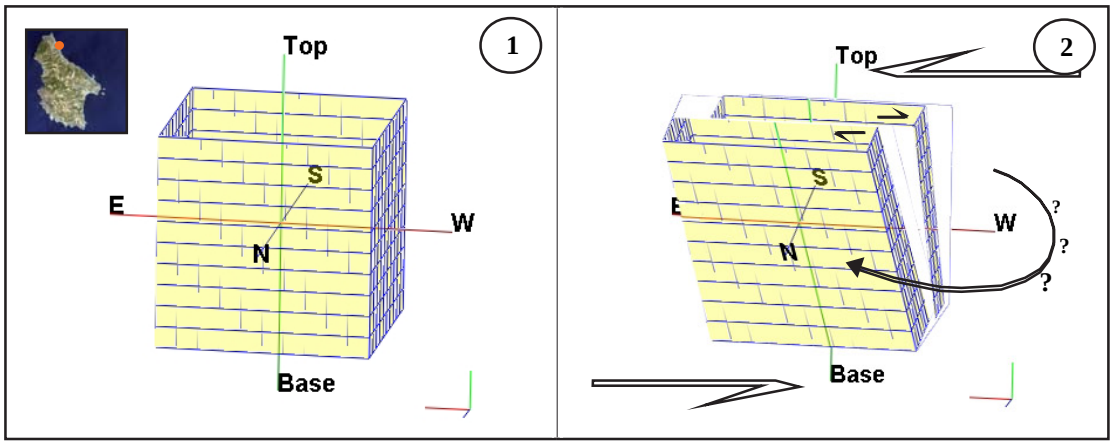

***Figure 30**:* 3D representation of shear sense kinematics at the outcrop of Plataia Ammos.

as extension fractures. However, Hancock (1973) proposed that veins could initiate as extension fractures, synthetic shear (Riedel) fractures or combinations of the two, while afterwards behave as shear fractures forming en echelon veins. Smith (1996) describes the kinematic process by which veins initiate as extension fractures and yet have a convergent configuration. On the outcrop of figure (27) we can determine the same kind of behavior. Specifically, we can observe a larger extensional fracture (fig. 27b-c) that has a tendency to form a sigmoidal shape. The latter geometry implys an extensional trending of NE-SW (fig. 27c, green arrows) and dextral shear sense of E-W. This extensional fractures is posterior compare to the vicinity of tension gashes at the same side of outcrop. The vicinal tension gashes are intersected by the posteriori larger extension fracture. If we accept that this direction of extension takes place today, then this fracture is the most recent, while the vicinal intersected tension gashes imply previous tectonic events. The latter forenamed sigmoidal shape of the extensional fracture infers that the dextral shear sense takes place until today at almost the same orientation of E-W. Finally, considering the larger size of extension that reveals compare to the vicinal prior fractures, the extension is getting more intensive at the Pleistocene.

Shear is preceded or accompanied by the development of these en echelon veins, tail cracks and solution seams. Deformed calcite veins and extensional fractures show dextral shear sense on vertical and horizontal plane. However, there are several veins in some exposed sides of this outcrop of Tripolis limestones that show different kinematics offset and confuse the shear sense (fig. c, blue arrows).

The tension gashes development indicates whether the fracture propagation and shear strain were concurrent or not. The vein shapes grade from straight to sigmoidal without commensurate increase in vein size. The occurrence of tension gashes swarm was the main result of a series of deformation episodes and not concurrent fracture propagation. Furthermore, it is problematic that there are some veins in many exposed conjugate arrays that show different kinematics offset (fig. 27c, blue arrows). At the figures 27b and 27c we can define fractures that were caused by extensional fracture propagation and don't show any shear. The latest was interpreted by the following hypothesis. A temporal change in the stress field could be a reasonal explanation. Another idea is the localized temporal and spatial variations of a stress field that influence these kinds of perturbations that occur on the geometry of minor structures such as en echelon vein arrays. Slip or/and fracturing of this kind may be short-lived processes, for example related to seismic events.

Plataia Ammos - Outcrop L22 - S/C′ fabric indicates top-to-the SW displacement

At the outcrop of the sample L22, which is located close to Plataia Ammos village, in the metamorphic nappe (below the detachment), many of thin shear zones were been observed (fig. 31). Most of them were belonged in grouped different shear zones of the same kinematics but of a variety of strain illustrations at the same outcrop. The range of the rock chemical, physical properties and rock's incongruity is the

result of the variety of grouped continued markers' lines of shear. The differential translation of no physical breaks that depicts shear markers shows ductile shearing sense. The divided differential translation of several separated shear zones of the same kinematics sense have a thickness of 5-10cm. The thicker that was observed has a thickness of almost 25 cm (fig. 31), while 2 m is the whole thickness of the appeared shear zone at the outcrop that illustrates part or the entire shear zone. It was difficult to determine the absolute borders of the shear zones but not the kinematics.

This outcrop of shear markers appears with a very dense layer of penetrative foliation. Progressive deformation by shearing results in rotation of plane of flattening toward parallelism with shear zone walls, as well as builds up (fig. 33) shear markers closer (Davis 1984). In this situation the rotation of plane of flattening appears with a dense layer of shear markers in a wavy form of pseudo S/C fabric. The latter fabric was confirmed as S/C′ fabric by closer observation (fig. 32b) and it is latter described. In addition, the shear markers occur into a sigmoidal form, implying the expansion of the thickness of shear zone and the consequent differential rotation of the flattening plane (Davis 1984).

According to Davis (1984), the shear zone expands in thickness during deformation, as a result of strain hardening. Consequently, a broader zone of original country rock becomes distorted. Foliation in the interior part of the zone, having formed first, will rotate the most during progressive shearing. Relatively newly formed foliation near the exterior of the shear zone will rotate least. Finally, the differential rotation of foliation creates the systematically curved sigmoidal foliation pattern that characterizes the shear zone contact. As it foresaid, the latter outcrop appears in a sigmoidal form (fig.33). This could be explained as expansion of thickness of shear zone and

Figure 31: Location of L22 sample - layer of dense shear markers.

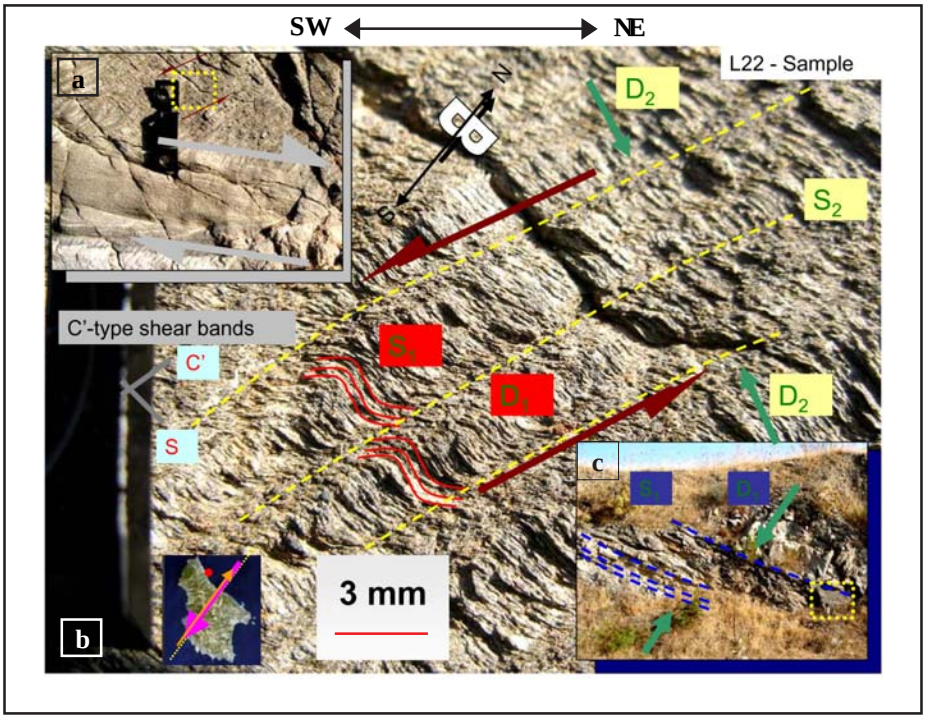

Figure 32: (a)Shear sense interpretation of the L22 outcrop's location sample. (b)A micro-view of the fig. 6a where the S/C' fabric is visible. (c) A macro-view of the fig. 31 where the outcrop is located.

consequent differential rotation of plane of flattening.

Assuming that the plane of flattening in the shear zone is the parallel horizon of the bedding of this outcrop of the shear markers then it manifests a penetrative folia-

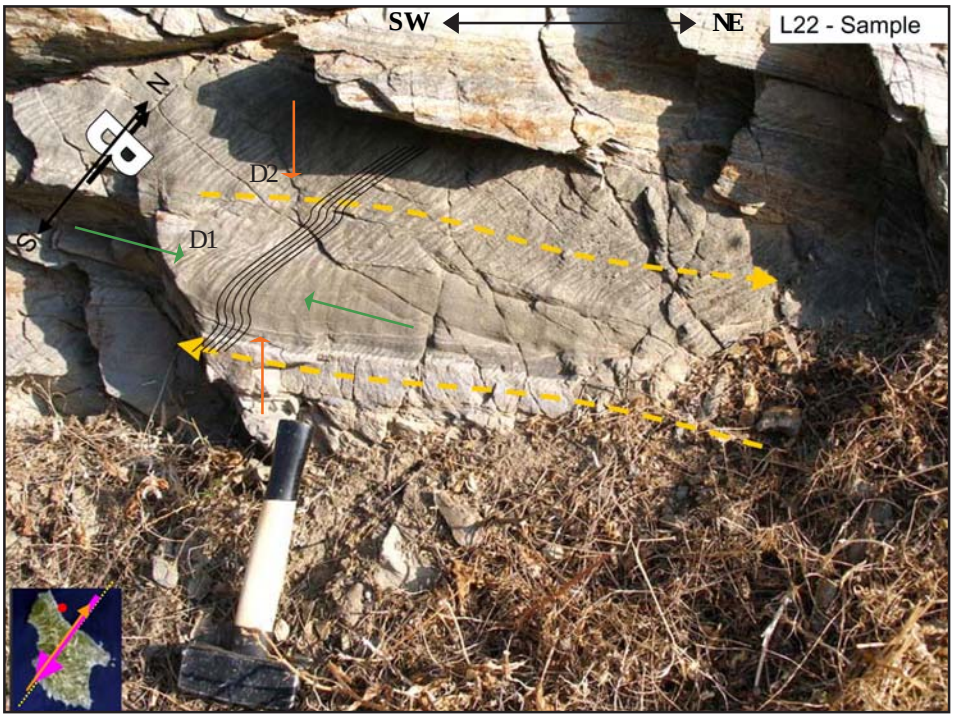

***Figure 33**:* A pseudo S/C fabric appears from the dense depiction of the shear markers at the outcrop of L22 sample location.

tion, inclined at an angle of almost 90 (?) degrees to the shear planes. A wider S/C fabric could be seen from the outcrop of L22 sample where the shear markers are not straight parallel lines to the flattening plane. Their systematical bends show an S and C fabric. These could be as a result of, D1 as ductile shear compression implying precursory an active proximate subduction zone, and D2 as compression from the rapid uplift and exhumation of the metamorphic nappe that occur from late Miocene until today, in this area. Further investigations about the kinematics of this location show obscure and confused sense of shear. From the other hand, the dislocation of the dense shear markers could show a kinematics of a dextral displacement of NE-SW trending.

Karavas area- Outcrop L09 - crenulation cleavage

At the outcrop of L09 location at Karavas village, crenulation cleavage (fig. 34) was observed. The preexisting continuous cleavage of the phyllitic schistosity cut by the crenulation cleavage, which is quite distinctive at the outcrop of L09 Sample location. The proportional relation of Micas and Quartz-feldspar-domains determine the crenu-

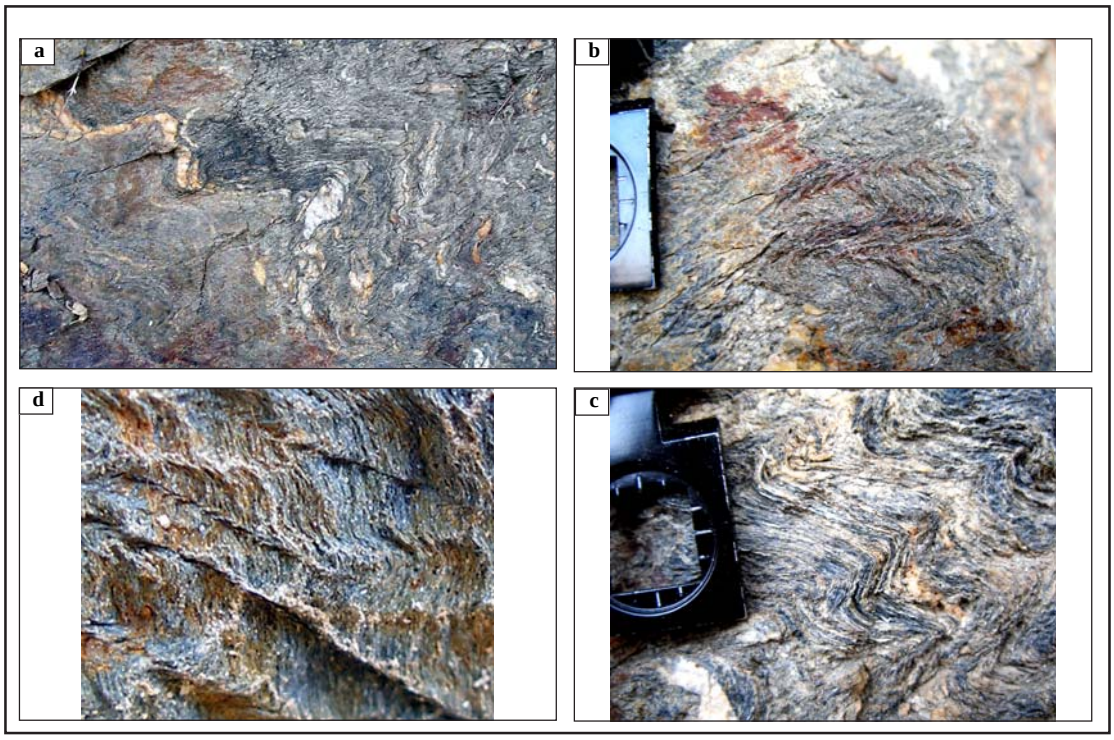

***Figure 34**:* Crenulation cleavage (discrete or zonal) created by analogous relation of Micas and QuartzFelspar domains. a,b,c: L09 Sample location at Karavas village, d: L10 Sample location close to Northwestern area of Agia Pelagia.

lation cleavage type. Discrete crenulation cleavage occurs at this outcrop with some kink bands. Discrete crenulation cleavage is the result of the relatively narrow micaceous laminae along which the continuous cleavage of adjacent microlithons is abruptly and sharply truncated (Marlow and Etheridge, 1977, Gray, 1979).

2. Agia Pelagia area (Eastern area of the map)

Agia Pelagia outcrop - Tension gashes indicate top-to-the SE displacement

At the street Agia Pelagia-Karavas, close to Agia Pelagia coast, a contact of lied Tripolis limestones to Metamorphic unit occurs (fig. 35a,c). At this outcrop a couple of tension, quartzed filled set of veins were observed. The tension gashes took place at the brittle region. It was hard to distinguish tips as they appear very close to each other, very dense in vein arrays. These en-echelon arranged set of veins opened to maximum width of 1-3 mm show a dextral sense of shear, inferring a top-to-the south-

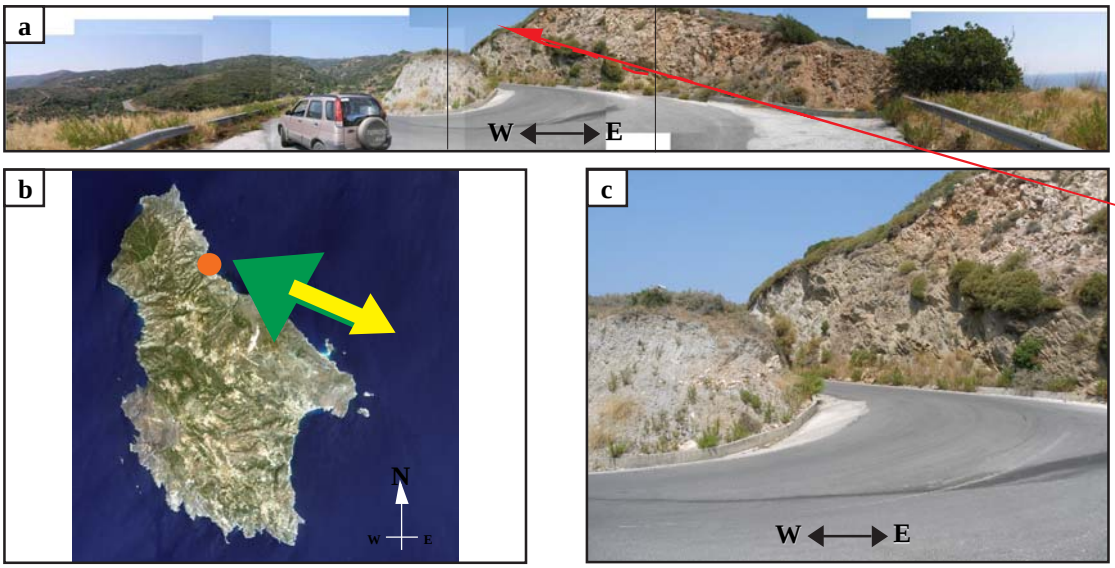

Figure 35: (a,c) Tripolis limestones lie on top of the metamorphic unit, close to Agia Pelagia village. (b) Geographaphic frame of reference that depicts the top-to-the southeast shear sense displacement of the outcrop close to Agia Pelagia area.

east displacement.

Agia Pelagia - Pindos unit structural observations

Many vertical faults of NW-SE trending, which located of both sides at the entrance road of Agia Pelagia area, appear as escarpments at the Cretaceous limestones of Tripolis, which probably die out in the metamorphic occurrence. The throw is not visible. At the area close to Kaki Lagada there is an overthrusted fault and brings the Cretaceous limestones of Pindos to lie against the Cretaceous limestones of Tripolis. Same kind of overthrusted fault appears at the area between Potamos and Agia Pelagia, which brings the Cretaceous limestones of Pindos to lie against the Flysch of Tripolis, the Cretaceous limestones of Tripolis and the metamorphic occurrences.

Part of the Pindos succession strata appears close to the coast between Agia Pelagia and Kaki Lagada. The Pindos upper Jurassic cherts succeeded by Cretaceous limestones and the latter series are covered by Flysch of Eocene. The Cretaceous Pindos limestones involve intense folds, in a macroscopic scale. Folding, normal strike faulting and rapid erosion gave rise to repetition of the outcrops of Pindos series in a NW-

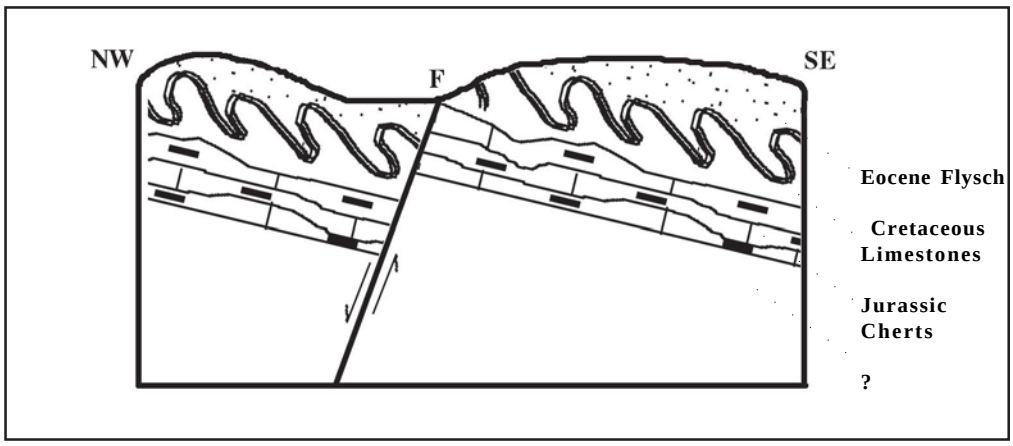

Figure 36: Normal strike fault, in section, crossing dipping strata, to show repetition of outcrops. The fault dips in the opposite direction to the dip of the strata.

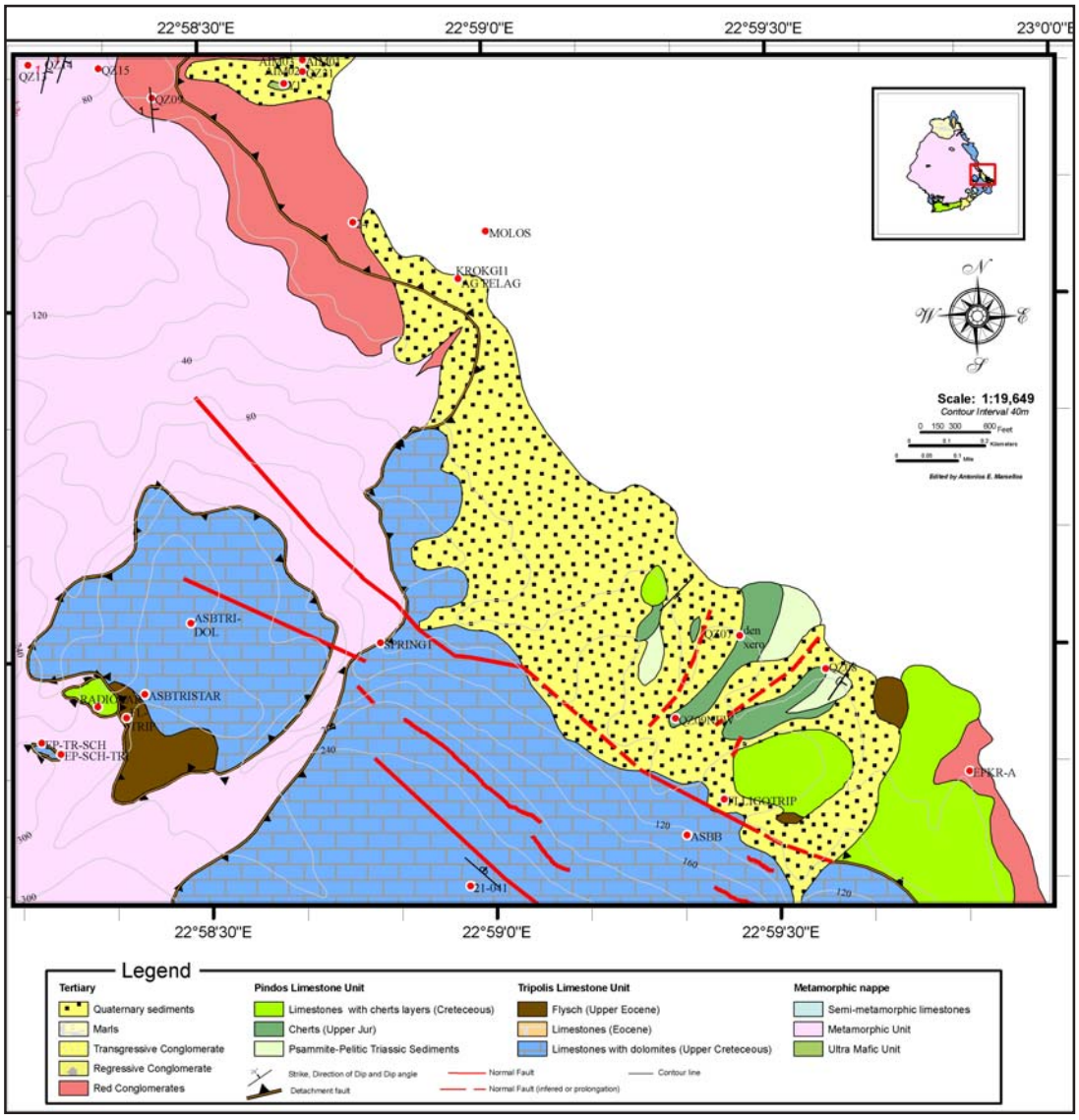

Figure 37: Part of the Agia Pelagia mapped area.

SE direction (fig. 37). The inferred faulting assumed that has a NE-SW trending according to the Pindos series outcrop repeated occurrences, while the folding trending follows the same direction of NE-SW. It is reasonable to assume that the fault dips in the opposite direction of the strata dip, at the direction of 315°NW, while the strata dip at 124°SE *(fig. 36)*. However, the evidence from such a small area at the map is often equivocal. The shape of the Upper Jurassic Chert and Pindos Flysch outcrops is probably partly due to a flexure in the beds, as a result of which the dip varies in direction and angle, and is very difficult to be estimated in such a smaller scale of mapped area. Between upper Jurassic cherts and Cretaceous limestones, both of Pindos unit, there is no clear contact because of multiple local alluvium covered strips.

Agia Pelagia - Ultramafic occurrence

There is an ultramafic occurrence at Agia Pelagia exit road to Karavas village. The outcrop appears among the metamorphic occurrence, the Cretaceous Tripolis limestones and the recently alluvium. It consists of serpentinite and chlorite. According to Theodoropoulos (1975) is certified as an altered peridotite, which consists of serpentine, chlorite and magnetite. From the field observation and according to the geotectonic setting of the island, this unexpected ultramafic occurrence could be explained and characterized as an olistholith or as a result of a small period of a tendency to create a deep ocean. Unfortunately, there are no geophysics measurements to reveal more evidence, while some thin sections of this outcrop reveal relict structures of a peridotite, very deform and altered chlorite, and the presence of the magnetite.

Agia Pelagia - Outcrop L10 and L11 - An old fault of almost 2,500 meters

At some outcrops very close to the outcrop location of sample L10 and L11,

systematic joints of rhombic development shaped occur. Brittle shear fractures observed that appear a saw-tooth like, zigzag pattern, determining a set of a sheared an echelon joint zones (fig. 38e). If we assumed that they have been experienced rotation of a horizontal axis, then it could be proposed a planar model of this structure in order to understand the orientation of the stress components (fig. 38d). A stress field with NNW–SSE compressional and ENE–WSW oriented extensional directions could be separated. This stress field could create the NNE–SSW and NW–SE oriented shear fractures, and NW–SE oriented normal faults. The lack of shear sense data from these outcrops could give two solutions. The first was the forenamed, while the second could be a stress field with NNW-SSE extensional and ENE-WSW oriented compressional directions. The second model contradicts the old fault pattern which is of NW-SE trending and parallel to the closer detachment fault orientation, while the first model agrees.

Based on the interpretation of digital terrain models of the area (SRTM elevation data), a 3D-model was constructed (fig. 38a, b, c) and revealed and old fault pattern (or pathway discharge) that occurred on this area parallel to the orientation of the closer detachment fault and provoke the forenamed shear fractures, confirming the existence of the first stress field forenamed model. The orientation of some DEM lineament sets related to the surface relief corresponds with orientations of structures measured in outcrops. With the help of DEM analysis, the youngest fault pattern was also precise, while the older, where we focus on this paragraph, was more difficult to

Figure 38 : (a-c). 3D representation of the Agia Pelagia's area topography accompanied with path profiles accross an inferred old fault line of the 2,500m length. (d-e). Determining the stress field of some observed brittle shear fractures of systematic joints of rhombic development shaped.
(next page)

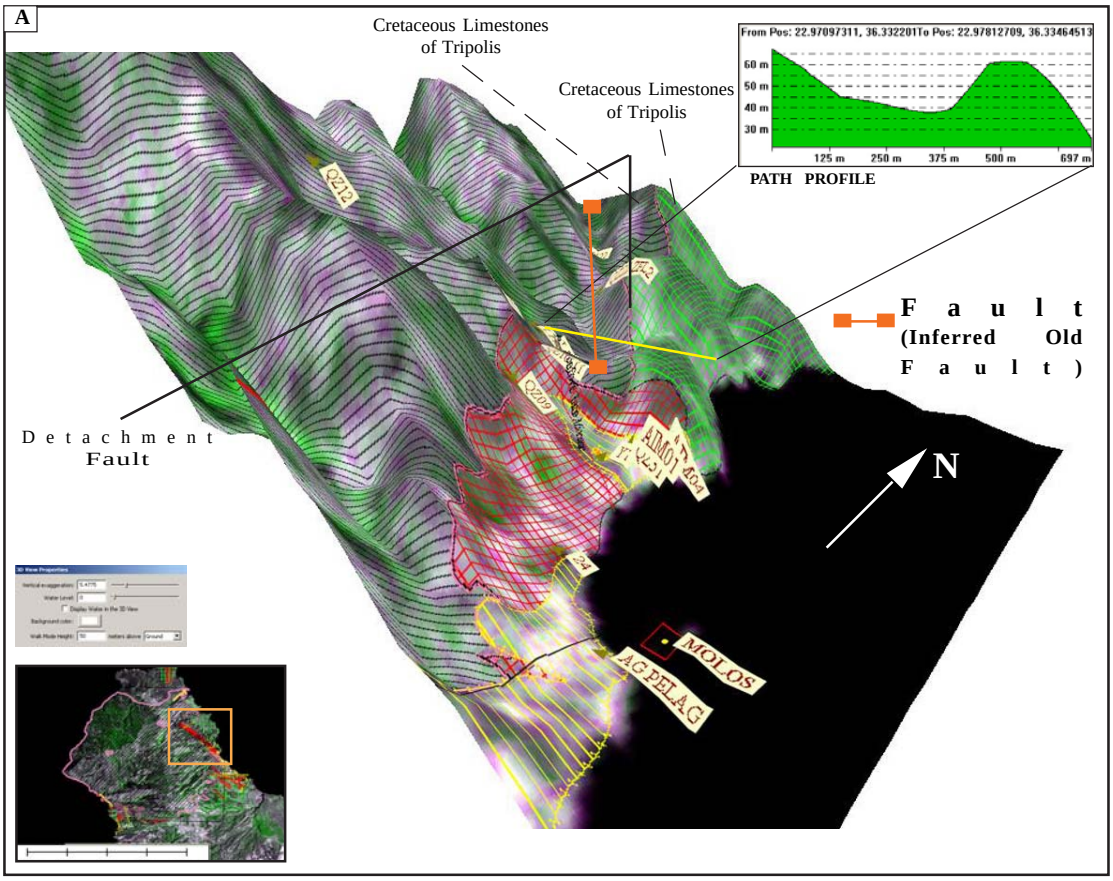
A
Cretaceous Limestones of Tripolis
Cretaceous Limestones of Tripolis
From Pos: 22.97097311, 36.332201To Pos: 22.97812709, 36.33464513
60 m
50 m
40 m
30 m
125 m
250 m
375 m
500 m
697 m
PATH PROFILE
Fault (Inferred Old Fault)
Detachment Fault
N
MOLOS
AG PELAG

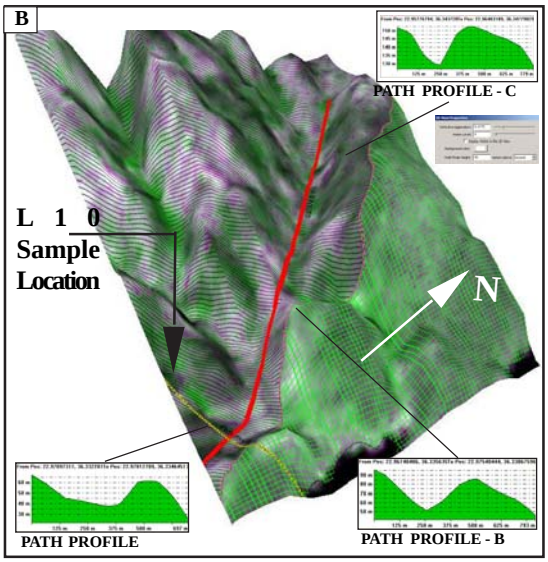
B
PATH PROFILE - C
L 1 0 Sample Location
N
PATH PROFILE
PATH PROFILE - B

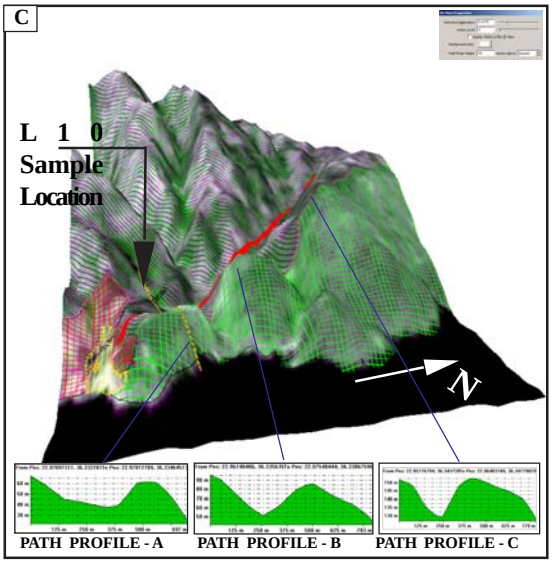
C
L 1 0 Sample Location
N
PATH PROFILE - A
PATH PROFILE - B
PATH PROFILE - C

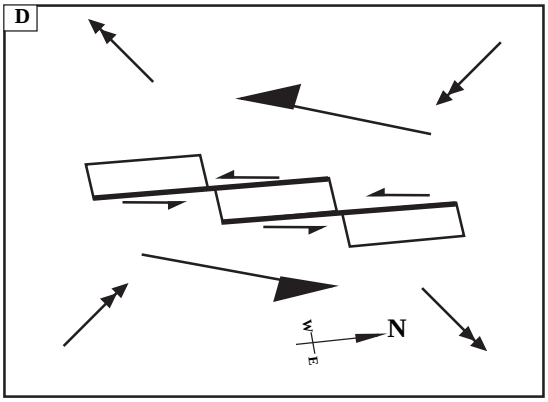
D
N
W
E


E
S S W
N N E

***Figure 39**:* Breccia and microbreccia of Pindos Eocene flysch on top of Tripolis Cretaceous limestones.

determine. However, an old fault of almost 2,500 meters and 135°SE revealed (fig. 38c), being parallel to the detachment fault of the Northeastern mapped area.

At Agia Pelagia area, the detachment fault brings the metamorphic occurrence below the Cretaceous limestones of Tripolis, while northern of Agia Pelagia, is covered by Neogene's red conglomerates, and southern of Agia Pelagia area, is covered by Tertiary sediments. The broad areas of Tertiary sediments consist of sandy and clay material. The origin of the latter weathering product is the limestone and metamorphic occurrences of the surround areas with an increased concentration of limestone or metamorphic material, depending of the distance from the parent rock. The conglomerates varie from some centimeters of pebbles to boulders (almost 50 cm in some places), and their thickness approach the 10m.

Agia Pelagia, Potamos area - Fault breccia

At the exit road of Potamos to Agia Pelagia, 1km far from the Potamos village,

***Figure 40**:* Z-Shaped drag fold form result from clockwise internal rotation and progressive deformation - outcrop of QZ22 sample's location.

Flysch of Pindos occur into a form of breccia on top of the Tripolis Cretaceous limestones, above the detachment fault. The clasts of breccia that are around 1mm diameter could be characterized as microbreccia or breccia (fig. 39).

Agia Pelagia, Karavas area - Outcrop QZ22 - Z-shaped Drag fold indicate top-to-the SE displacement

At the outcrop of the sample QZ22, where is located at the north exit road of Agia Pelagia to Karavas village about 1.5 km northeastern of Agia Pelagia village, a minor structure of a Z-shaped drag fold studied. A stratum of a horizontal quartz vein was deformed by frictional drag into folds (fig. 40) that are convex in the direction of relative slip.

The distortion of the depicted quartz vein stratum of the outcrop sample's QZ22 location, that drag folding occurs, is a result of shearing. The convex of the folding was used to determine the direction and sense of slip. At the drag fold's outcrop it was observed that strata on the hanging wall of thrust-slip and reverse-slip faults are dragged

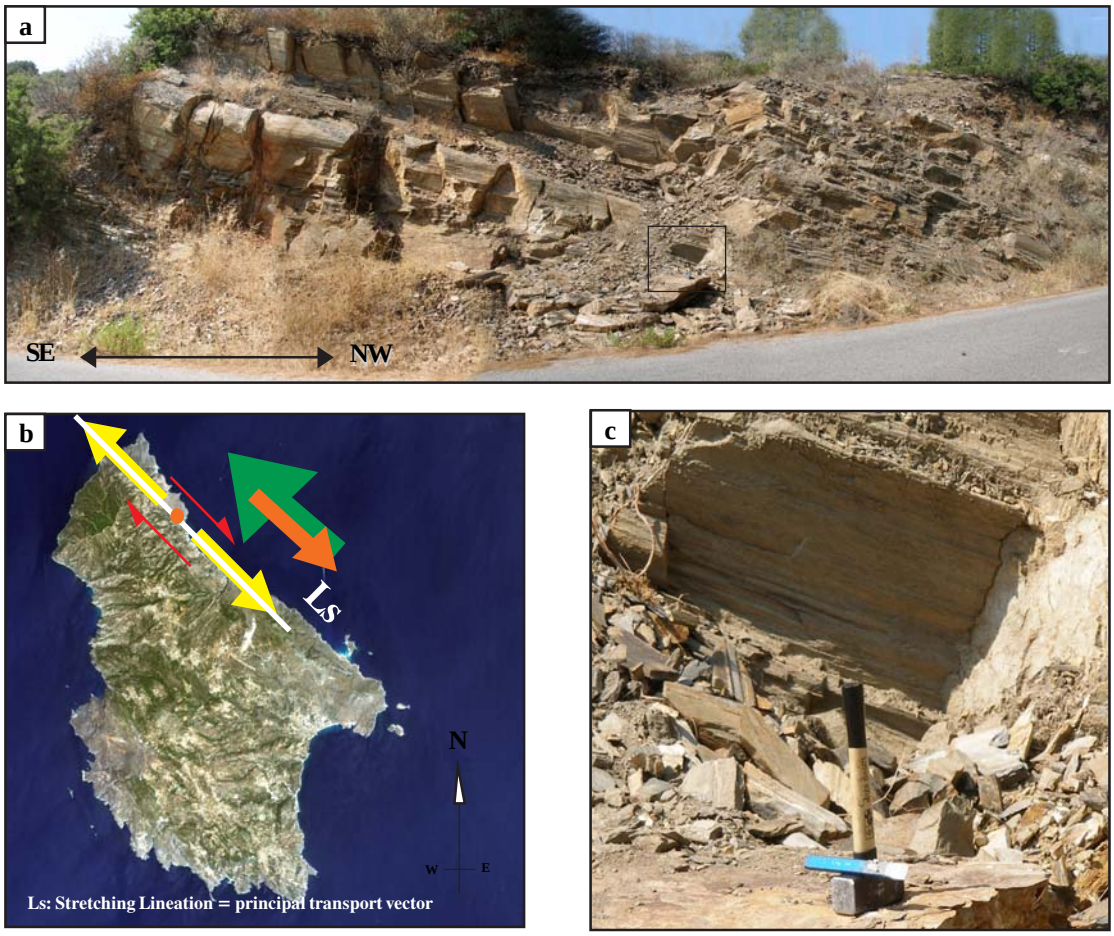

Figure 41: (a,c). Strong stretching lineation plunging northwestern at the outcrop of L23, close to Agia Pelagia area. (b). Geographic reference frame that depicts the shear sense observed indicators from the same outcrop.

into an anticline, whereas strata on the footwall are dragged into a syncline. Tight asymmetrical drag folds were observed downplunge and were characterized as Z-shaped. The high clockwise rotation that constructed the asymmetric, Z-shaped drag fold reflects a right-handed shear, specifically a dextral displacement of top-to-the southeast trending.

The latter displacement that appears on the Z-shaped drag fold may be associated with a NW-SE folding event or otherwise with the maximum compressional axis of NW-SE trending that occurs today, while the maximum extensional axis occur on NE-SW trending with normal faulting and scarps. Under a vertical compressional component (σ_2) the z-shaped fold was compressed, since the two convex folds occur in a

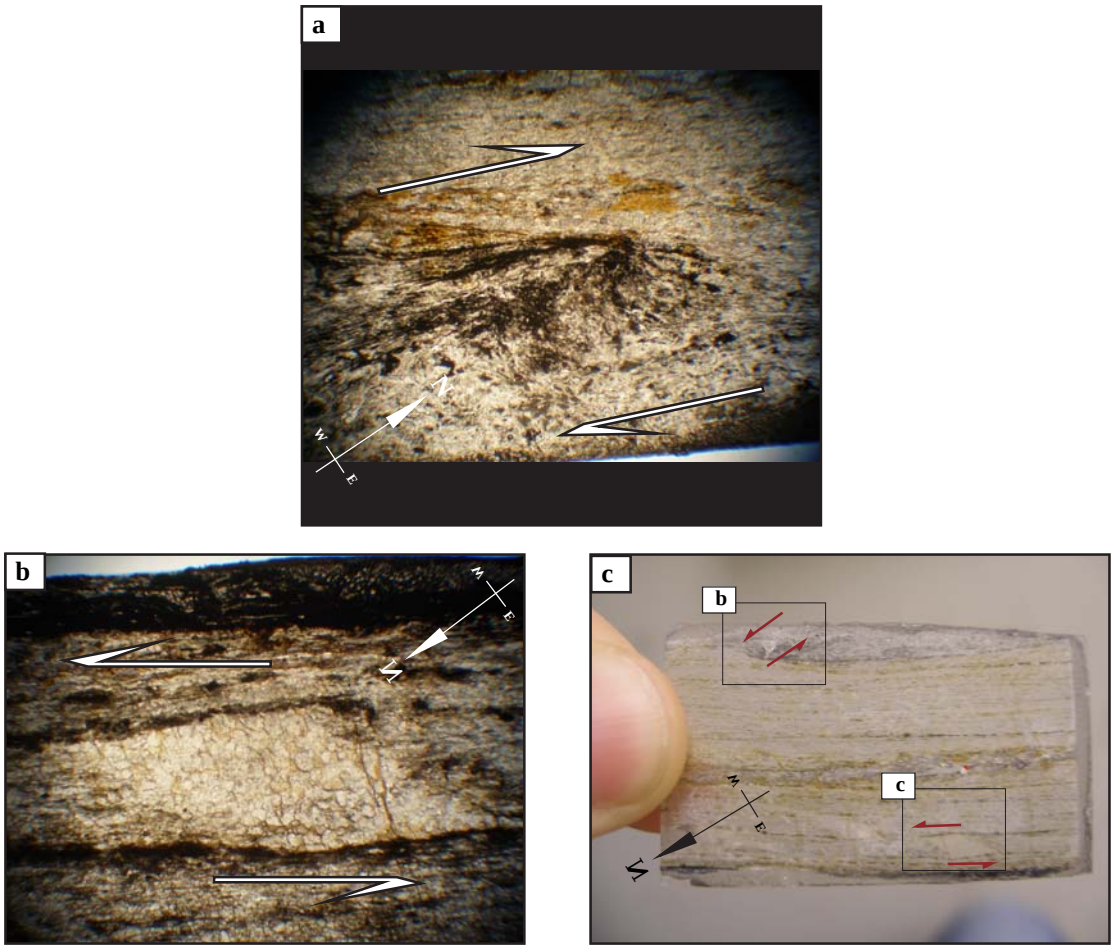

Figure 42: (a,b)Thin section of Sample L23 under plain polarized light, (c) , close to Agia Pelagia area.

tighter – compacted – version of a z-shaped drag fold, while brittle faulting produced small offset of the z-drag fold.

Agia Pelagia - L23 outcrop - LS shear fabric indicates dextral shear sense and top-to-the SE displacement

A strong stretching lineation plunging to the northwest developed in the metamorphic unit, occurs on a big recumbent fold, close to Agia Pelagia (L23) location area (fig. 41a). This is an L-S shear fabric which may be folded by one or more folding phases. The latter described structure usually occurs in many mobile belts, where the earliest regionally extensive and pervasive deformation is typically an intense L-S shear fabric, which is often subsequently folded by one or more folding phases (Goscombe,

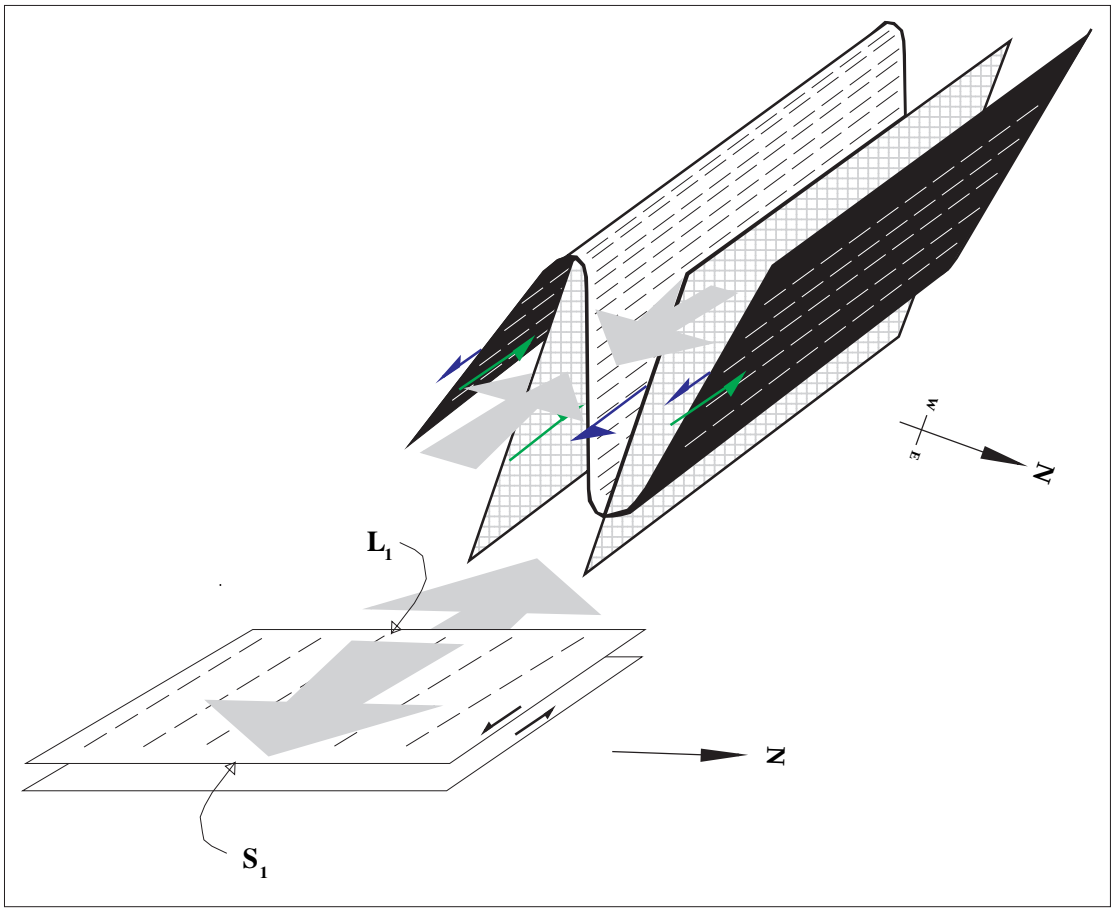

***Figure 43**:* Sketch of the folding stretching lineation and associated shear sense of the outcrop of the sample location L23 at Agia Pelagia area.

1991, Goscombe et al., 1998).

According to Goscombe (1999), the stretching lineation and asymmetrical structures, employed to evaluate shear sense, are frequently formed in this earliest non-coaxial shear episode. As a result of later folding events, the early stretching lineation (fig. 41c) - thought to represent the principal relative transport vector - and shear sense indicators no longer reside in their original orientation and evaluation of regional tectonic transport can only be deduced, after removing later folding effects.

The geometry of refolding of early stretching lineations and associated sense of shear indicators could easily lead to grossly incorrect tectonic interpretations of orogens and orogenic events. To evaluate this outcrop of L23 sample location correctly, the acute angle (φ) between the refolded transport vector and the fold axis needs to be

considered. This is illustrated by the geometry portrayed in figure (43). The acute angle (φ) was measured to be zero, inferring a co-linear relationship between stretching lineation and fold axes. The latter estimation of the acute angle (φ) results in shear sense inversion. Specifically, after some examinations of shear sense indicators at thin sections (fig. 42a-d), it was concluded a dextral sense of shear.

To ascertain the regional tectonic transport in these mobile belts, the way up of the sequence needs to be known, so that over-turned limbs with inverted early shear sense can be recognized. In most high-grade metamorphic belts, way up indicators are rare or absent, because of the overprinting metamorphic events. Thus, an alternative analysis is required to decide which of the two opposing shear senses is the original tectonic transport sense. The determination of which way is up of the sequence at the limbs was impossible, however most of the shear sense indicators close to this location refer the same shear sense kinematics, implying that the limbs of the fold were not overturned.

The XZ section (i.e. parallel to the lineation and perpendicular to the foliation) shows L-S fabric. The left-lateral offset of the quartz vein (fig. 42c-d) indicates the sinistrial shear sense kinematics of NW-SE trending. In the 3D-sketch of the folded stretching lineation structure (fig. 43) this gives a top to the southeast sense of shear. In the geographic reference frame, it appears with the orange shear sense arrow. Moreover, optical mineralogy analyses provided significant evidence for the P-T conditions of the metamorphism.

Agia Pelagia - Outcrop L23 - Blueschist (HP/LT) metamorphism

The thin sections reveal blueschist character with glaucophane and crossite dominated plus other mica minerals. The foliation is instense and consists of mineral band-

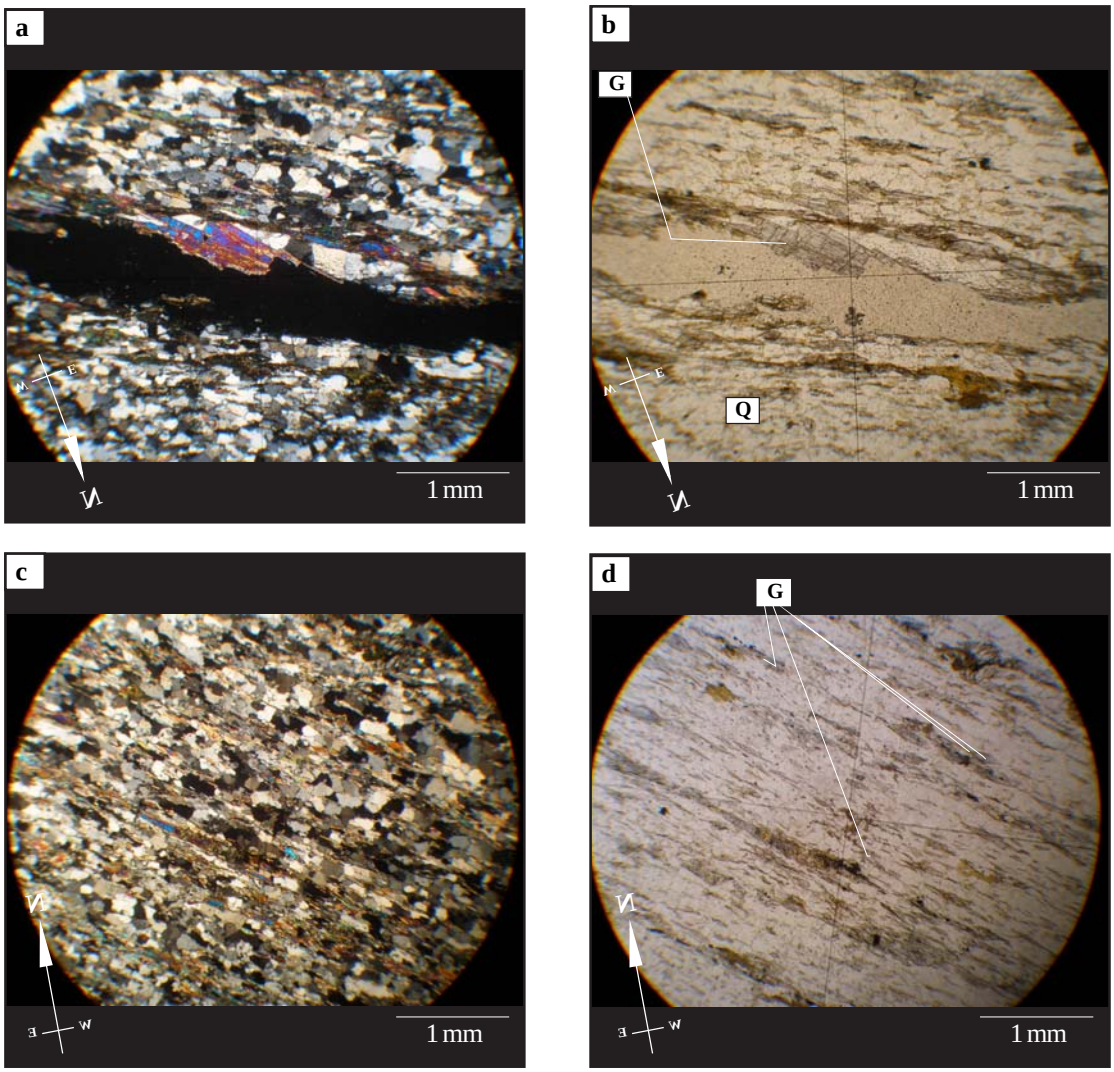

***Figure 44**:* (G) Glaucophane, (a,c) Photomicrographs under cross polarized light, (b,d)photomicrographs under plane polarized light of sample L23 at the area Agia Pelagia.

ing. Even that the blueschist character reveals a low grade metamorphism of HP/LT the texture appears mineral segregation into separate bands of micaceous and amphibole minerals that separate from the quartz and some rare altered feldspars. The latter may indicate deformation tendency to gneiss foliation.

The relief in thin section appears as moderate to moderately high positive (fig. 44b,44d, 45a, 45c). Both glaucophane and crossite crystals appear colorless to low blue in thin section with distinct pleochroism. However, the crossite in this thin section appears with almost no variation in indices of refraction, consequently it reveals a very

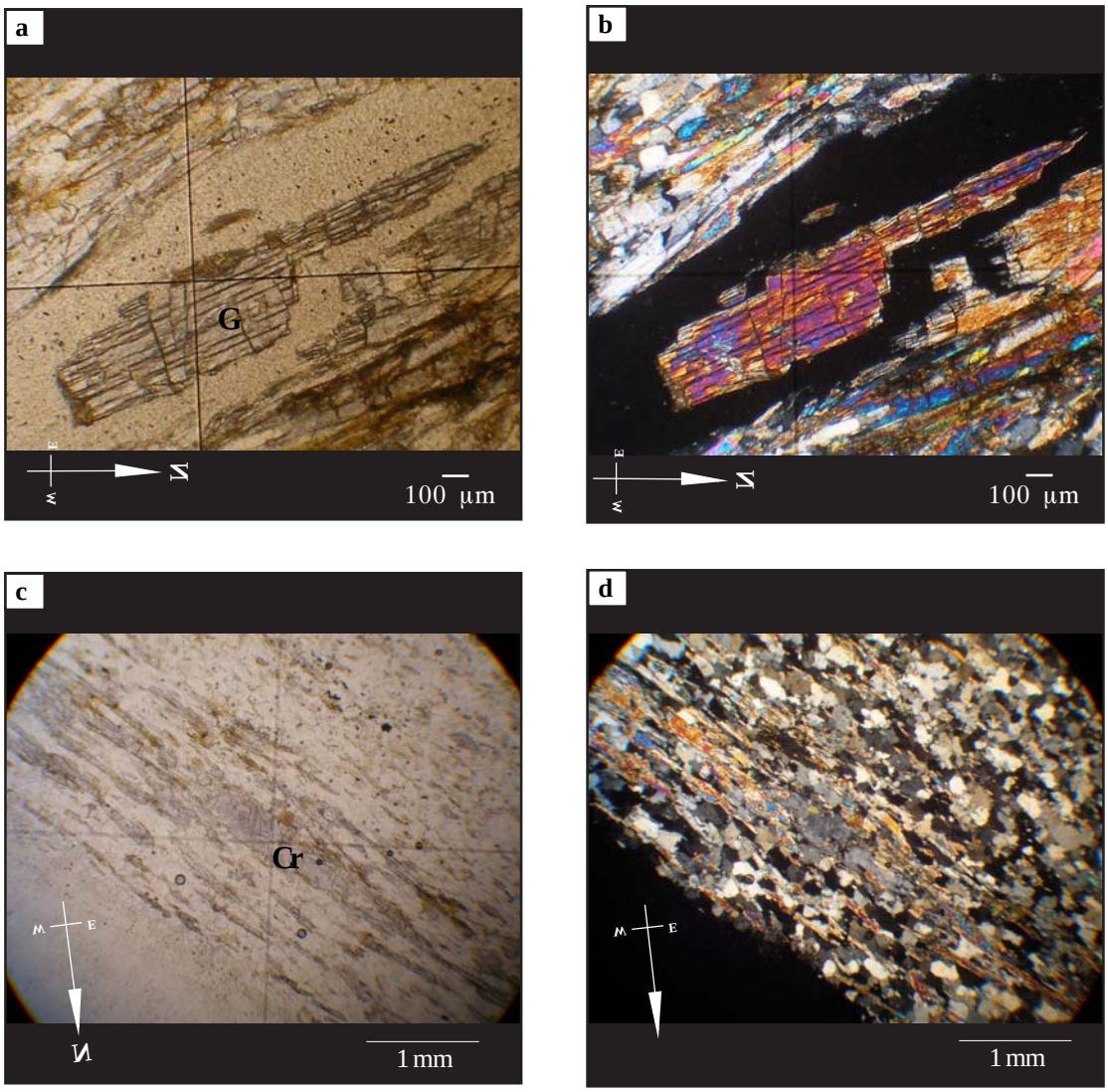

***Figure 45**:* (G) Glaucophane, (Cr) Crossite. (a,c) Photomicrographs under plane polarized light, (b,d)photomicrographs cross polarized light of sample L23 at the area Agia Pelagia.

low to clear birefrigence. The latter could probably be explained as an alteration of the crossite to quartz. They form bladed to slender prismatic crystals and shows prismatic cleavage, while less commonly fibrous. The cleavage is a typical amphibole cleavage that intersects at about 55° and 125°. Any kind of twinning was not observed. The interference colors in thin section are upper first to lower second order (fig. 44a, 44c). The determination of 2V angle was very difficult for the glaucophane, but for the crossite (fig. 45c-d) was estimated an angle of higher value than 45° that results to

crossite.

Glaucophane and crossite are characteristic minerals of HP/LT regional metamorphic rocks, which, because of their presence, we should called the (L23, close to Agia Pelagia area) quartzites as blueschists. Glaucophane and crossite are usually associated with lawsonite, which was not observed in the thin sections of the sample L23 location. However, Glaucophane has been used as a characteristic mineral of the glaucophane metamorphic facies, as well as has been used to characterize a relatively high pressure metamorphism such of this of blueschist phase, which is related to orogenic deformation, such of this of Kythera Island. Frictional resistance of downward movement of a subducted slab would be a suitable model of place that metamorphism took place. This conditions generate deep-focus earthquakes, as well as lead to high-pressure metamorphism at shallow depth.

Characteristic blueschist metamorphic assemblages are formed at the expense of partially subducted melange sediments and underlying, ophiolitic oceanic crust (Miyashiro, 1973). The low temperature character of blueschist metamorphic assemblages is attributed to the downsinking of relatively cool rocks into relatively hot regions (Ernst, 1975). The glaucophane schists facies includes the derivatives of sediments (pelites, cherts, calcareous rocks and greywackes) and basic lavas, tuffs and intrusives (Coleman and Lee, 1963). The above evidence confirm the pelitic character of the protolith of the L23 blueschist rocks.

The high-pressure metamorphism takes place at depths of 20 to 35 km. Tremendous vertical faulting is required to lift these rocks to the level of surface exposures. The presence of blueschist facies metamorphic rocks at the surface is yet another testimony of the great structural relief bound up in the recently Hellenic orogenic belt,

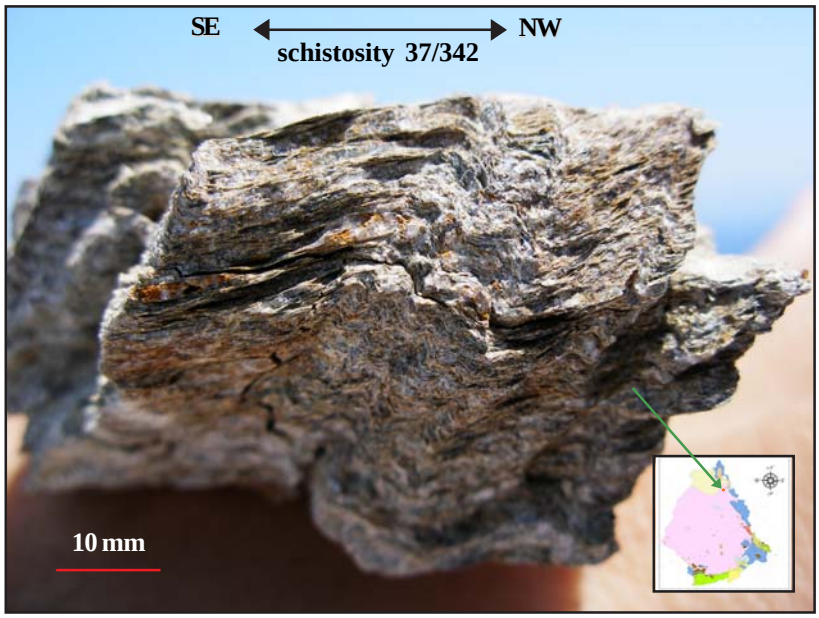

***Figure 46**:* Dextral Kink Band form at a mica-schist (sample L17) close to Plataia Ammos village.

as well as of the regional, epizonic character, metamorphism accompanied by intense deformation.In addition, it has to be note that at Cyclades area (Central Aegean) a lot of blueschist and greenschist zones have been studied that occur close to the MCL (Middle Cycladic Lineament).

Plataia Ammos - Outcrop L17 - Kink bands

According to Ghosh (1968), the mechanical idiosyncracy of the layer-parallel shortening of the multilayers of the sample L17 depicts that this district of metamorphic nappe buckled into short-wavelength folds. Such a minor folding is illustrated at the figure (46), and occurs as dextral kink folds, very abundantly, at these well-foliated phyllitic rocks on this outcrop location of L17 sample.

Further explanation of the main cause of the kink bands could be given by the cohesion of the rock. This mainly consists of quartz, micas and feldspar. They are able to construct individual strong layers with simultaneously low cohesive strength between their contacts. The latter according to Donath and Parker (1964) is the mainly cause

of such structures, of individual thin bedded layers that are folded and tend to retain their primary, original thicknesses.

The kink bands are part of the folding event of NW-SE trending that occurred on the Kythera Island. According to Dewey, 1965; Ramsay, 1967; Ramsay and Huber, 1987, kink bands commonly form in polydeformed areas and they are associated with compressional deformation, particularly with the late stages of orogenesis. For the later reason and above indicated folding orientation, the kinking of this sample L17 was the latest folding episode that took place on this district of L17 sample's location at Kythera Island and it is of NW-SE trending.

Potamos area (South of the mapped area)

Potamos area - Quaternary Sediments

Transgressive and regressive sequence appears respectively in an opposite sorting direction of diminishing or increasing the particle size of the sediments at the layers of the outcrops. The latter outcrops appear at Scandia, a small area southeastern of Potamos village. From a first approximation is hard to distinguish the two sedimentary formations. The highest energy deposition environment appears at the higher elevated layers of largest sediment grains, while at the lower layers, hardly appears the finer offshore. This transgressive sequence consists of conglomerate of 1cm – 8cm limestone detrital pebbles and cobbles. Although, any metamorphic conglomerate is absent, there are a lot of slate and quartzite fragments at the main matrix. The latter formation comprises the neogene disconformity that lies above the Tripolis and Pindos limestones, and the metamorphic nappe.

The regressive sequence takes place eastern of the latter neogene sedimentary

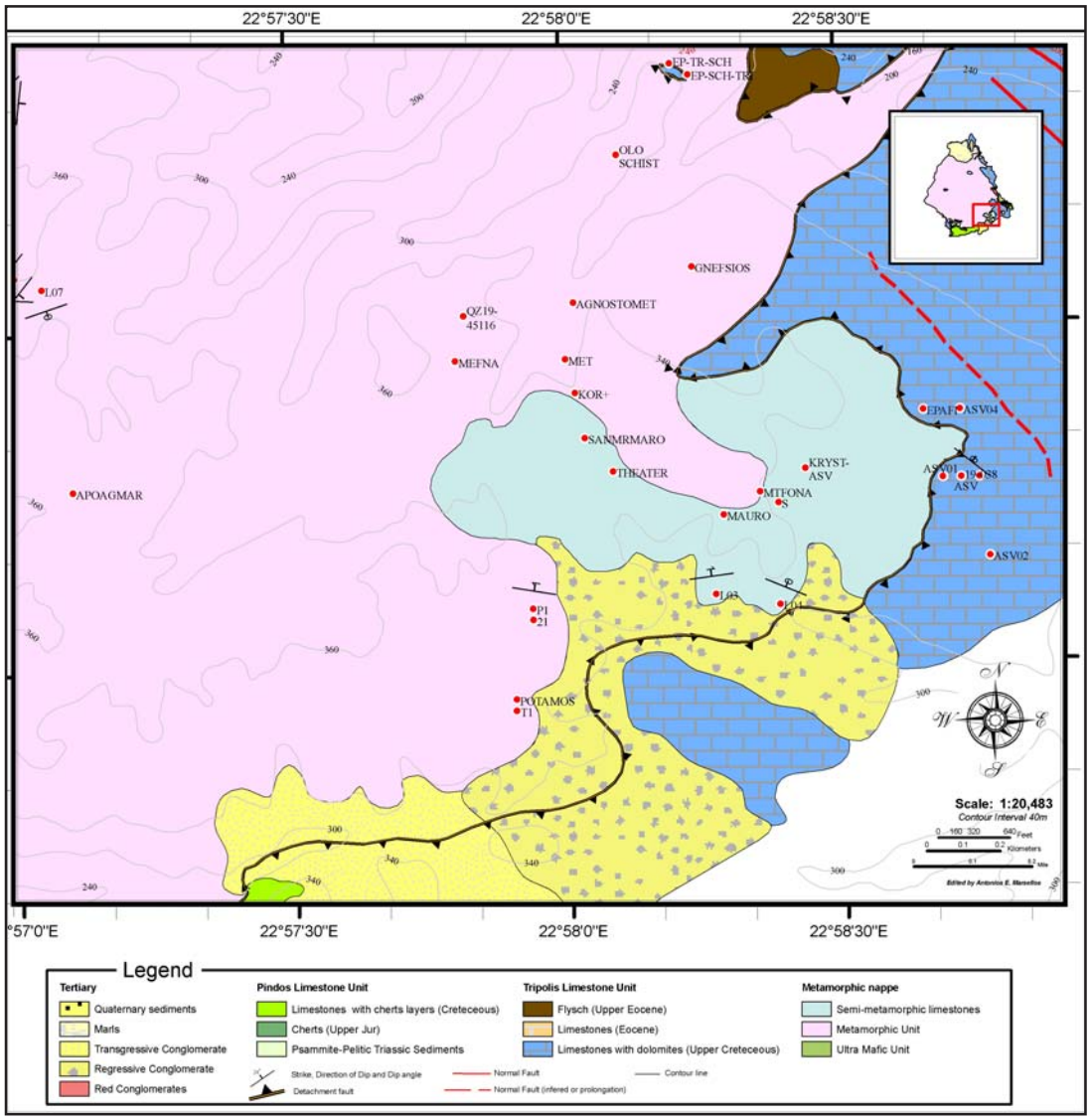

***Figure 47**:* Part of the Potamos mapped area.

sequence. It consists of gravel size's conglomerates. Western of Potamos, the apparent detachment is inferred, that crosses these sediments and continues to bring the upper Cretaceous limestones of Pindos to lie against the metamorphic nappe. Eastern of Potamos, the detachment fault brings the Cretaceous limestones of Pindos to lie against the semi-metamorphic and metamorphic occurrences. The same rock (marbles) forms an outlier at the west side of the mapped area (close to Ligia area), at the north side of the mapped area (close to Plataia ammos area) and at the center (Karavas).

Potamos area - Mylonitic occurrence - Ultramylonites

At the southeastern area of the semi-metamorphic occurrence, it appears a mylonitic formation. The latter evidence confirms the high strain environment of ductile shear zones (or brittle-ductile) that occured to these rocks. The mylonitic foliation of the forenamed rocks contains very lenticular, individual crystals. Ribbons and fragmented grains are illustrated with breccia streaks at these mylonitic outcrops. There are a lot of porphyroclasts and plastically deformed mineral assemblages of mica and quartz. The matrix grain size of less than 10μm and the matrix percentage of more than 90% extract their characterization of an ultramylonite and in some places of a phyllonite. The white represents porphyroclasts and "breccia streaks" or trails from porphyroclastic material; the black represents finely comminuted material and dark minerals (fig. 48, 51). As a first determination for the protolith of this mylonite could be possible derived from a parent rock of more coarse-grained original fabric, such as a granite. However, later explained observation in thin sections describe characteristics similar of the PQU.

It should be note that it was not found any other similar mylonitic occurrence of such a very high deformed and low grade metamorphism rock at the mapped area, beside the southeastern of Potamos area. In addition, this location has a lineation parallel (NNW-SSE) to the fold axis of the inferred broad antiform of the metamorphic occurrence and foliation almost parallel to a horizontal plane.

Mylonitic occurrence - Dislocation creep indicates top-to-the NE displacement

The indicated above relic structures of a more coarse-grained original fabric illustrate the shear sense movement, at the following figures (fig. 48-51). The figure (fig. 49) shows the quartz deformation from dislocation creep at a direction of NNE-

Figure 48: An outcrop close to Potamos (theatre) area showing a mylonitic formation.

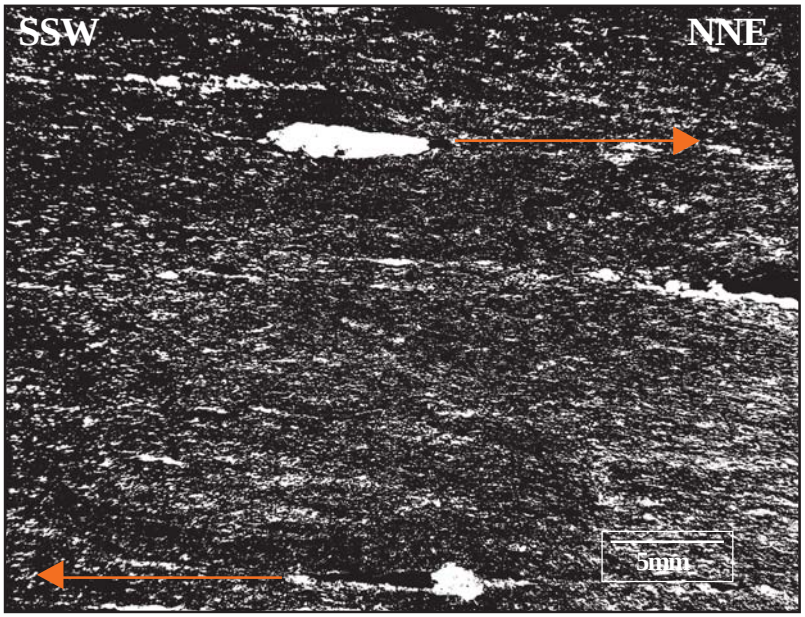

Figure 49: Macro-Photograph, of an outcrop close to Potamos (theatre) area, from the L04 sample location, shows a mylonitic formation and its interpreted dextral shear sense kinematics.

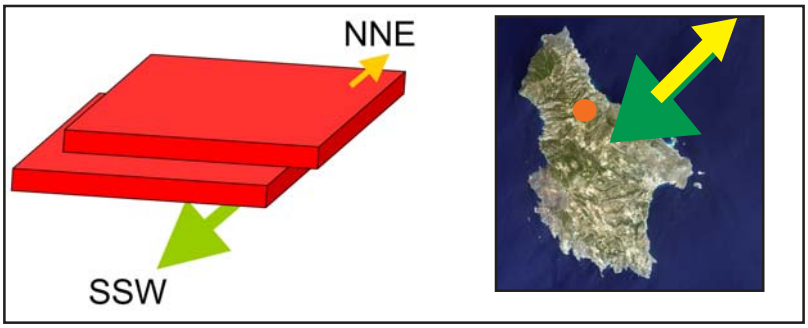

Figure 50: Geographic frame reference that depicts the location of the mylonite and the accompanied shear sense. (L04) Sample location, Southeastern of Potamos.

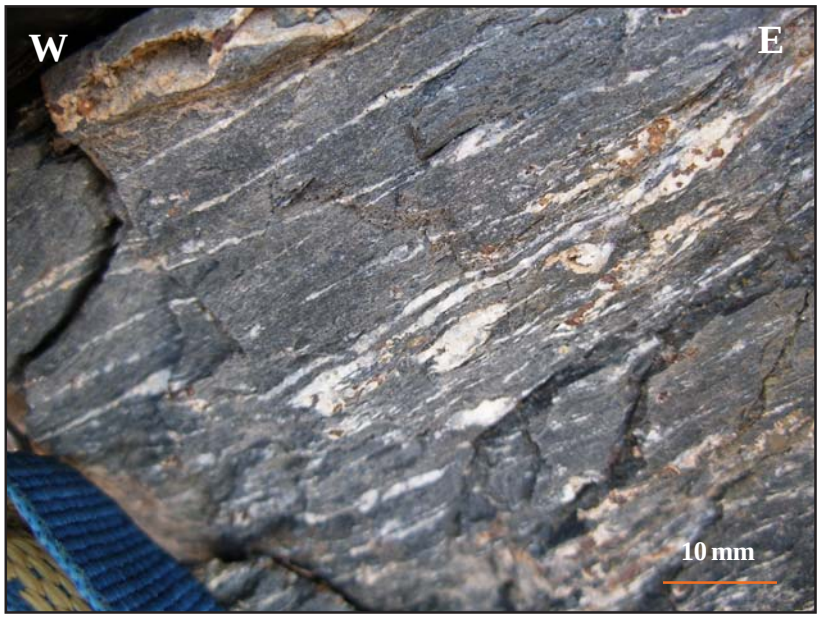

***Figure 51**:* Outcrop of the mylonitic formation at the L04 Sample location of Potamos area (southern mapped area).

SSW. While the feldspar is the stronger mineral, quartz deforms by dislocation creep NNE-wards and SSW-wards depicting a dextral shear sense of a top-to-the northeast displacement.

In this outcrop, was identified a very cohesive, foliated fault rock implying the mylonitic texture. The tectonic fabric was well developed to be identified as a mylonitic rock. Mylonites are the typical product of dynamic metamorphism. This metamorphism is usually even more local in its occurrence than regional metamorphism. Taking into account that this kind of metamorphism takes place along fault planes or shear zones of intense deformation of rock in the immediate zone of movement, we could result that there is an unambiguous indication of a detachment fault. This brittle-ductile shear deformation event took place in easily plastic rock types, where all floating in a matrix of more easily deformed minerals and rocks. Under conditions of high stress concentration, high confining pressure, and moderately temperature, mechanical comminution, recrystallization accompanied by growth of hydrous minerals due to movement of fluid into the zone of deformation, wall rocks along the inferred detach-

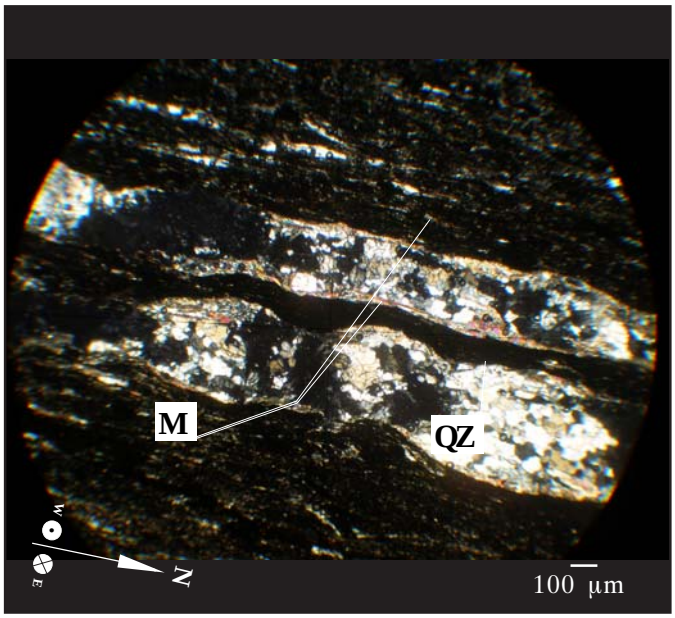

***Figure 52**:* Thin section cut parallel to lineation and normal to foliation of mylonitic rock sample L05, close to Potamos area. (M) Mica, (QZ) Quartz. Photomicrographs under cross polarized light.

ment fault were converted into mylonitic rocks. As it was forenamed, hydrous minerals such as micas occur in the mylonite formation due to movement of fluid into the zone of formation or their presence is attributed to relicts of the protolith.

Mylonite - Determination of Protolith

At the handspeciment view the fluxion structure is hardly recognizable, cause to extreme comminution and recrystallization. However, in some thin sections parallel to lineation and normal to foliation were determined rare occurrences of not mylonited quartzes and micas (fig. 52), implying that the protolith of the mylonite could be part of the PQU. Further from the forenamed outcrop, the mylonite occur more platy and phyllosilicate-rich determine a phyllonite. The latter could confirm that the protolith is the PQU.

As the rocks of the PQU close to the outcrop of Mylonites occurrence exhibit effects of both brittle and ductile deformation related to exhumation, there is good reason to believe that the deformation during the emergence of these rocks was con-

centrated along discrete and widely spaced deeply penetrating shear zones. Furthermore, we could determine that this is a non-coaxial shearing of the high pressure rocks (PQU), which took place during extensional tectonic events at 300-350^{o}C, when strain localization occured in response to decreasing P-T conditions, as well as localized mylonitic formation occured. Concluding, we can estimate the sense of shear, which is illustrated (fig.56) and discussed later. This is in a good agreement with evidence regarding other movements along the detachment at a close distance of 500m, which can be observed in outcrops of ductile and brittle shear zones.

A first approximation for the construction depth of the mylonite could be a place where there is a considerable degree of freedom for rotation because a high degree of preferred orientation (such as of the micas and quartzes) appears to be produced by very high strains and any kind of rotation would be difficult. For the above reason, it is possible that mylonite took place when the sediment or the PQU was still wet and soft; consequently fluid factors and “dewatering” under stress, would be a good time fora cleavage development.

One of the most important structures associated with mylonitic shear zones is the extension lineation. Even though, there is a very pure lineation of mylonitic occurrence at Potamos area, it indicates an almost N-S to NNW-SSE trending. This develops progressively towards the shear zone, while the extension lineation gives the trend but not the sense of displacement.

Sense of displacement in the mylonitic shear zone at Potamos area is given by an asymmetric structure of a metro-scale, which is the most reliable kinematic indicator. The latter was derived by an outcrop of S/C′ shear bands (fig. 56), 5 metres away from the mylonite outcrop, inferring a dextral sense of shear. That implies a top-to-the

southeast displacement and is discussed later on this research.

Potamos theatre - Marbles and stylolites

The semi-metamorphic occurrence or otherwise named as recrystallized limestones (sometimes occur as marbles) occur close to mylonite's outcrop area of about 500m eastern distance from the previous outcrop. These are light beige, beige grey, beige brown or brownish-grey colored, sometimes with a light yellow to pink hue, and partly contain white calcite veins and some stylolites (fig. 53). A stretching lineation is not developed and either observed. It is very difficult to determine the transport direction in these calcite deformed limestones or otherwise named as marbles, because foliation and stretching lineation are not developed. However, the development of some stylolitic teeths could may indicate sense of shear.

Stylolites formed by dissolution of carbonate, leaving dark accumulations of more insoluble material. The wave-like or tooth-like, serrated, interlocking surfaces seen in microscopic slab of the sample (19038), are thought to have been formed by pressure solution. The dissolution process reduces pore space under pressure during diagenesis, while it associates shear sense movement. Stylolitic surfaces produced by tectonic stress of shortening (Nickelsen, 1972) from tectonic orogen or from burial and compaction. The semi-metamorphic marbles that carry these stylolites do not preserve or indicate any bedding, as well as any folding, implying that these stylolites are primary formation during compaction.

Teeth and cones of stylolitic surfaces are oriented perpendicular to axial surfaces of folding (Alvarez, Engelder, and Lowrie, 1976), implying the direction of greatest principal stress (σ_1). According to the depicted arranged en-chelon stylolites of the sample (19038), there is a semibrittle dextral shear sense. Although ductile or

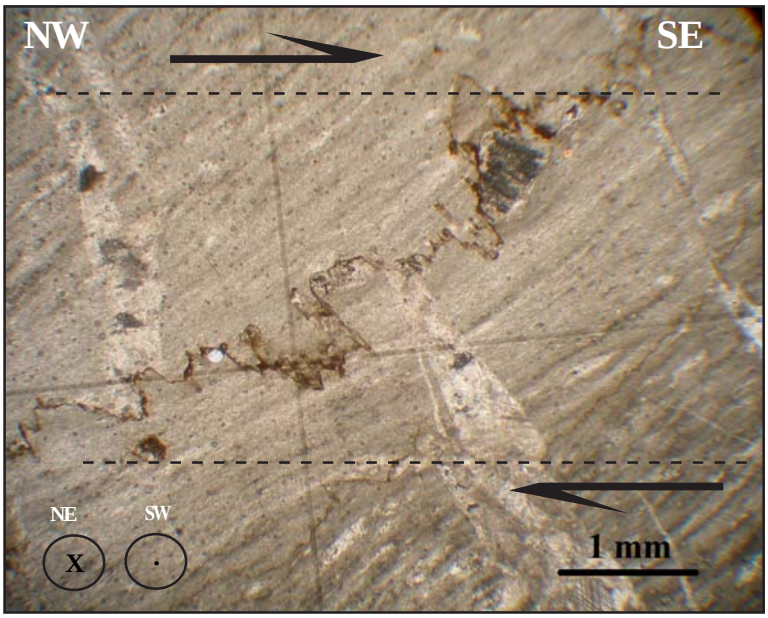

***Figure 53**:* Stylolites at southeastern area of Potamos (recrystalized limestone), microscope's photograph of the sample (19038).

semibrittle-ductile shear zones contained by this sample, brittle deformation dominates along the zone and is accommodated by fractures, filled by calcite veins.

Potamos Theatre - Shear Boudins indicate dextral shear sense and top-to-the SE displacement

Close to the forenamed outcrop of semi-metamorphic marbles, at southeastern area of Potamos, boudins occur (fig. 54a-b) in a stretched quartzite layer (white-reddish), covered top and bottom by phyllites (gray). Structural field data show the boudins to be bounded as pinch-and-swelling structure. Movement of small normal faults permitted the layer to further stretch its length. The brittle-plastic (or brittle-ductile) behavior pinched the quartzite layer and drifted away, while medially gaps developed in between the pinch-and-swell quartzite layers. The boudinage occurred on a NNW-SSE direction as a result of viscosity contrast, between the quartzites and phyllites. According to Schopfer & Zulauf (2002), pinch and swell structures develop at an approximately 1.5 viscosity contrasts, whereas boudins develop at viscosity contrasts of

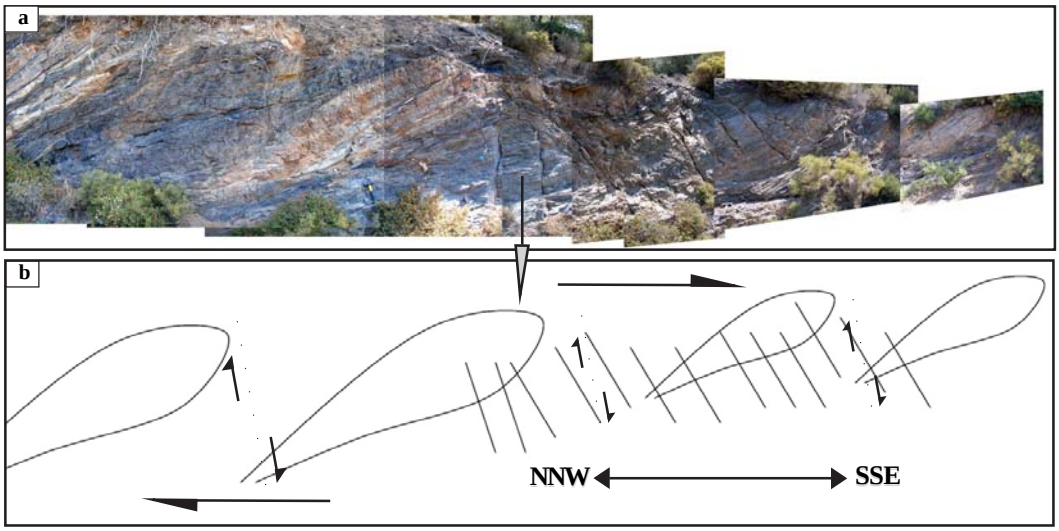

***Figure 54**:* Pinch-and-swell structure of quartzite layers in a less viscosity formation of phyllite series show a boudinage of NNE-SSW trending.

approximately 2.0-2.5. In this case, an explanation dealing with deformation by ductile conditions may be a reasonable scenario for the construction of the elongate inclined pinched and swelled shape of the boudin structures (fig. 54a).

The forenamed asymmetric extensional structure of boudins and pinch-and-swell structure occurs less than 150m away from the Mylonitic shear zone and forms a reliable kinematic indicator which is consistent with the kinematic indicators of the mylonitic shear zone. The pinch-and-swell structure shows almost distinct shapes. Rotation is the main characteristic of their shear boudins and dragging out of leading with the shear sense. The rotation is antithetic (back-rotation) with respect to the shear sense (Hanmer, 1986), and implies a dextral shear sense character of top-to-the southeast displacement.

Potamos Theatre - Slickefibres of NE-SW trending

Lineations developed in the fractured rock, such as striations on slickensides and fibrous crystal growths on NE-SW trending were observed at an outcrop close to sample location of L03, at Potamos theatre area (fig. 55). These slickenfibres used to deter-

Figure 55: Outcrop of quartzites at Potamos area that hosts slickensides of NE-SW trending, close to sample location of L03.

mine displacement direction, but only to indicate the last-stage movement direction or local displacement, since they may not represent a movement history of such long-lived and mobile zones.

Potamos Theatre outcrop - S/C´ shear bands indicate top-to-the SE displacement

The asymmetric S-C ´ structure of the two combine foliations S and C ´ reliably gives the sense of shearing. This was revealed from an outcrop five metres away from the mylonitic occurrence. This is a dextral shear sense of NW-SE trending, implying a top-to-the southeast displacement. This kinematic indicator shows the mechanisms of shearing that accommodates the bulk deformation (Lister and Snoke, 1984). Very close to this outcrop, it rises to prominence of the increased shear strain accumulation, where the S foliation rotates towards the C foliation and loses its integrity (Berthe et al., 1979). The product at this stage of deformation that occurs is a mylonite with just one well developed foliation and appears as a crushed and foliated matrix proportion of 90% determining a typical ultramylonite.

The acute angle between the two foliations S and C ´ (fig. 56c), is another impor-

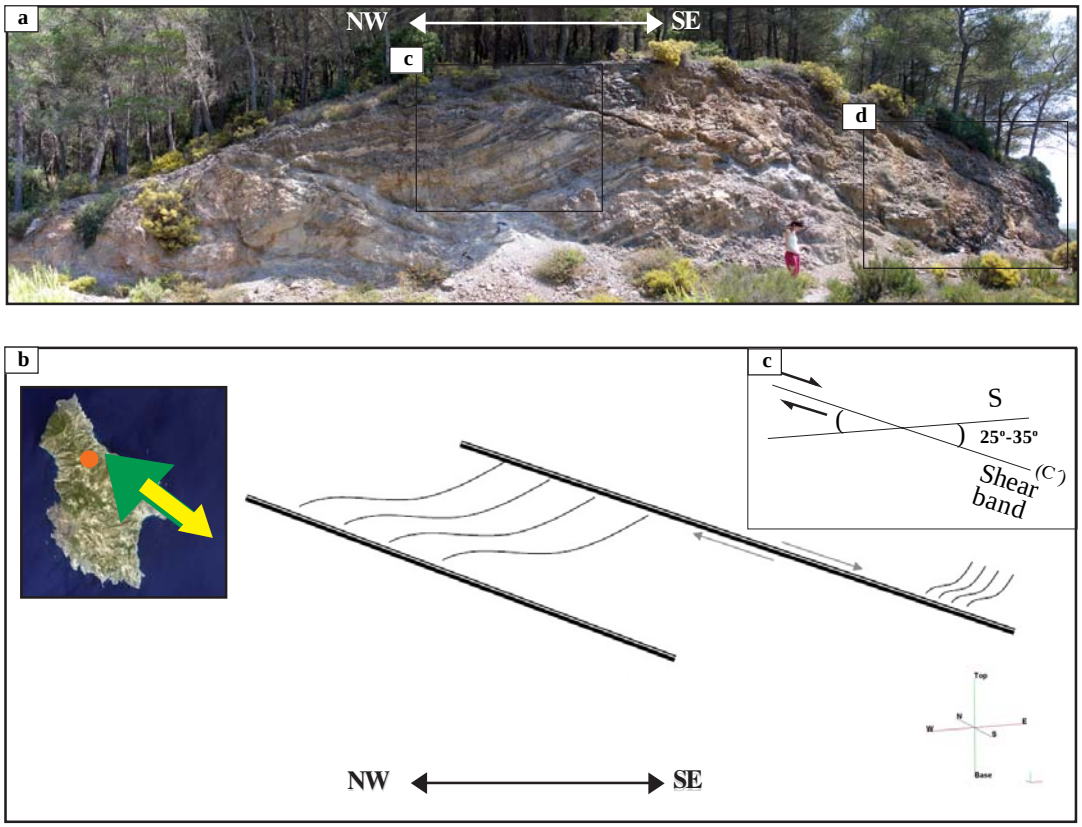

Figure 56: Macro-scale of a S/C´ fabric close to the mylonitic occurrence, Potamos.

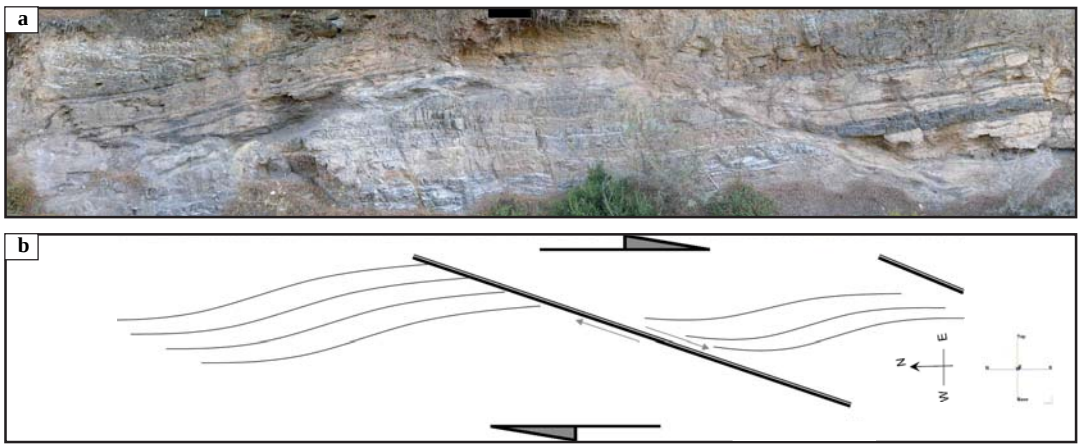

Figure 57: Strain path model of the simple shear zone complex depicts on the outcrop of the mylonite sample outcrop location.

tant characteristic that was considered. The acute angle of approximately 30 degrees (25^{o}-35^{o}) of the intersection of the two foliations implies their simultaneous occurrence, otherwise if were intersecting at angles $>45^{o}$, then are almost certainly of different ages and are superimposed (Mawer, 1989).

Potamos, Karavas - Brittle Ductile fault - Fault Gauge and S-Slip Boudins indicate top-to-the Southwest displacement

Northwestern of the exit road of Potamos to Karavas village, it was observed a fault gauge, grey to black in color zone of 1-2cm width accumulation of tiny crystals fragments (less than 0.1 mm). This special type of cataclasite formed by rapid fault movement at high crustal levels (e.g. earthquake possible related) and seems as a pseudotachylite but is not. Considering that this fault occurrence is less than 1000m far away from the outcrop of the mapped detachment fault and the mylonitic occurrence, we could conclude that this fault rock was caused by grinding or fracturing at semi-brittle region. In addition, there are fractures in almost parallel orientation of the forenamed brittle fault. Under such a tectonic setting of normal faulting, very high extension and simultaneously uplift, is reasonable to assume that a powerful shock under instantaneously imposed strain formed this fault. This brittle-ductile fault was created in depth no more than 10km, as a result of rapid movement inducting thermal fragmentation. Moreover, along the fault gauge line, trails of a series stair-stepping shear sense movement were observed (fig. 58-60). These consist of large lozenge shape and monoclinic shape asymmetry fragments. These boudin blocks have an asymmetric, rhomb to lens-shape similar to that of σ-type mantled porphyroclasts (Passchier and Simpson, 1986; Goldstein, 1988); shapes with tapering wings.

According to Swanson (1992), the forenamed boudins are shearband boudins with

Figure 58: Brittle-ductile normal fault that hosts fault gauge and stair-stepping boudins parallel to the fault plane. Potamos area, L08 sample location.

the previous characteristics. They have one curved and one planar side, similar to σ-type porphyroclasts. They lie with their long axis parallel at the fault surface and show a steeper inclination at their opposite side, while they appear as pinch and swell structures at the edges. According to this forenamed kinematic indicator characteristics and its dextral sense of shear, this fault behaves as a normal fault(fig. 58).

The forenamed pinch and swell structure at L08 sample location is an asymmetric boudinage which may develop in shear zone or moreover under high shear strain values as the model of Goldstein (1988) depicts at the figure (fig. 60b). It should be note that these fractures were form at the transitional shear zones with brittle, solution-transfer, and crystal-plastic deformation processes operating synchronously within the whole shear zone and cyclically (Mawer, 1989). Asymmetric boudin models have been proposed from many authors, such as Hanmer (1986) and Goldstein (1988). According to the boudins description of Goldstein (1988), the outcrop of pinch and swell structure that occurs at Potamos (L08 sample) location is in agreement with the

***Figure 59**:* Outcrop of Potamos area of L08 Sample location shows asymmetric boudinage

.

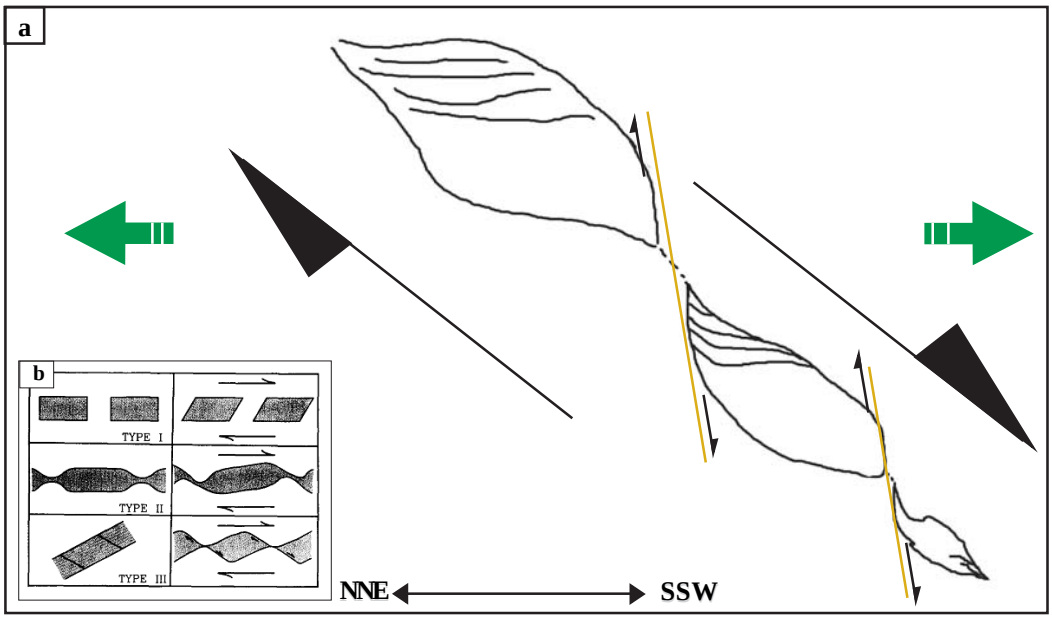

***Figure 60**:* a. Scheme of the fig. 59 that shows the kinematics of non parallel shearing and externsional fields, b. Three types of asymmetric boudinage which may develop in shear zones (right column) from Hanmer, 1986; Goldstein, 1988.

final step (d) of the model of the figure (fig. 61), where at high shear strain values, boudins become completely separated and their corners experience ductile shape modification.

From a comparison of the forenamed outcrop with the three models depicted at

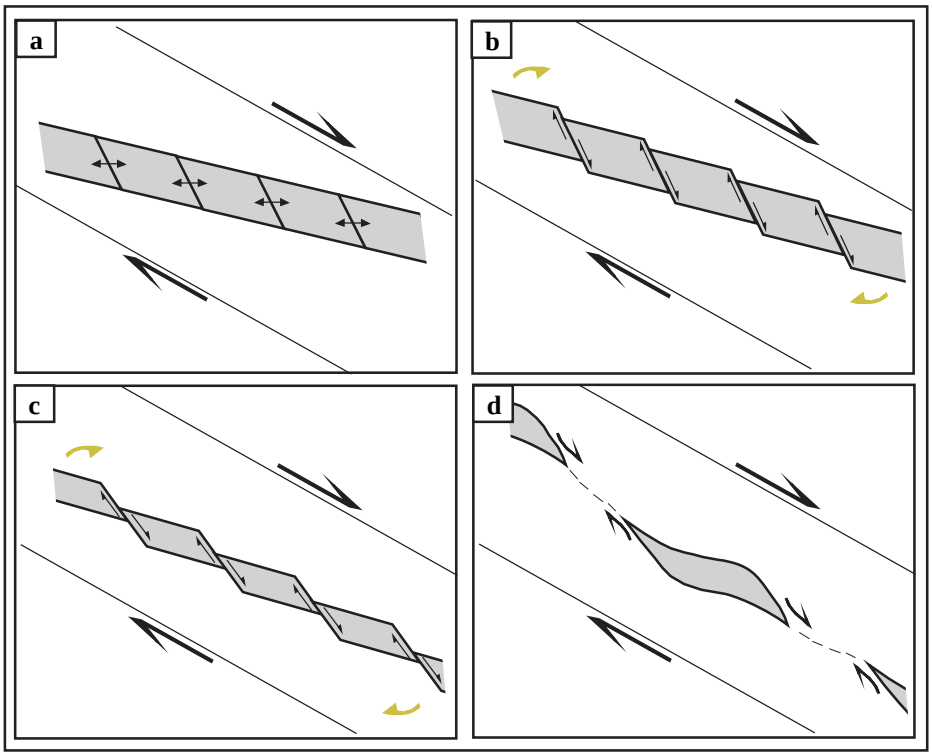

***Figure 61**:* Proposed model for the formation of the asymmetric boudins by Goldstein (1988).

the figure (fig. 60b), this outcrop may correspond to the type III. Hanmer (1986) proposes the type I and II asymmetric boudinage which require the existence of either blocky or pinch and swell boudins prior to shearing. The type I and II presupposes the existence of parallel trending of shearing and extension, while the type III mechanism that produce asymmetric boudinage comprises non parallel orientation of shearing and extension. In detail, the type III asymmetric boudinage, proposed by Goldstein (1988) requires that layering be inclined to the shear zone and lie in the extensional field. According to Goldstein (1988), the latter asymmetric boudins, form as a result of layering lying within the extensional field of a shear zone, implying that extension and shearing worked together for some period of time.

Asymmetric boudins within foliation-oblique boudin trains can be applied as shear sense indicator if these structures could be confidently identified as shearband boudins.

The previous ambiguity was solved by the evaluation of asymmetric boudins as shear sense indicators according to Goscombe and Passchier's (2003) evaluation of asymmetric boudins as shear sense indicators.The forenamed evaluation was followed and explained further in detail.

Proceeding to the four steps, the attempt is described as follows. The figure (fig. 63a) describes the measured components θ, L, D, W and N. The boudin axis (L_b) is at high angle to the stretching lineation (L_s). The boudins correspond to the secondary shape characteristics of shearband boudins as discussed below and shown in figure (fig. 63). Boudin shape is quantified by θ angle, which is 38^o. The length (L) of the boudins is 21.3cm, 16cm, 5.7cm, and the width (W) of the boudins is 10cm, 7cm, 2.4cm respectively from the larger to the smaller boudin. The displacement (D) between individual boudins measured parallel to Si_b and normal to L_b is 19cm and 9.25 cm. The dilation (N) of Si_b measured normal to Si_b is 2.5cm and zero or almost -1cm. Another important aspect, besides the geometry, is the orientation of the boudin train with respect to the main foliation in the rock matrix. The foliation is oblique to the boudin train. While the first and the second boudins are clearly separated, the third almost begins to overlap with the second.

As a first approach, the geometry characteristics of the previous boudins express the following aspect ratios to be not as high as the average values of Goscombe (2003), however they prove the presence of shearband boudins. The L/W is 2.13 (21.3/10), 2.28 (16/7) and 2.47 (5.7/2.3) respectively from the larger to smaller boudin. The latest decrease of the measures implies presence of the (σ_2) compressional axis which disrupts the mutual arrangement between the boudins. According to Goscombe & Passchier (2003) studies and further literature of the previous aspect ratios of shearband

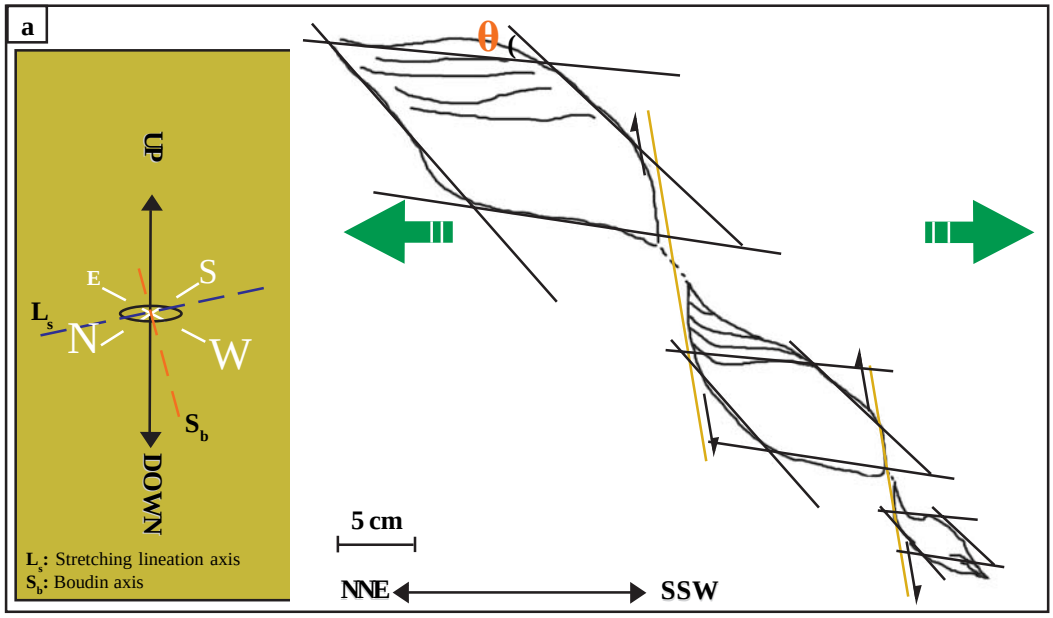

Figure 62: Scheme of the fig. 20 that shows the orientation of foliation vs boudin axis .

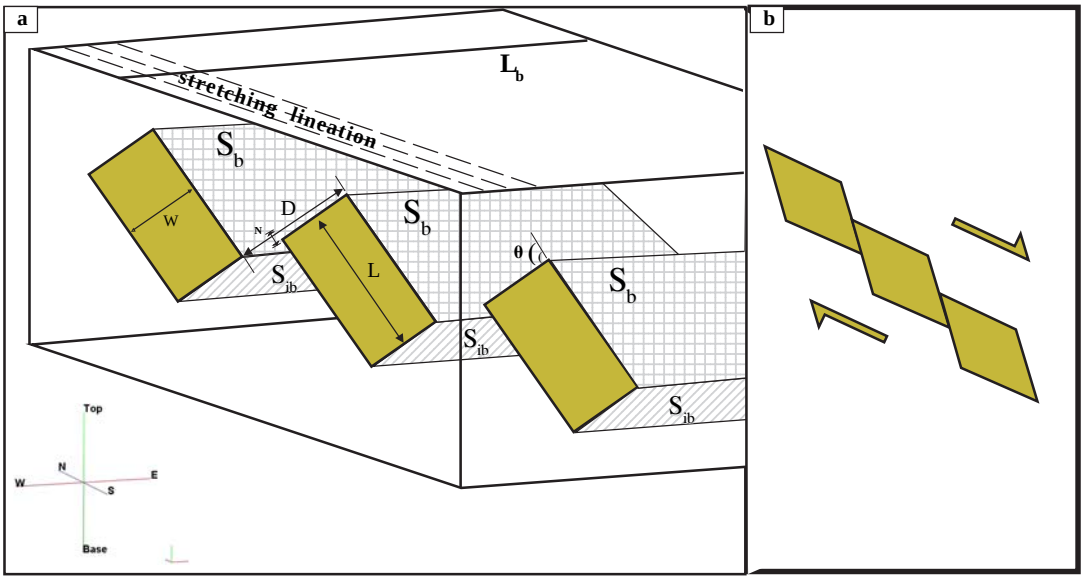

Figure 63: 3D structure (of the fig. 62), that shows the geomteric parameters of the shearband boudin fabric.

boudins, the forenamed described boudins are dominant S-slip boudins. The normalized displacement (D/W) is 1.9 (19cm/10cm) and 1.32 (9.25cm/7cm), while the S_{ib} dilation (N/L) is 0.039(2.5cm/21.3cm) and zero. The S_{ib} dilation appears low or none, which is in agreement with 39 boudins from elsewhere and from literature that have been studied from Goscombe & Passchier (2003). The latter ratios confirm that the

***Figure 64**:* A δ-type porphyroclast with folded tails.

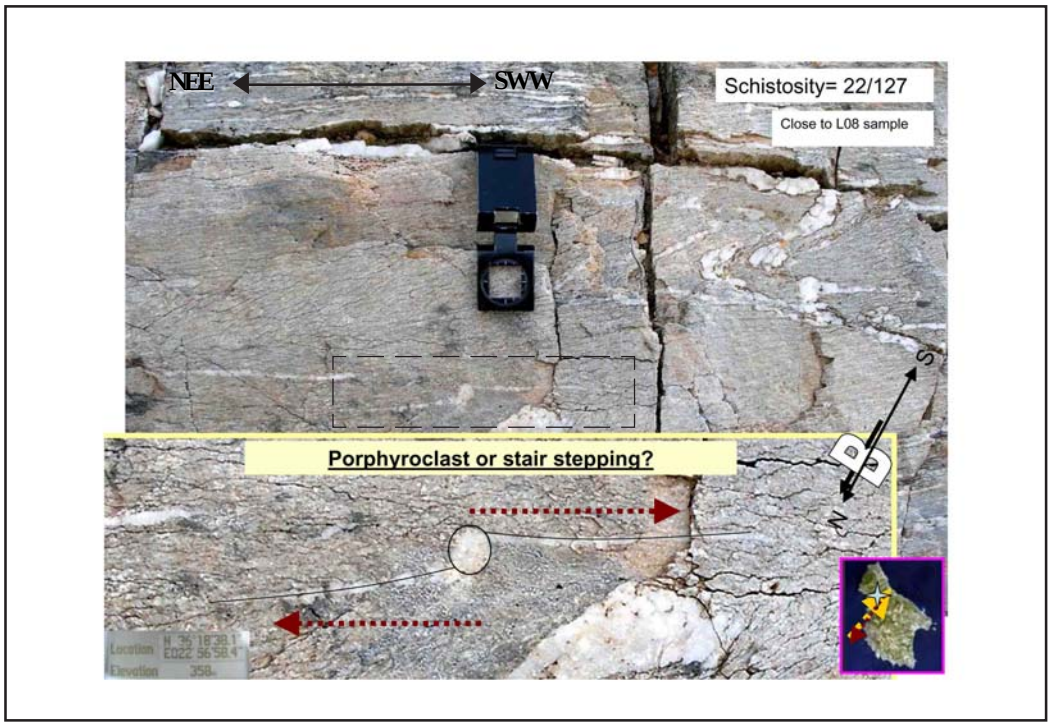

***Figure 65**:* A δ-type porphyroclast.

shearband boudins of Potamos area L08 location are dominant S-slip boudins.

Given such geometry, the sense of displacement on boudin-seperating shears would be in harmony with that of the overall shear zone which is later described and confirmed by near outcrops. For the locality illustrated at the outcrops of Potamos loca-

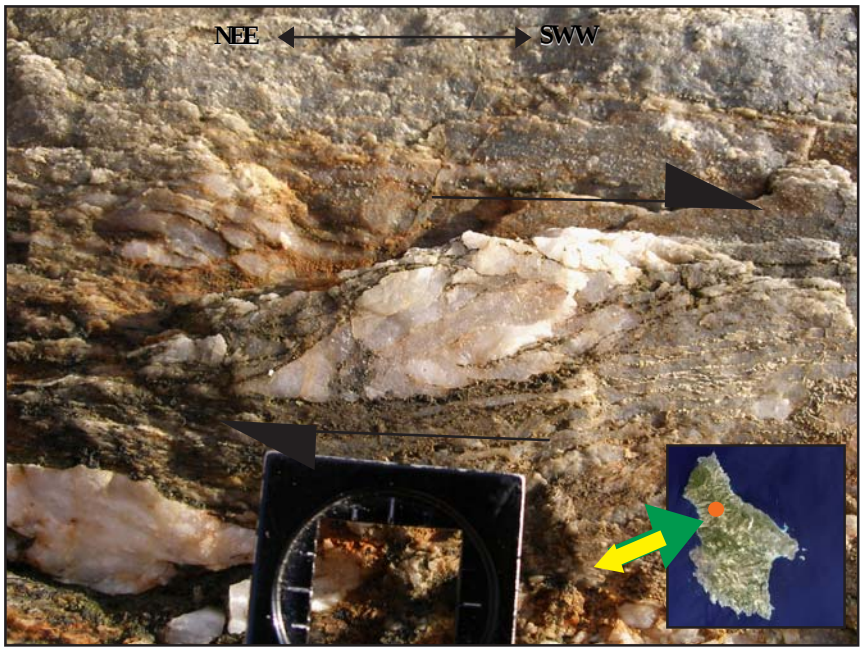

Figure 66: Quartz fish that implies a dextral shear sense of NEE-SWW trending, close to the Potamos area, location sample of L08.

tion, shear sense indicators such as C and S structure and microstructures of a wide variety of asymmetric structures describe a dextral shear sense of a generally NE-SW trending, implying a top-to-the southwest displacement.

Potamos - L08 outcrop - δ-type porphyroclast indicates a dextral shear sense of a top-to-the SW displacement

At the same outcrop, porphyroclasts of relic brittle deform feldspar crystals show the brittle deformation kinematics, as the quartz deformes around them. The sheared feldspar clast is small, rounded, implying the high deformation intensity. The nature and attitude of this crystal illustrate important kinematic indices. This porphyroclast can be termed as a δ – type porphyroclast. It occurs with a slightly elongate clast and in extented considerable distance of tails (horizontal lines) that cross an inferred central reference plane. These tails are thin, and present tight embayments that exist between the tail and porphyroclast. The kinematics analysis of the δ-type porphyroclast indicates a dextral shear sense (fig. 64, 65) of NE-SW trending.

Figure 67: Asymmetric structure of an S/C fabric on the outcrop of L08 sample Location of Potamos area.

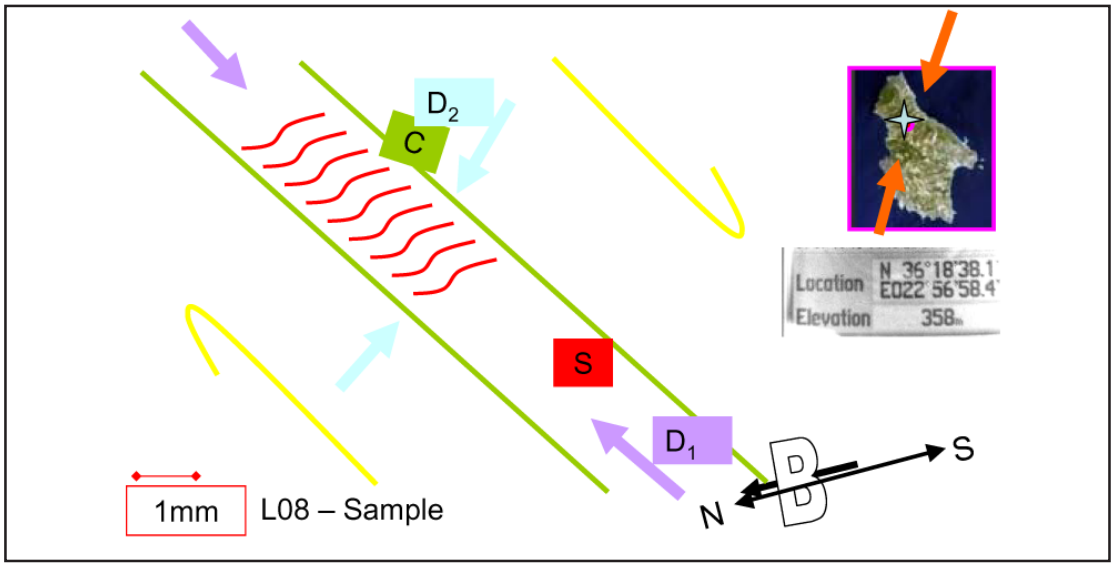

Figure 68: Schematic interpretation of the S/C fabric from the previous figure.

Potamos - L08 outcrop - Quartz fish indicates a top-to-the SWW displacement

Quartz fish, with a parallelogram-shape form, occurs close to the forenamed outcrops of Potamos area showing in agreement the dextral shear sense (fig. 66). It appears a lenticular shape with curved sides, ending in sharp tips. The sides of this fish are straight and parallel to foliation. The orientation of the microfault planes of the fish is parallel to the shortest side, continuing parallel or at a small angle to the long

axes of the fish. The microfaults separate the fish in smaller parts, implying the rapid deformation. The fragmentation of the fish infers the transitional zone brittle-ductile that deformation took place.

Potamos - L08 outcrop - S/C fabric indicates a top-to-the SW displacement

In a high strain experienced rocks as phyllites-quartzites are, at this outcrop of L08 Sample, were found two commonly develop fabrics (fig. 67) in association with the forenamed shearing. These were commonly developed simultaneously. They termed as S-C fabrics. The C surfaces are parallel with the shear zone margin, while the S surfaces are oblique to the C surfaces. The two cleavages are very distinctive at the field as well as at the figures (fig. 67, 68). The S-C surfaces configure a span angle of 20-45 degrees. As the angle decreases, so the density of C-surfaces increases. Concluding, we can estimate the sense of shear, which is illustrated (fig. 68), appears to be of dextral sense of NE-SW trending, implying a top-to-the southwest displacement. The presence of the indicated above S-C fabric, at the same outcrop, corroborates the kinematics evidence of the forenamed δ-type porphyroclast.

Potamos area - L01, L08 outcrop - Tension gashes indicate top-to-the SW displacement

At the L01 Sample's location outcrop, a tension, quartzed filled joint was observed (fig. 69). This was extracted from a cross section of a hand specimen. Unfortunately, it was difficult to observe the whole veins set, because of the development direction which was toward the inside of the bedrock, and any effort to extract them provokes ruins of the continued inferred tension gashes. However, I should note that close to this outcrop (1m distance), I was able to observe a different cross section of a joint set (fig. 70) with the similar direction of the previous oucrop, which is discussed

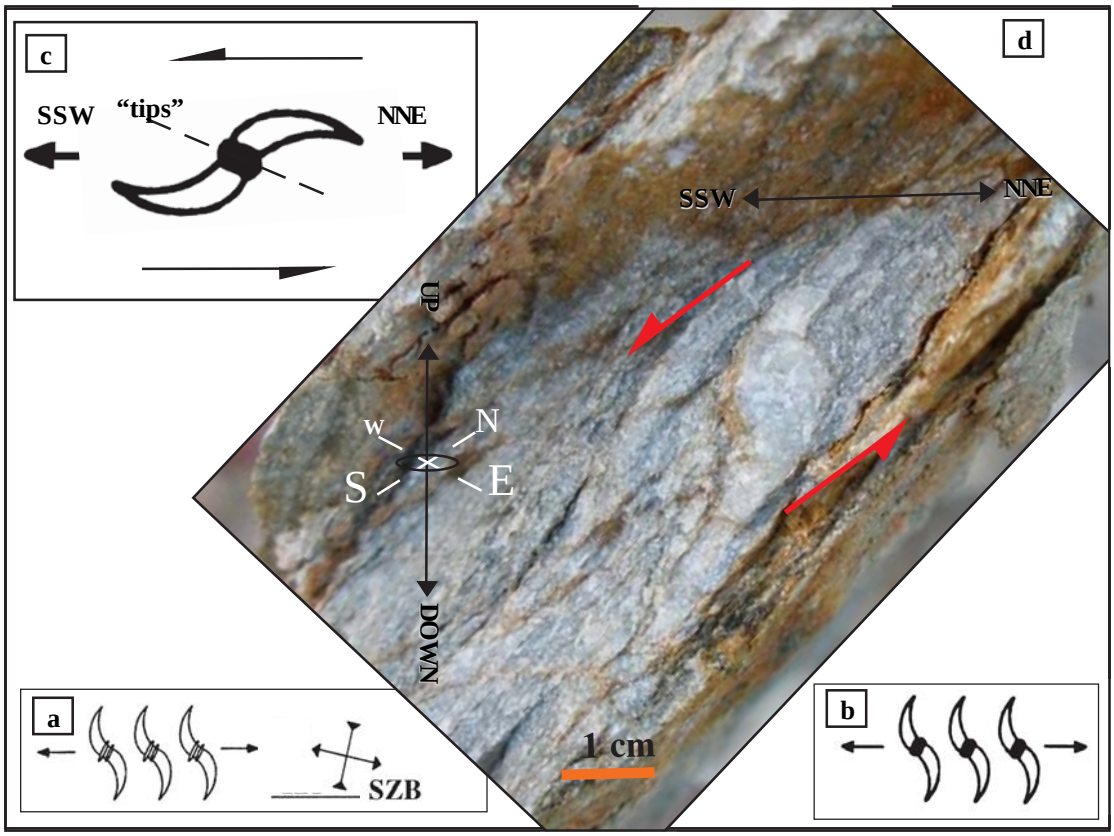

***Figure 69**:* (a) Schematic diagram of tension gashes in en-echelon arrangement in a shear zone with tips presented, ISA as Instanteneous Shear Axes and SZB as Shear zone boundary(from Passchier & Trouw, 1996), (b) Schematic diagram of tension gashes in en-echelon arrangement without tips, (c) Schematic diagram of kinematics analysis of the right adjusted photograph of the L01 Sample with inferred tips of less than 45 degrees. (d).

***Figure 70**:* Cross section of tension gashes in en-echelon arrangement implying inverted shear sense in a shear zone of SSW-NNE trending, without intensified tips.

later and it seems as a tension gashes set. In addition, the inferred direction of those forenamed small deformed cracks (implied as tension gashes) development, is of NNE-SSW trending.

If I assume that this single tension joint (fig. 69d) is a part of a tension gash development, then this is another testimonial of the indicated above kinematics analysis of the forenamed observed shear markers, at the southwestern mapped area. A small description follows of the single observed tension gash. According to this tension gash kinematics analysis, the maximum instantaneous extension is of NNE-SSW trending and took place at the brittle-ductile region. Additionally, the observed vein is without tips or it has the sight of implied tips that were not built up enough to be clarified as tips (fig. 69c). This could be happened, because of two main reasons. An absence of tips could be explained as a very rapid extension or shortening and not progressive deformation. The latter could be further strengthened by the correspondence of the almost straight veins and not curved that accompany the edges of the tension joint. From the other hand, this may not be a tension gash but a porphyroclast. It could be a porphyroclast, if the kinematic analysis should be reversely, in vertical direction, which contradicts to the all forenamed shear markers.

In terms of the second outcrop of the tension gashes set (fig. 70), these en-echelon arranged sets of veins were created closer to the brittle than to brittle-ductile region. The latter derives from the brittle evidence synchronous fracturing and solution-transfer and quartz precipitation. They opened to maximum widths of 1 cm, at low angle to the main foliation (i.e. they are near horizontal planar structures (25-30 degrees)). They are the structurally latest mineralized strain features, partly to completely mineralized with quartz-dominated assemblages. In this outcrop Riedel struc-

Figure 71: Quartzites host a boudinage of pinch and swell structure, implying extension of NEE-SWW trending, close to the Potamos area, location sample of L08.

tures are oversheared and apparently indicate an incorrect sense of shear. The latter is very common in mylonitic shear zones, and shows the danger of misinterpreting.

Specifically, these fractures were formed primary under shortening or stretching shear zone. The veins form as infilled extension fractures oblique to the shear-zone boundaries, and with continued deformation they become folded and rotated to sigmoidal shapes. Secondary, they were folded by a vertical compression axis. The observed curved veins were formed under a high compression of a secondary event (folding), to construct folded tension gashes and distorted shear sense indicators, confusing the kinematics analysis as they illustrate an opposite direction of shear sense (fig. 70).

According to Mawer (1989), long, thin veins such of these (fig. 70) become folded by buckling as they rotate during shearing, undergo a shear of the reverse sense to the overall shear zone, resulting in minor folds of the vein with apparently the wrong asymmetry for the major zone of shear. These sorts of structures are relatively common in

greenschist-facies shear zones. The synchronous and cyclical operation of brittle-solution-transfer/crystal-plastic deformational mechanism is particularly clear in this case.

These outcrop locations at the north area of Potamos village - systematically - show the kinematics of the metamorphic nappe exhumation process. Consequently, it should not be taken care about of penetrative structures or localized micro-shear apparent displacements. This area represents a bulk deformation of the NNE-SSW kinematics orientation and direction of sinistral horizontal displacement. Finally, it is reasonable to validate that the south-center part of the mapped area has a sinistral shear sense of a NNE-SSW trending, implying a top-to the south-southwest displacement.

Potamos area - Outcrop of L07 - Pinch and swell quartz boudinage

Close to the location sample of L07, at Potamos area, pinch and swell quartz structures occur in the quartzite layers, implying the extension of NNW-SSE trending (fig. 71). The basic reason for this structure is the differences in competency between the boudin layer and the adjacent quartzite mica-riched rock. Lenticular boudins formed by complete necking-down in response to tensile stress. The specific boudins are deformed and appear a smooth sinistral rotation in a fashion which may be an inconsiderable indication of shear movement and could be as a result of the continuous foliation. Foliation is parallel to the boudin trains. However, it should be note that the dextral shear movement to the layering in the adjacent quartzites is in agreement with the previous found kinematic indicators.

According to Hanmer (1986), the previous forenamed pinch and swell structure corresponds to type II. The lattest is supported by the criteria that type II boudins are not display a clear truncation of any internal fabric of the boudinaged layer. In addi-

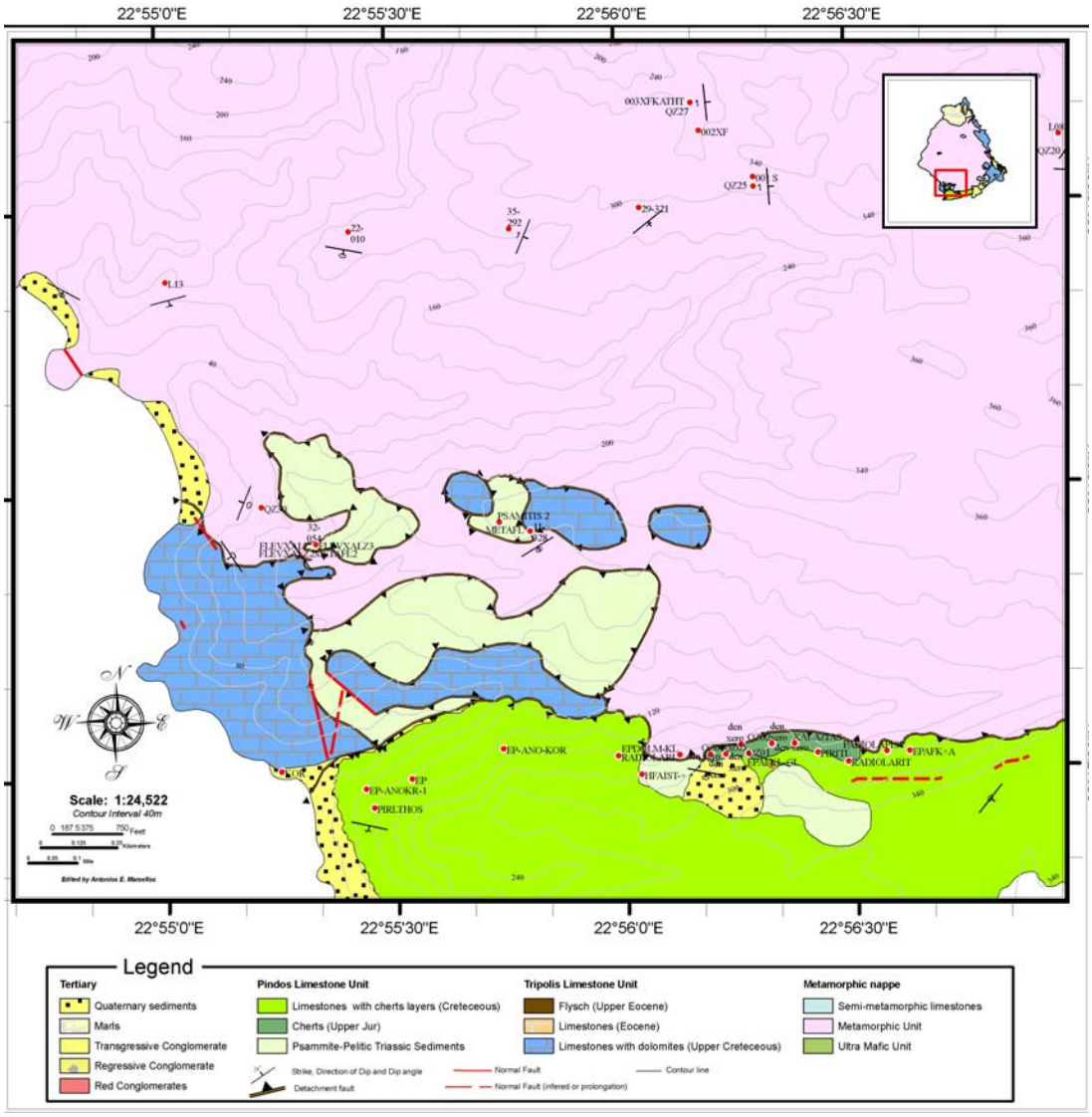

Figure 72: Southwestern mapped area of the detachment fault

tion, the same boudinaged layer does not appear any significant rotation of the boudins. Finally, we could conclude that this quartzite layer appears an intensive extensional boudinage as a posteriori tectonic event of shearing as there is no clarified evidence of intensive shear sense. Shearing could have been paused, or took place apriori or in a NNW-SSE trending which is not being visible on this outcrop, while extension continues until today. Normal faults on pleiocene and pleiostocene sediments confirm the extensional field that occurs until today.

Moreover, Gaudemer & Tapponier (1987) have suggested that fractures which

are integral to the formation of type III boudinage may initiate as shear (mode II) fractures. If we compare the shearing and extension roles the figures (fig. 58 and 71), then we could conclude that intensive shearing took place first (fig. 58), while extension followed until today (fig. 71). In detail, it is not clarified if the extension started at the same time as shearing, but during the shearing event, extension had already begun.

4. Likodimou area (souhwestern area of the map)

The detachment fault brings the Tripolis Cretaceous limestones, Pindos Jurassic cherts and Pindos Flysch to lie against the metamorphic occurrence. The west side of the map is not as high sequence faulting area as the east side is.

They were found two faults of NW-SE and NNW-SSE trending, close to the coast and at the north side of the street Logothetianika - coast of Likodimou, and bring the flysch of Tripolis to lie against the Cretaceous limestones of Tripolis (fig. 72). Any wrench movement at the faults was hard to be distinguished. The NW-SE trending fault is almost vertical to near upright and dipped to west, while the NNW-SSE trending fault is almost vertical to near upright and dipped to east. A throw of 2m is visible of both faults. The area between the faults is therefore a fault-trough. The contact between the Cretaceous Pindos limestones and its succeeded flysch is covered locally by a strip of alluvium in the river.

Likodimou area - Seath folds between Cretaceous Pindos limestones and Jurassic Pindos cherts.

The Upper Jurassic cherts of Pindos are succeeded by the Cretaceous limestones of Pindos. The latter contact appears, in some places, to have been intruded by the upper Jurassic chert of Pindos, the underneath layer or to the opposite (fig. 73). It

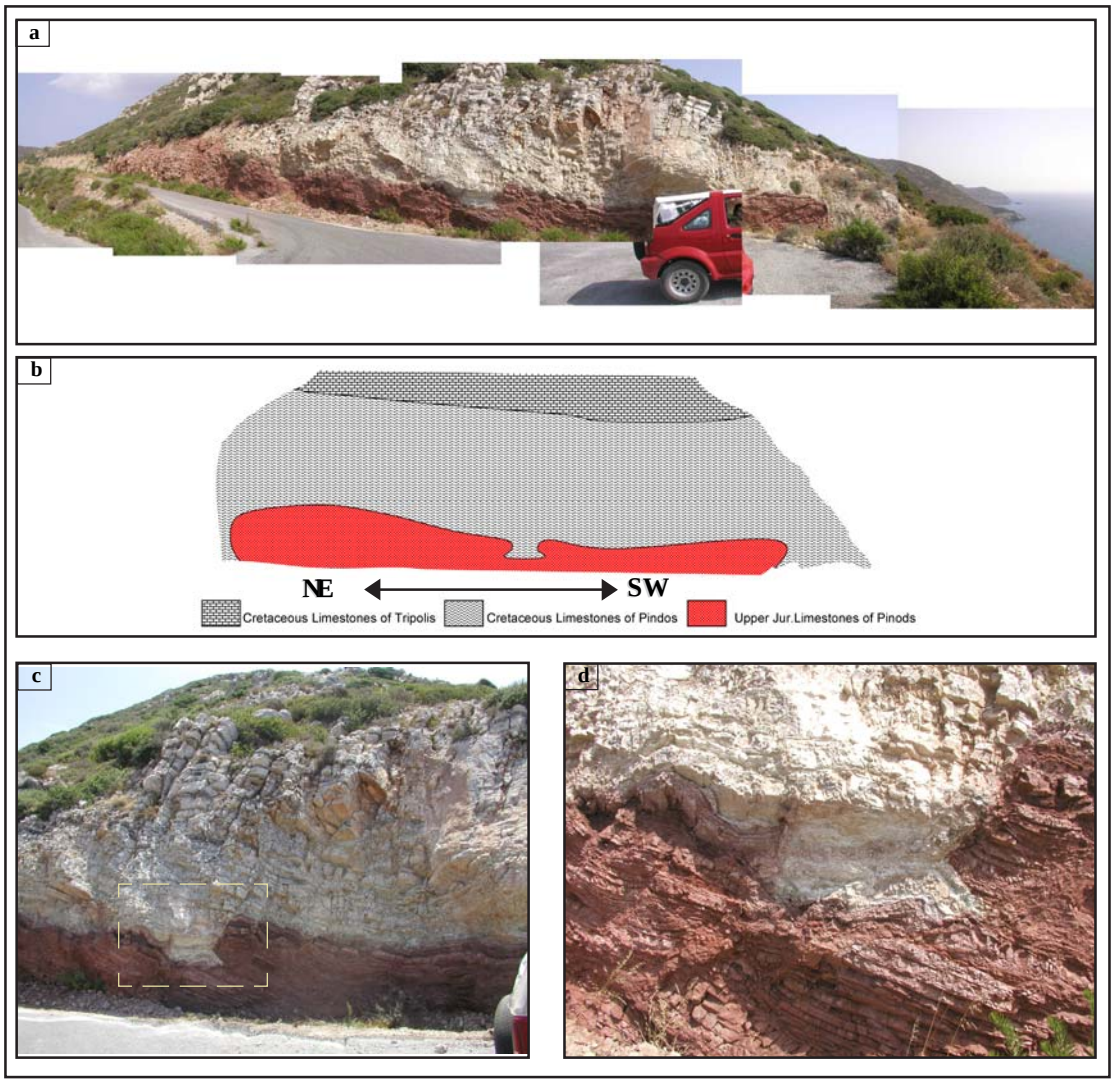

Figure 73: (a,b,c) Seath fold structures (a,b: major seath fold, c,d: minor seath fold) that may be related to the pre-extensional crustal thickening episode of pre-alpine orogen, which culminated in the Late Eocene in the Aegean region,

seems that have undertaken a big stress, which concluded to create small minor structures of folding and faulting associated with hydrothermal liquid alteration among this contact. The below upper Jurassic cherts yield effortlessly to folding by penetrative movements of the above Cretaceous Pindos limestones, along preexisting weaknesses of the underneath upper Jurassic Pindos cherts. The structures occur by the form of Seath folds, which could be related to the pre-extensional crustal thickening episode of pre-alpine orogen, which culminated in the Late Eocene in the Aegean region (Blake et al., 1981; Bonneau and Kienast, 1982).

***Figure 74**:* Neogene disconformity on top of Cretaceous folded Pindos limestones

At the east side of the Likodimou mapped area, at the exit road of Logothetianika village to Likodimou beach, there are limitless folds of Upper Cretaceous limestones of Pindos. The latter limestones appear also at the Likodimou beach, below the neogene sediments. Between the latter two observations the limestones appear to be not folded and inclined between these two locations, at the road that connects the Likodimou beach and the Logothetianika village. The latest observation could be derived from the aspect that we see through the cross section of the fold axis of the folded Cretaceous limestones of Pindos.

Likodimos area - Neogene unconformity on top of isoclinal folded Cretaceous limestones of Pindos

The limitless but mostly isoclinal folds of Cretaceous Limestone of Pindos achieved a true bending but without significant slippages between the layers. The Cretaceous limestones of Pindos are of pelagic deep sea sedimentation and they lack non rigid layers. Although the stiff layers retained their original thicknesses, in contrast they

Figure 75: Quaternary sediments in a form of alluvial fan model.

Figure 76: Neogene disconformity on top of Cretaceous folded Pindos limestones

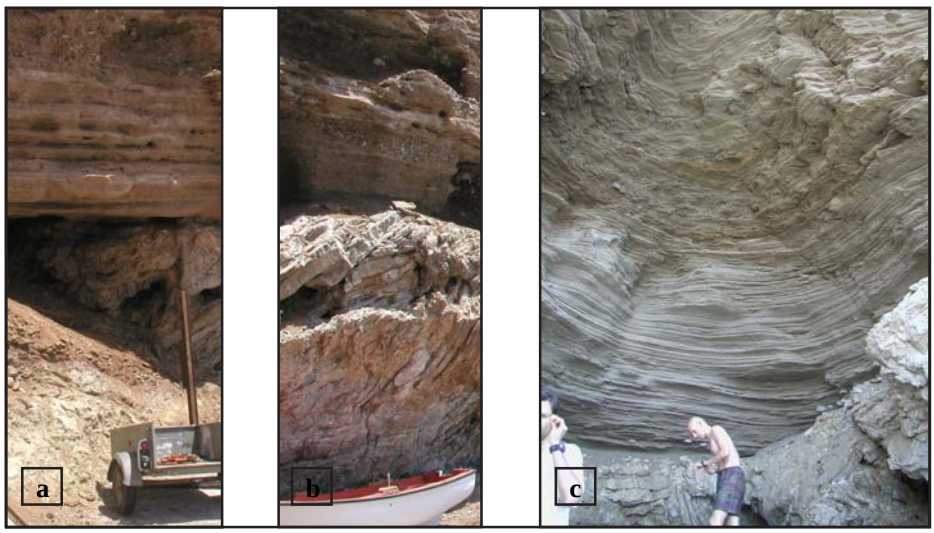

Figure 77: Quaternary deposits of various diameter of gravel, cobbles and pebbles on top of the Cretaceous folded Pindos limestones

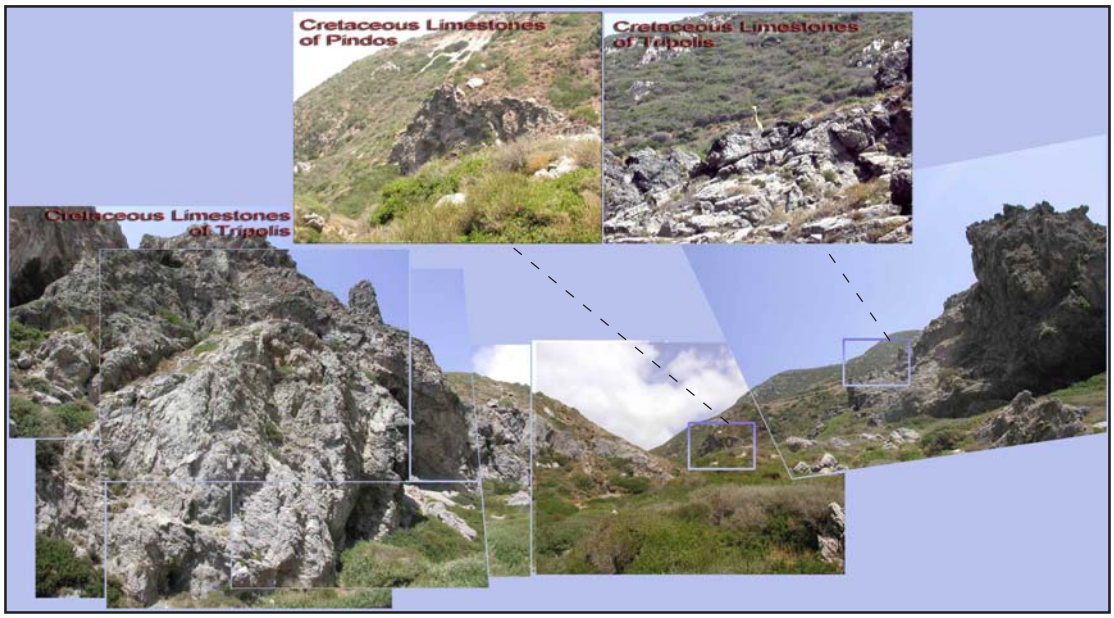

Figure 77: Tectonic escape of Tripolis unit - Likodimos area.

appear as flexural-flow folds without any high ductile layers. As it was forenamed, the folded upper Cretaceous limestones of Pindos were covered by the neogene disconformity (fig. 74). According to Papanikolaou (1986), the Pindos nappe limestone was moving for 35 myrs. The duration of this "travel" started from middle Eocene, when its flysch sedimentation stopped, until the middle Miocene, where the neogene sediments were deposited at the syncline of Epirus – Akarnanias (Northwestern Greece). This time period represents almost the whole orogenic history of Hellinides. As a result we could conclude that the folding event of Pindos limestones took place before the middle Miocene at Cretaceous limestones of Pindos occurrence at Kythera Island.

Likodimos area - Quaternary sediments

At the Likodimos coast area, quaternary sediments appear in a form of an alluvial fan model (fig. 75), and lie uncomfortably on the folded cretaceous limestones of Pindos, and mark the locally incoming of tectonic uplift and sea submerse conditions at the Neogene time in comparison to the folding of the older sedimentary series. The

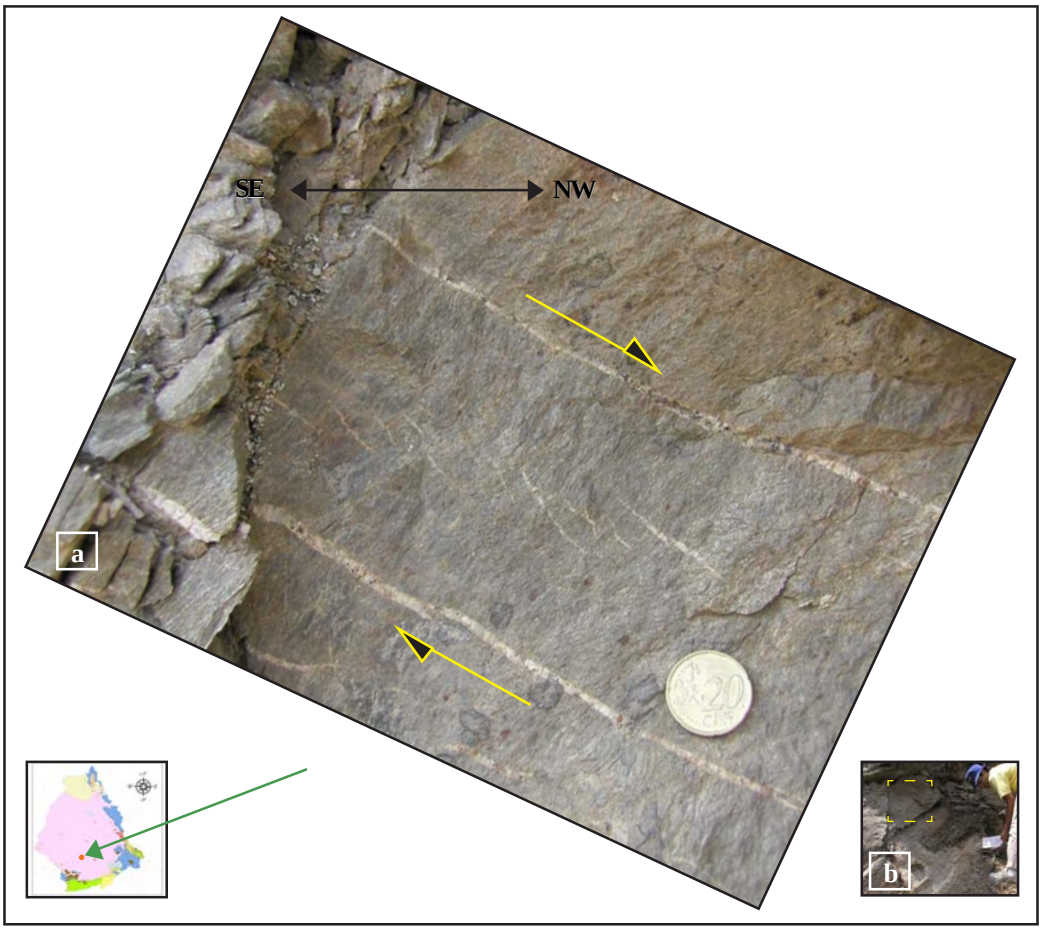

Figure 78: Tension gashes at the location area of sample QZ27 - 3km Northwestern of Potamos village.

quaternary sediments appear as almost horizontal sandstone bedding and terrigenous sediments of gravel debris flows, pebbles and cobbles (from bottom to top – Likodimou coast area). According to the indicated above series of sediments, these could be characterized as regressive sediments. The gravel sediments are red, probably because of a combination of a source area that supplies iron-rich minerals and a semiarid climate that produces an oxidizing vadoze groundwater zone. The regressive deposits are characterized by a thickness of 7-8m, while the gravel debris are of 6-7m. The sandstone occurs in 1-2 m thickness at the bottom and toward the top more coarse grains with pebbles and cobbles appear (fig. 77a-c). Both of quaternary deposits are southeastwards inclined about 2-4 degrees (fig. 75). The latter denotes the presence of the

detachment fault to be in a nearby distance at an opposite direction (north) of the dipping quaternary sediments. Furthermore, it would be wrong not to note that the transition from the folding Cretaceous limestones of Pindos to tertiary sediments appears within a 30-40cm layer of limestone gravel with a red silk matrix (fig. 76). The latter interfered layer denotes the rapid exposition of the folded Cretaceous limestones of Pindos to a sedimentation process of a deep sea and better explained to a rapid and small period of transgression setting. The latter interefered layer could be explained as a transgressive sediment layer or (?) as a high shear sense movement between the folded Cretaceous limestones of Pindos and the neogene sediments, that detached Pindos limestones' fragments.

Likodimos area - Tectonic escape of Tripolis limestone's unit below the Pindos limestone's unit

Cretaceous limestones of Tripolis unit appear to have tectonic escape caused by the rapid uplift and exhumation of othe metamorphic nappe. The latter observation was made close to the Likodimos area, north of the Likodimos coast. At this area, Cretaceous limestones of Tripolis appear to have escape tectonically between the below clastic Triassic sediments of Pindos and the metamorphic nappe, and lie against the Cretaceous limestones of Pindos and the Metamorphic nappe (fig. 77).

Agia Marina - Outcrop of QZ27 - Tension gashes indicate an opposite shear sense of the major pattern - Bookself structure

At the QZ27 Sample's location outcrop (fig. 78), a tension, quartzed filled set of veins was observed. It is believed that these are tension gashes according to their description. This is a testimonial of the kinematics analysis of the area close to the sample QZ27. Dextral displacement information on a dipping surface towards north-

Figure 79: Sinistral tension gashes at Ligia coast area (C2 sample location).

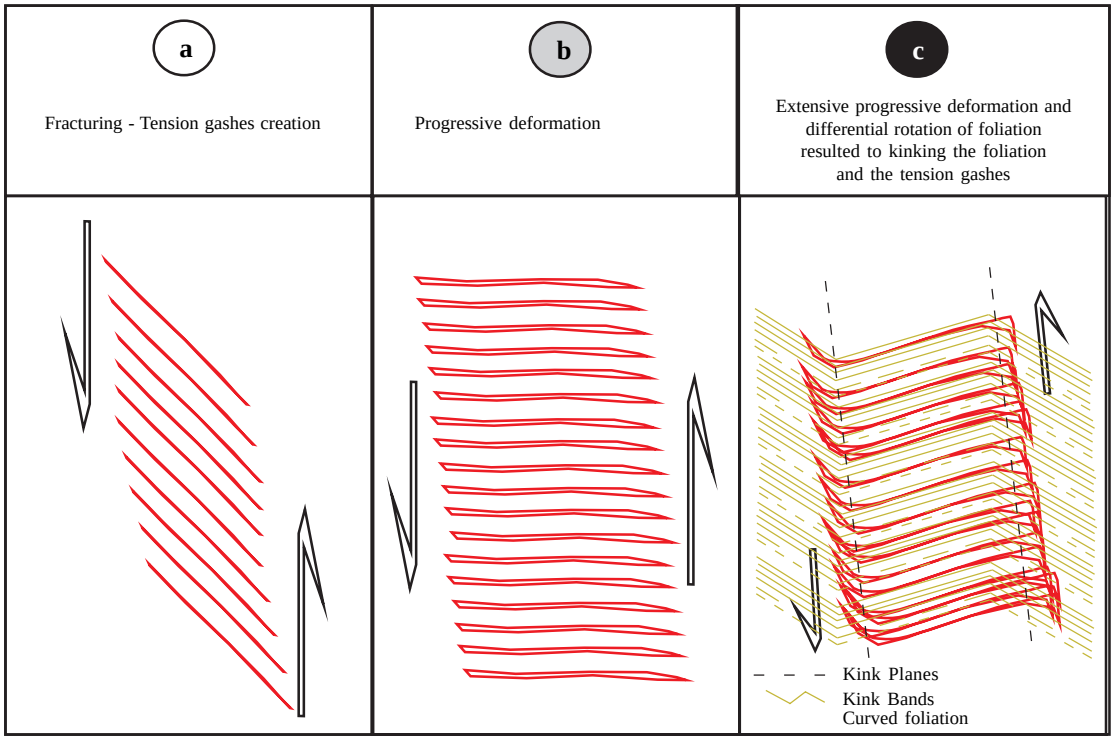

Figure 80: Schematic evolution of the depicted tension gashes of Ligia coast area (C2).

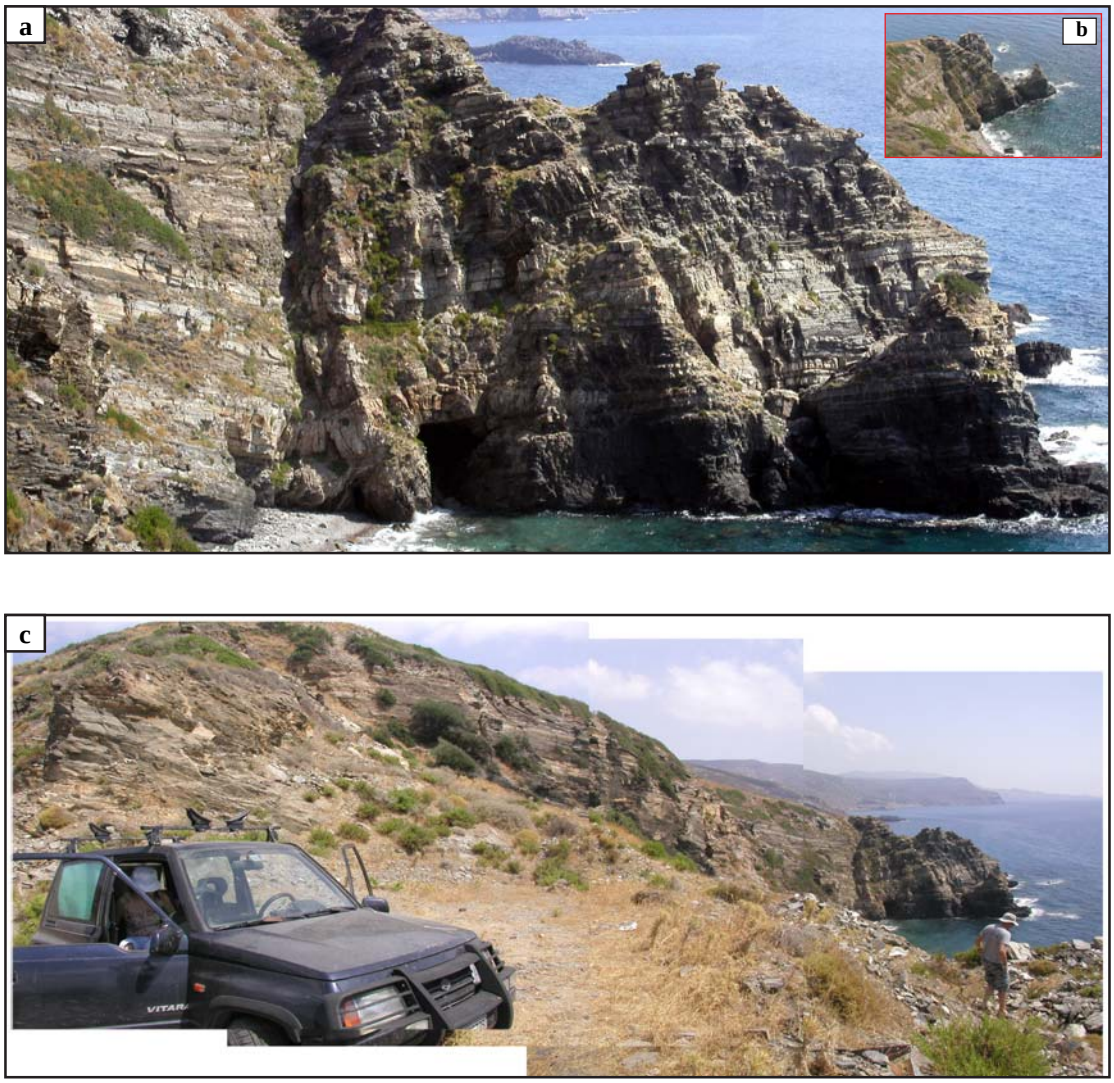

Figure 81: C2 Location, Ligia area.

west derives from the kinematics analysis of the QZ27 sample of tension gashes. The tension gashes took place at the brittle region. It was hard to distinguish tips or their angle at the observed veins. However, one or two were found, as well as, most of these edges were almost straight veins, but two of them appear lightly bending at the edges of the tension joints, to confirm that lightly progressive deformation took place during those tension gashes formation.

These en-echelon arranged set of veins opened to maximum width of 1-3 mm at approximately vertical angle to the main foliation (80-90degrees). It is unknown if they were formed primary under shortening or stretching shear zone because it was

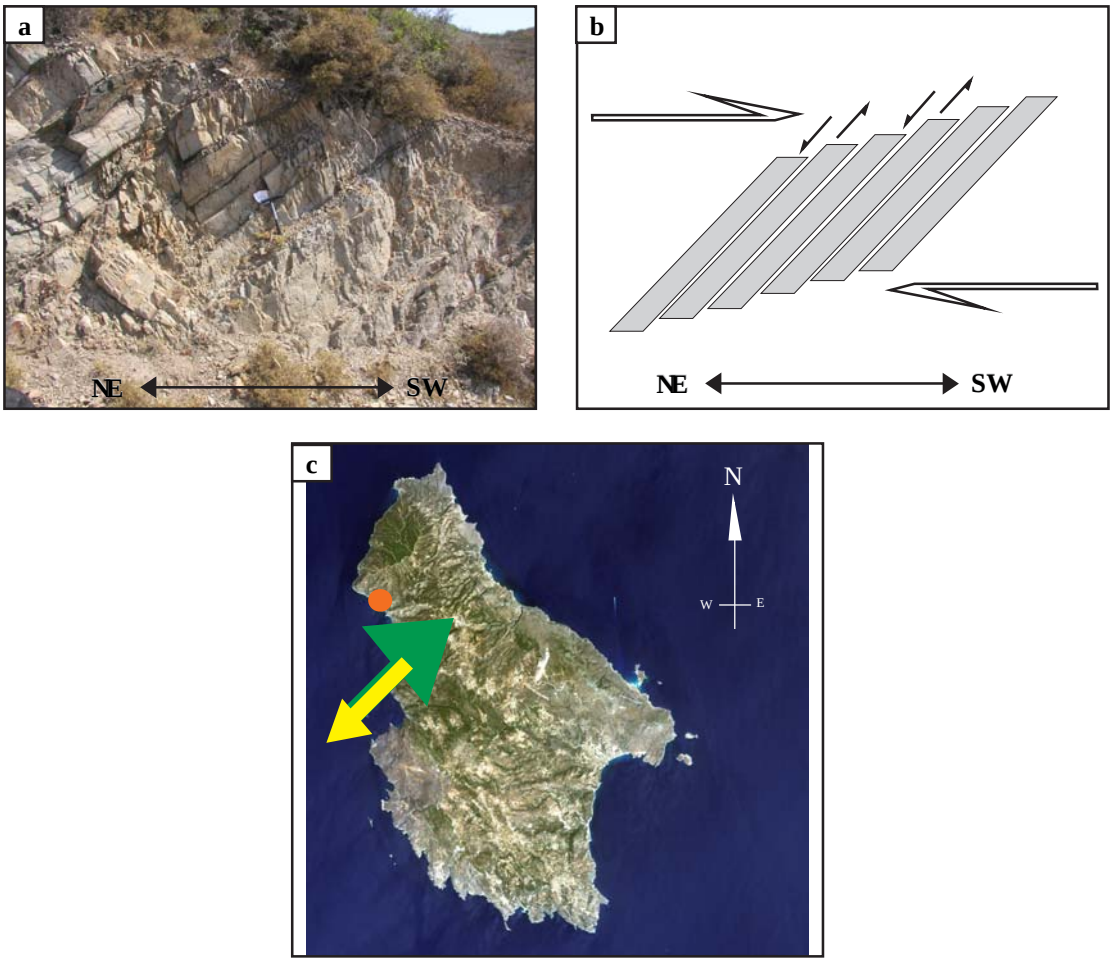

***Figure 82**:* a. Location of sample Metafl2 at the outcrop of the intermittent well bedding quartzites layers by shaly layers, b. schematic diagram to illustrate the interpretetion of quartzite layers' sinistrial shear sense within a top-to-the-southwest shear zone, c. geographic reference frame depicting the kinematics of the shear zone on the locality of Metafl2 (red spot).

difficult to observe their tips.

Ligia area - Outcrop of C2 - Vein set arrays of tension gashes indicate an opposite shear sense of the major pattern - Bookself structure

At the Ligia outcrop location of sample C2 (fig. 79), quartzed filled set of veins, almost parallel to foliation were observed. The forenamed en enchelon gash vein sets are arranged in perpendicular bearing lines to the outcrops of NEE-SWW trending. Each vein trends at almost vertical angle to the line of bearing of the set as a whole. Some veins are thickest at their centers and some other are thickest towards their margins. Progressive deformation caused bending at the gashes' margins while the

Figure 83: An S-shaped drag fold result from counterclockwise internal rotation, close to location sample of L13 (flevxalz or Metafl2).

occurrence of some thicker gashes owe to combination of two or more gashes of different size. The character of these en echelon fractures implies that these are tension gashes.

Primary, the veins formed 45 degrees to the shear zone by simple shear (fig. 80a). New formed veins accumulate at the same location, and they were continuing to form in accordance with the instantaneous stretching axes of NEE-SWW trending. Multiple generations of old and younger veins, more or less deformed respectively, and form curved vein geometry. Once formed, progressive deformation provoked veins to start shortening; they partially rotated over (fig. 80a-b), toward the direction of a sinistrial shear. The foliation, which was observed at the outcrop, possible formed, primary, from rapid uplift, when the metamorphic nappe was exhuming to the surface. Finally, the differential rotation of foliation creates the curved – almost sigmoidal – foliation pattern. Folded foliation was the last event, showing Kink bands. The Kink Planes are of vertical lines to the surface (fig. 80c), implying a parallel compressional

axes of the same trending as the outcrops show at the Ligia area (NEE-SWW).

The main goal to study the shear zone and the responsible cause, that provoke the fracturing, was accomplished by determining the sinistrial shear at the forenamed outcrop, but this outcrop appears as an exception comparing to the outcrops closer to the southwestern part of the detachment fault, implying an interpretation of an apparent shear sense and not the correct. However, further investigation below displays another explanation of the forenamed sinistrial shear sense.

Ligia area - Outcrop of METAFL2 - S-shaped Drag Fold and tension gashes indicate an opposite shear sense of the major pattern - Bookself structure

An outcrop close to the QZ30 by the name of METAFL2, shows well defined bedding quartzite layers plunging 32°NE intermittent by phyllite layers (fig. 82a). An S-shaped drag fold (fig. 83) was observed on one of the quartzite layers indicating the sinistrial sense of simple shear movement. This is the same sense of shear as the C2 location, which is almost 500-700m northern of the current discussed location. The fold occurs on a NE-SW trending outcrop, implying the same kinematics bearing. The fold was further composed as tight asymmetrical drag fold by counterclockwise internal rotation, identifying the sinistrial sense of simple shear.

The C2 location is prominently a bookself structure. The previous kinematic indicator should be observed under a smaller scale. In a wider angle of observation, a deformation apparatus of wedge models and normal faulting reveals an opposite kinematic sense. The wedge models deformation takes place at the depth of the 40-70 km, where the Benioff zone occurs. Normal faulting creates horst and graben at the surface. From a close observation of scarps and fault lines of NW-SE trending, and kinematic indicators at the forenamed location, close to areas Likodimou and Ligia show

***Figure 84**:* A pinch-and-swell structure showing a boudin by layer-parallel stretching at oucrop of L13 sample location.

the presence of a horst at the shoreline of the forenamed area and a graben towards the island on NE-SW trending. The latest region of normal faulting appears significant rotation of hanging-wall and footwall strata, and it could be characterized as a case of listric normal faulting (fig. 81). This could be reasonable if we consider the presence of a larger low-angle fault, which has provoked a profound crustal stretching. The latest result could be derived from a detachment fault which is located at the vicinity.

According to the figures (fig. 82a-b and fig. 83), we can determine the dextral kinematic sense of this area. That derives from the observation of the extensional crenulation of the quartzite which developed as a consequence of coaxial flattening oblique to a pre-existing foliation (Platt and Vissers, 1980). The quartzite layers at this situation act anisotropically and create antithetically rotated extensional structures defining a dextral kinematic sense. When the quartzite layers lie at a low angle to the shear zone, then the displacements indicate with confidence the bulk shear sense. At our outcrop of Metafl2 the bulk shearing appears in a more complex way. The relative

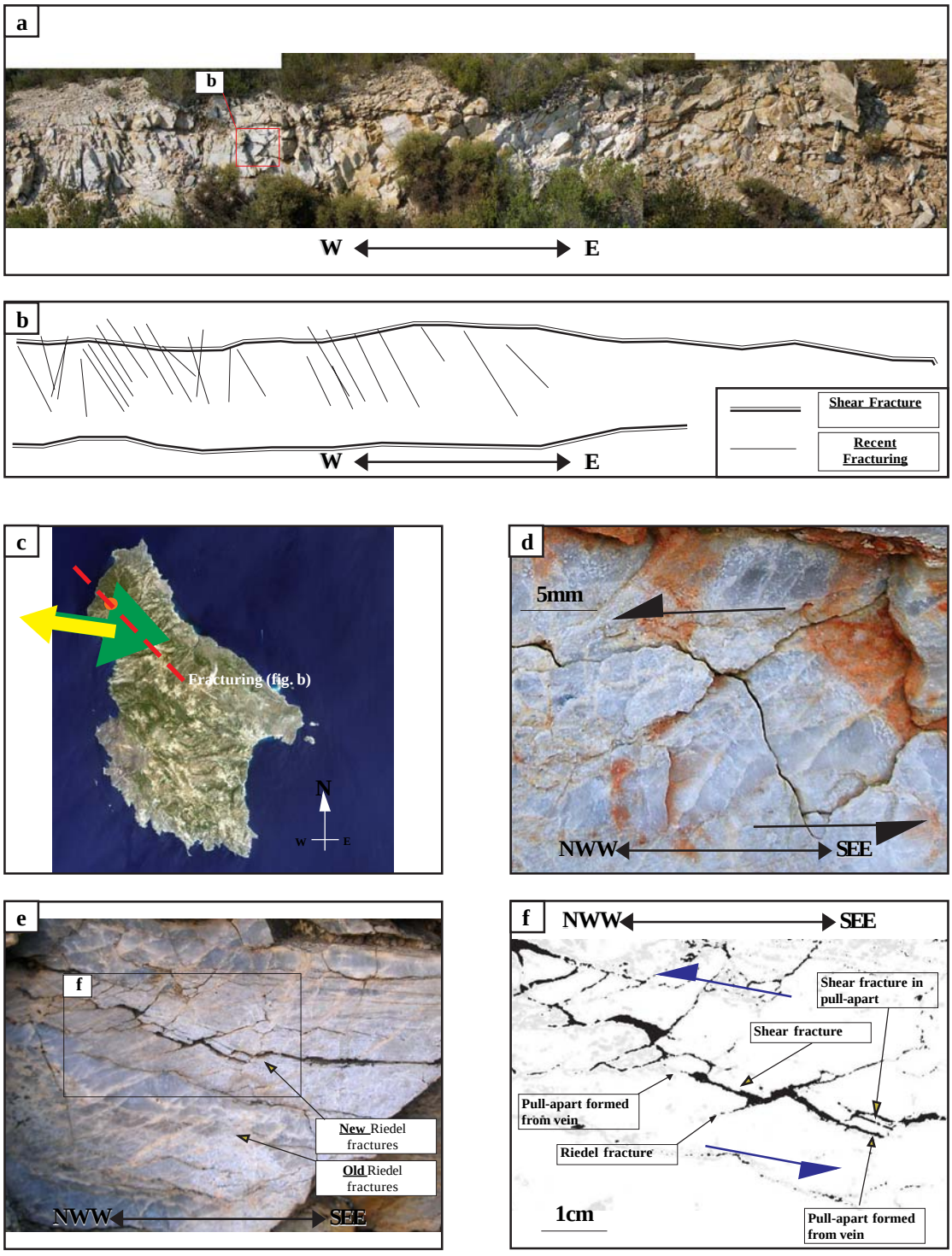

Figure 85: , (a) Outcrop marbles that hosts swarm of tension gashes that indicate a top-to-the southeast displacement, (b) scheme of interpretation of the (a), (c) geographic frame reference that depicts the determined shear sense indicator (e) pull apart array of tension gashes, (f) scheme of interpretation of the (e).

movements of the shaly-quartzite layers initially oriented at high angles to the shear zone show antithetic displacement. Synthetically rotation of the shaly-quartzite layers

provokes antithetic displacements.

The latter observation could be better explained by the example of rigid body movements along surfaces. Bedding surfaces were activated during flexural-slip folding. The beds slip relative to one another, like pages in a book (Davis, 1996). The well illustrated phenomenon of the sheared stack of books or cards by Etchecopar, (1977) emphasized the opposite sense of shear of the quartzite layers that occurs at the outcrop of Metafl2. The C2 location (fig. 81) is prominently a result of flexural-slip folding or a bookself structure. Specifically, antithetic microshears are produced during synthetic rotation of the fragments as a domino-like microstruture (fig. 82b). This assumption resolves the ambiguity that the sinistrial sense of shear is an exemption of the overall scene at the western mapped area below the detachment, while it reveals the opposite, dextral shear sense and specifically top-to-the southwest displacement.

Ligia area - Outcrop of L13 - Pinch and swell boudin structure

Northwestern of the QZ30 and METAFL outcrop, there is a boudin quartz formation at the outcrop of L13 sample location (fig. 84). A pinch-and-swell structure hosts the quartz's boudin. This formation was caused in a ductile setting by layer-parallel stretching. The latter hypothesis is further strengthened by the correspondence of the ductility contrast between the layers. The stiffer layers (quartz parallel veins to bedding) appear to have been pinched, necked but not break. The soft layers which are mostly phyllite don't host any special cleavage besides the cleavage which is associated to boudins. Layer-parallel stretching on the outer arc of an inferred antiform, that hosts the metamorphic nappe, could explain the achievement of boudinage and pinch-and-swell structures that occur on the outcrop of L13 sample location.

Natura area - Outcrop of L18 - Marbles host swarm of tension gashes - Indicates a

top-to-the West displacement

At the sample location of L18, marbles occur on top of the metamorphic unit. This outcrop of W-E trending hosts numerous tension gashes which show a dextral shear sense, inferring a top-to-the west displacement, however a more precise determination of shear follows below. At this outcrop the vein array set of tension quartzed gashes took place at the brittle region and caused as a result of shear on NWW-SEE direction (bearing of outcrop). It was hard to distinguish any tips as they appear in planar shape to almost sigmoidal. Sigmoidal shape takes place, due to passive rotation of the central portion of fractures in the deformation zone and continued growth at the fracture tips (Olson & Pollard, 1991). In addition, it was observed that these en-echelon arranged set of veins have an opening width of 1-9 mm. Moreover, the figure (fig. 85f) demonstrates how vein arrays evolve into pull-apart arrays through dilation of the veins between overstepping shears in a micro-scale that may be eventually faulted (Gammond, 1983; Peacock & Sanderson, 1995). Specifically, vein arrays evolved into pull-apart arrays through dilation of the veins between overstepping shears were observed and may be eventually faulted (Cowied & Scholz, 1992). In a metro-scale, it was observed a large shear fracture (fig. 85b) accompanied with recent fracturing of NW-SE trending and northeastern dipping , which in some places reveals normal faulting. The latter implies broken and displaced blocks of marbles on a direction that reveals dextral shear sense kinematics of NEE-SWW trending.

Lineation

They were found a large variety of lineation. From lineations, as parallel alignements of elongate, linear fabric elements in the rock bodies, commonly penetrative at the outcrop of hand speciments of observation, to lineations of very penetrative

intensity fabric that the lineated rock depicts a very etched grain, which is visible from a couple meters away of the outcrops (L23 Sample location). Secondary lineations were able to found on the metamorphic specimens showing their deformation during metamorphism and shearing, or either one as a separated process. They were distinguished almost all the types of lineations, such as strong stretched lineation , horizontal stretched lineation constructed by a parallel-linear arrangement of minerals in the rock, intersection lineation, crenulation lineation and mineral lineation. However, possible mistakes may be hidden under the complex tectonic history of Kythera Island that may host more than one lineation's family, as multiple extensional events.

At the north area of the island, most of the lineations show a NW-SE and NE-SW trending. The latter implies the complex tectonomorphic history of Kythera Island. Furthermore, according to the mapped lineations (fig. 86a) we could estimate a pattern of an inferred broad antiform of a NW-SE fold axis that hosts the PQU, as well as an inferred broad syncline of a NW-SE fold axis western of the above forenamed antiform.

A subsidiary syncline is indicated by the arrow of L21 sample – west area of the map – lineation which trends NNE-SSW. The latter deviated lineation from the main pattern of the antiform may imply the continuity of the folding event of NE-SW trending, consequently it indicates an inferred broad disrupted syncline. The syncline has undergone serious normal faulting that stops to the northwestern coast of Kythera Island. Finally, more lineament analysis using remote sensing would be beyond the scope of this thesis research, which is a future study on this area.

Map of shear sense indicators

The map area of the north part of Kythera Island is interpreted as two different

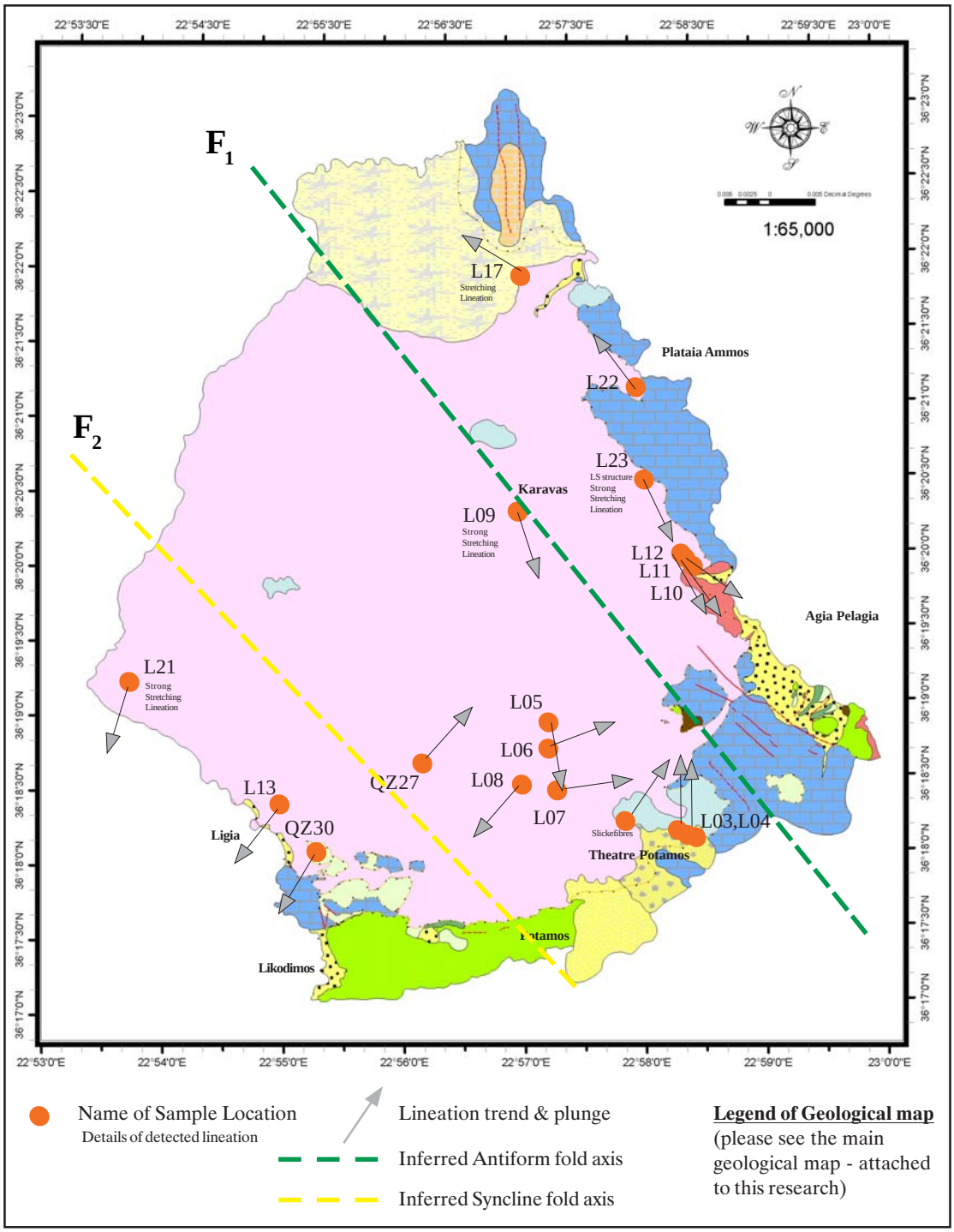

Figure 86a: Plotted lineations from some of the sample locations of field measurements on the constructed geological map.

kind of broad verging shear-sense indications. The one occurs at the west coast line of the north part of Kythera Island, determining an almost top-to-the southwest displacement. The other occurs at the east coast line of the north part of Kythera Island, determining an almost top-to-the southeast displacement. The sense of shear is almost constant across east and west coasts of Kythera Island.

All the above interpreted outcrops that host shear-sense indicators were plotted on the mapped area (fig. 86b) of the current research. These results support an ideal model of a symmetrical displacement of simultaneously top-to-the southeast or east and top-to-the southwest or west direction. The overall map distribution of the shear-sense indicators along the inferred detachment fault determines a symmetrical gravitational displacement caused from the antiform of the Late Miocene folding event. Considering the simultaneously folding – associated with the rapid uplift and exhumation - and extension event on the trending of NW-SE, we may conclude that the detachment is occurring paralleling to the Kythera strait on the same direction. Although, a spatial reconstruction map of the above interpreted shear-sense indicators would be fascinated in order to clarified the exact architecture of this kind of detachment, this kind of research would be beyond this first step of mapping the shear sense indicators.

Riedel Fractures on a very small scale - Mountain ridges Agia Moni and Agia Elesa

Pull-apart arrays through dilation of the veins between overstepping, may eventually faulted (Cowie and Scholz, 1992). Pull-aparts occur in dilational jogs between overstepping shear fractures (Sibson, 1989) or between extensional fractures (Riedel fractures) over several orders of magnitude (Aydin and Nur., 1982), from the milli-

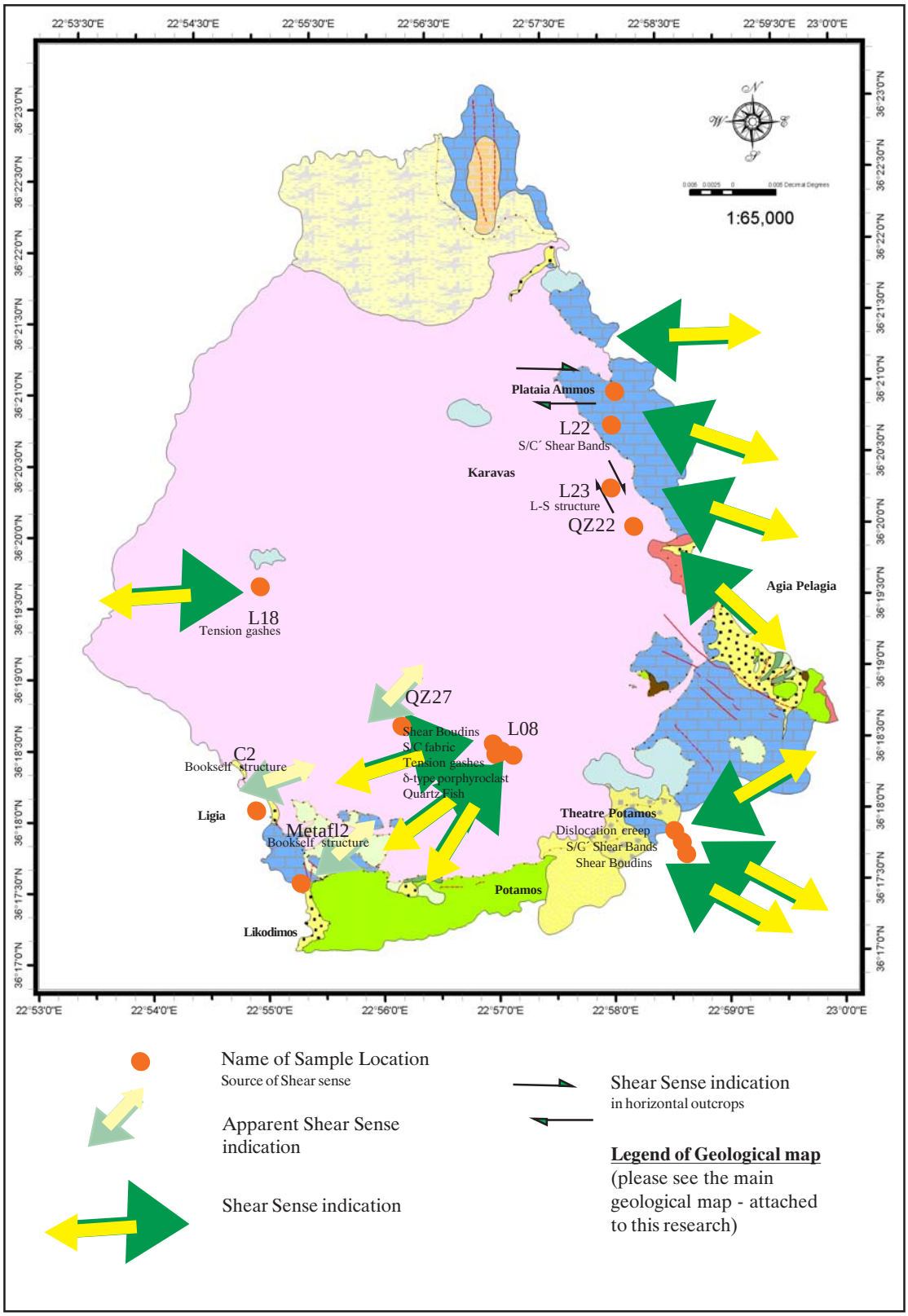

***Figure 86b**:* Map distribution of shear sense indicators across the inferred detachment.

meter-scale to sedimentary basins on the kilometer-scale (e.g. Hempton and Dunne, 1984). Examples of the forenamed structures of metro-scale observed at the Plataia Ammos area, as well as of macro-scale at the mountain ridges of Agia Moni and Agia Elesa (fig. 88a-b). The latter observations of mountain ridges of Agia Moni and Agia Elesa from the SRTM model and aerial photos revealed faults (fig. 87-89) that play the roll of Riedel fractures of a kilometer-scale. These faults have an orientation of NWW-SEE. Dextral shear sense of W-E direction is revealed from the forenamed observations, implying the large extension that Kythera Island has undergone and continues on NE-SW trending.

Peloponnesus-Kythera-Antikythera straits act as a less rigid micro-plate

The rotation of Kythera Island, according to many authors is very light or absent. At the contrary, observing the revealed faulting patterns (fig. 17) from the submarine studies (Lyberis et al., 1982), and our observations on lineations, on extensional fractures that instruct pull-apart structures on a kilometer-scale, as they were discussed above, it could be a reasonal explanation to imply that Kythera belongs to a block more loosely attached to the borders of the shear zone between Peloponnesus and Crete or entirely floating. In other words the Kythera-Antikythera strait could act as a less rigid micro-plate or there is a detachment fault of SW-NE direction that provides conditions for more freedomly floating of the upper crust, above the ductile region towards the African subducted plate.

Lineations and porosity characteristics, using Landsat 7 (ETM) images

A network of some measured lineations exposed at several outcrops (fig. 86) over an area of the exhumed PQU were mapped. The later data were plotted onto a Landsat image (ETM, with bands 2,3,4 and 3,4,5) providing the opportunity to study

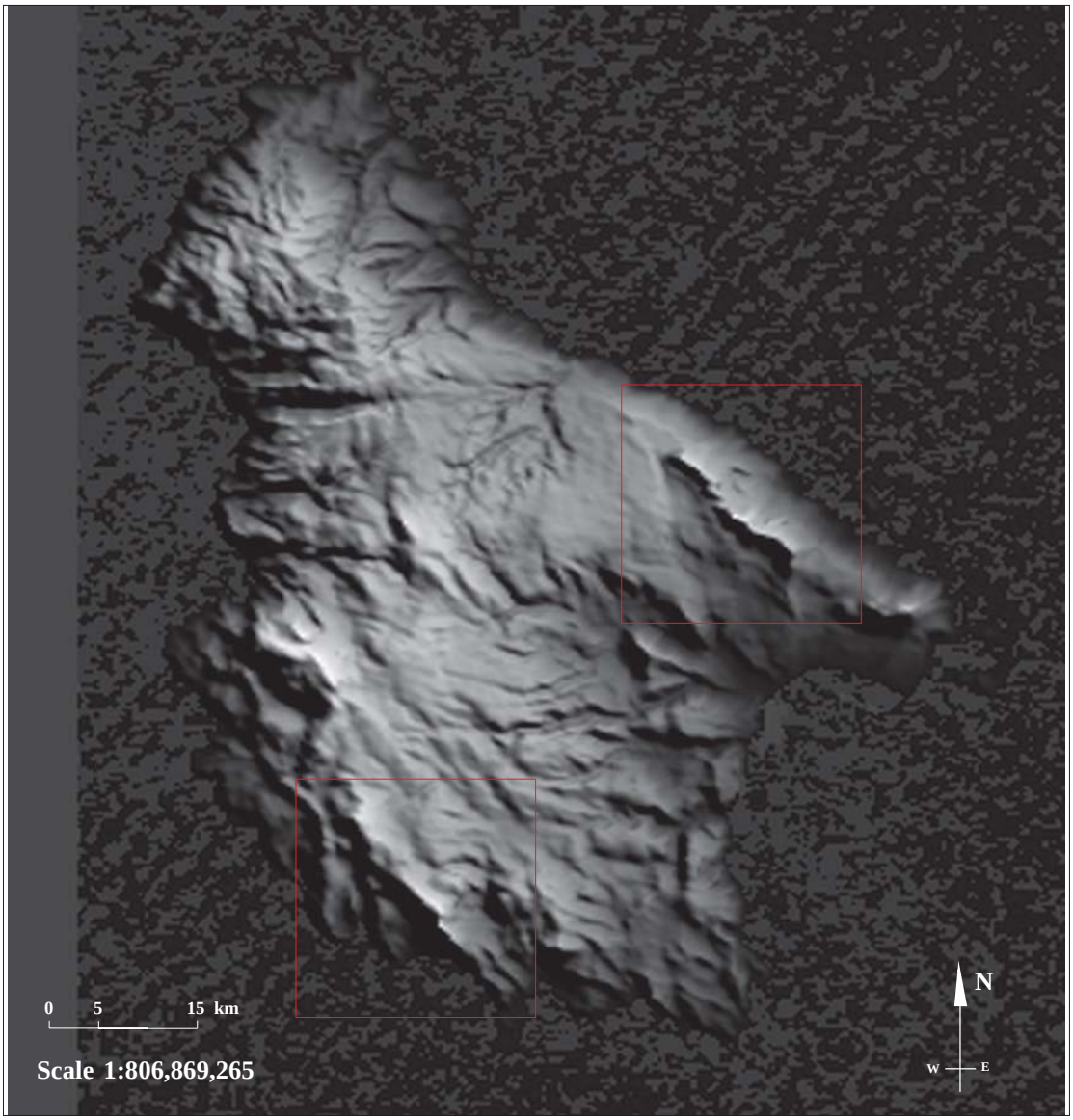

Figure 87: A grayscale gradient color DEM (Digital Elevation Model) constructed from a SRTM (Shuttle Radar Terrain Model of a 1arc degree resolution)

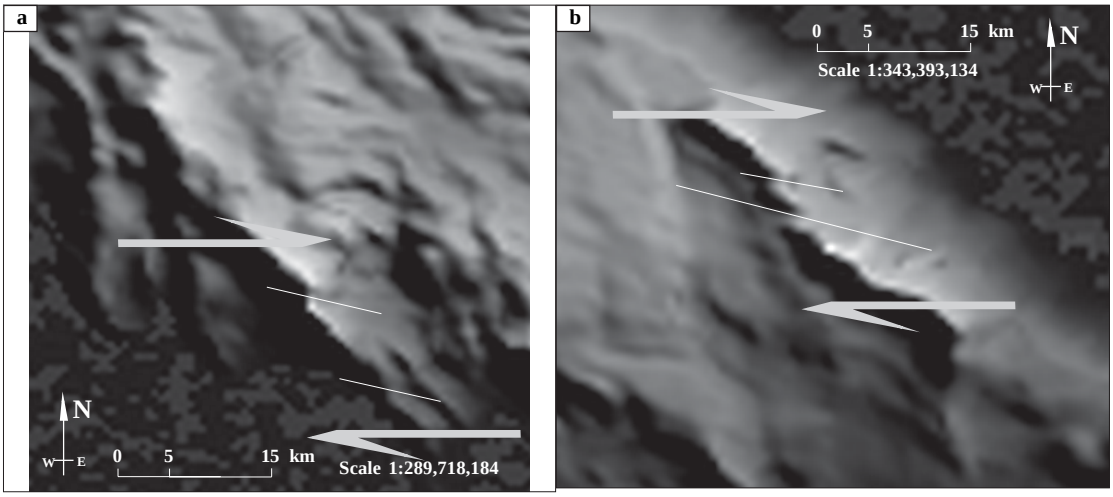

Figure 88: Magnification of the previous figure, at the locations of (a) Agia Elesa and (b) Agia Moni.

***Figure 89a**: Riedel fractures on a kilometer scale. Agia Moni Mountain ridge, aerial photo from 250 m above sea.*

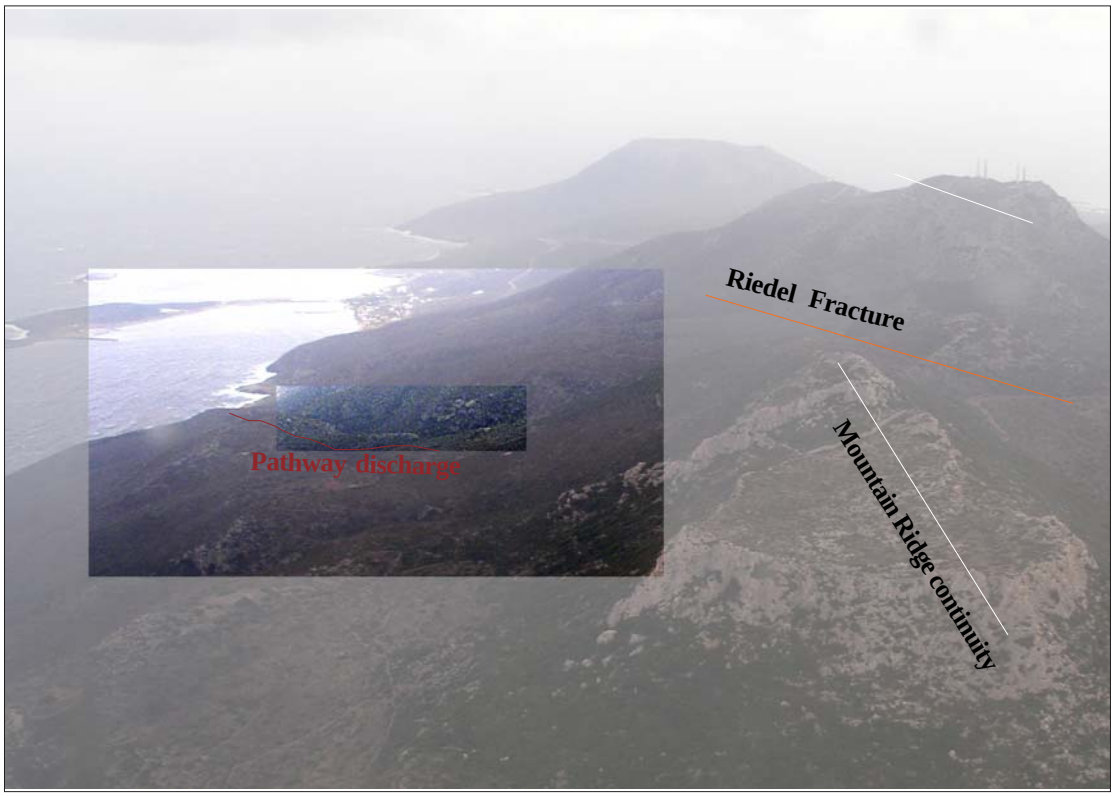

***Figure 89b**:* Interpretation of the fig. 89a, showing the Riedel fracture which may be related to the pathway discharge among the two splitted mountain ridges and continues to a pull-apart initiation.

possible correlations between fault geometry, lineation patterns, large folds related with water runs off and infiltration with related dipping and plunging of lineations and linkage at larger scale. Cataclastic shear zones show ubiquitous fracturing, comminution, and formation of porosity and permability. Because of the greatly contrast of the schistosity and lineation dip against the topography, the folded axis of the big antiform of the metamorphic basement is observed at the Landsat image of visible and near- and mid-infrared bands. It is possible that the water is infiltrated in different directions following the identified and mapped rock lineations. These data are on the Landsat image, implying or confirming the hypothesis of the broad antiform of NNW-SSE direction. This antiform axis appears lightly bended in a way that shear provokes, simultaneously. The assumed shear that may have bended this antiform is in agreement with the shear sense that occurs at the Riedel fractures at Agia Moni and Agia Elesa mountain ridges. It would a fascinated research to extend this discussion on these satellite observations, which will be on further investigation on future research, as well as it would be out of the scope of this research to discuss the preliminary image processing (atmospheric correction, image enhancement, principal components analysis, etc) of the satellite image prior to observation.

GIS Map Seismicity reveals two possible strike slip faults or the lowest rigidity of the southwestern part of the Hellenic Arc.

Two GIS maps (fig. 92a-b) of seismicity of the East Mediterranean area, focus on Greek Territory, were developed in order to observe unrevealed patterns of spatial seismicity patterns. The latter observation of the GIS maps was focus on the southwestern part of the Hellenic Arc, close to Kythera straits (fig. 92a-b). However, it is

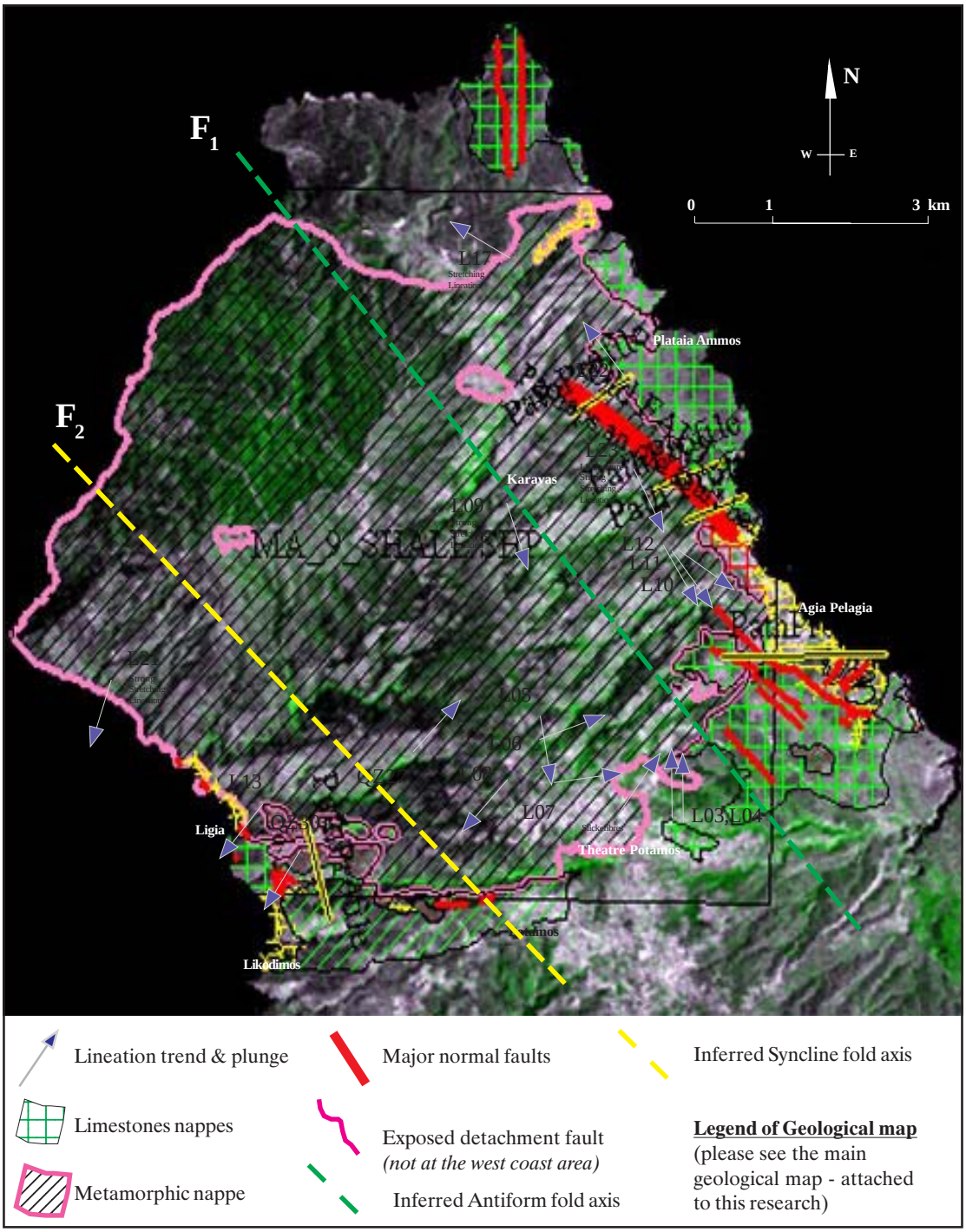

***Figure 90**:* Plotted lineations from some of the sample locations of field measurements on the composited GIS map of the Landsat ETM (year 2000) imagery of 3,4,5 (visual and near infrared) bands, and some of the geological rock formations in generic mode (limestone nappes vs. metamorphic nappe).

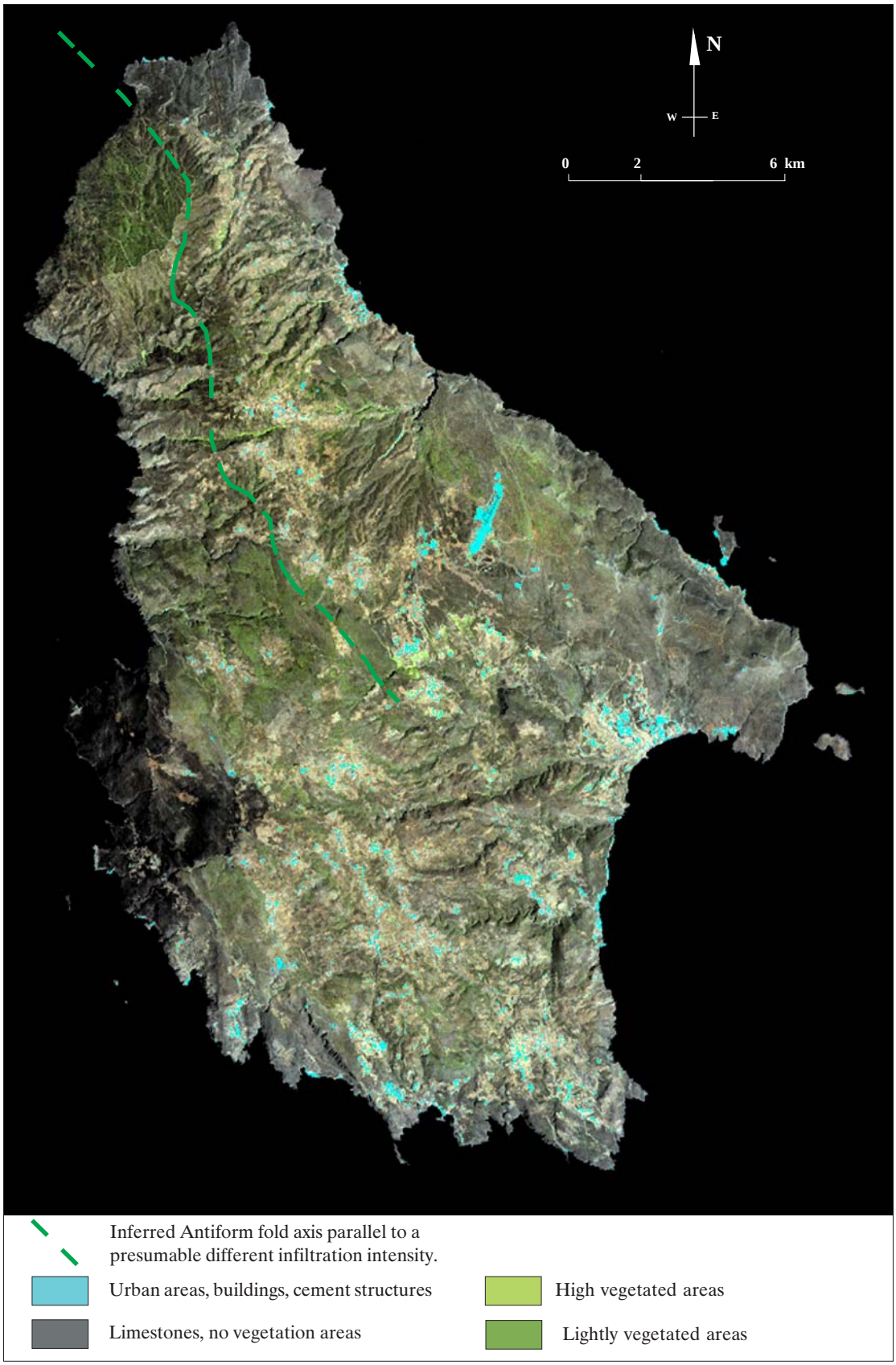

***Figure 91**:* Landsat ETM (year 2000) imagery of the whole Kythera Island of 3,4,5 (visual, near and mid infrared) bands with 30m/pixel resolution, that shows the inferred "bended" antiform fold axis, following the infiltration contrast of water.

not the scope of this research to discuss the further procedure of these GIS maps development (database conversion and integration, projection and datum, etc).

Tzannis & Valianatos (2003) observed similar earthquake foci databases (1903-2002 and constructed GIS maps of 1965-2002), predicting an earthquake southwestern of Kythera Island to be occured in 2003 of more than 7.0 Ms, and revealed seismic release patterns that can possibly be explained with a family of NE-SW oriented, left-lateral, strike-slip to oblique-slip faults and capable of producting earthquakes of a Ms 7.0 magnitude.

At the GIS maps that I developed on a ARCGIS9 platform (fig. 92b) I easily observe two linear more “silent” areas (red dashed lines) that do not occur so many earthquakes as at the vicinal areas. This “silent” areas occur in a direction of E-W and NE-SW direction, implying unrevealed strike-slip faults or areas of very low rigidity and high strain that host perhaps the maximum deformation of the outer Island Hellenic Arc.

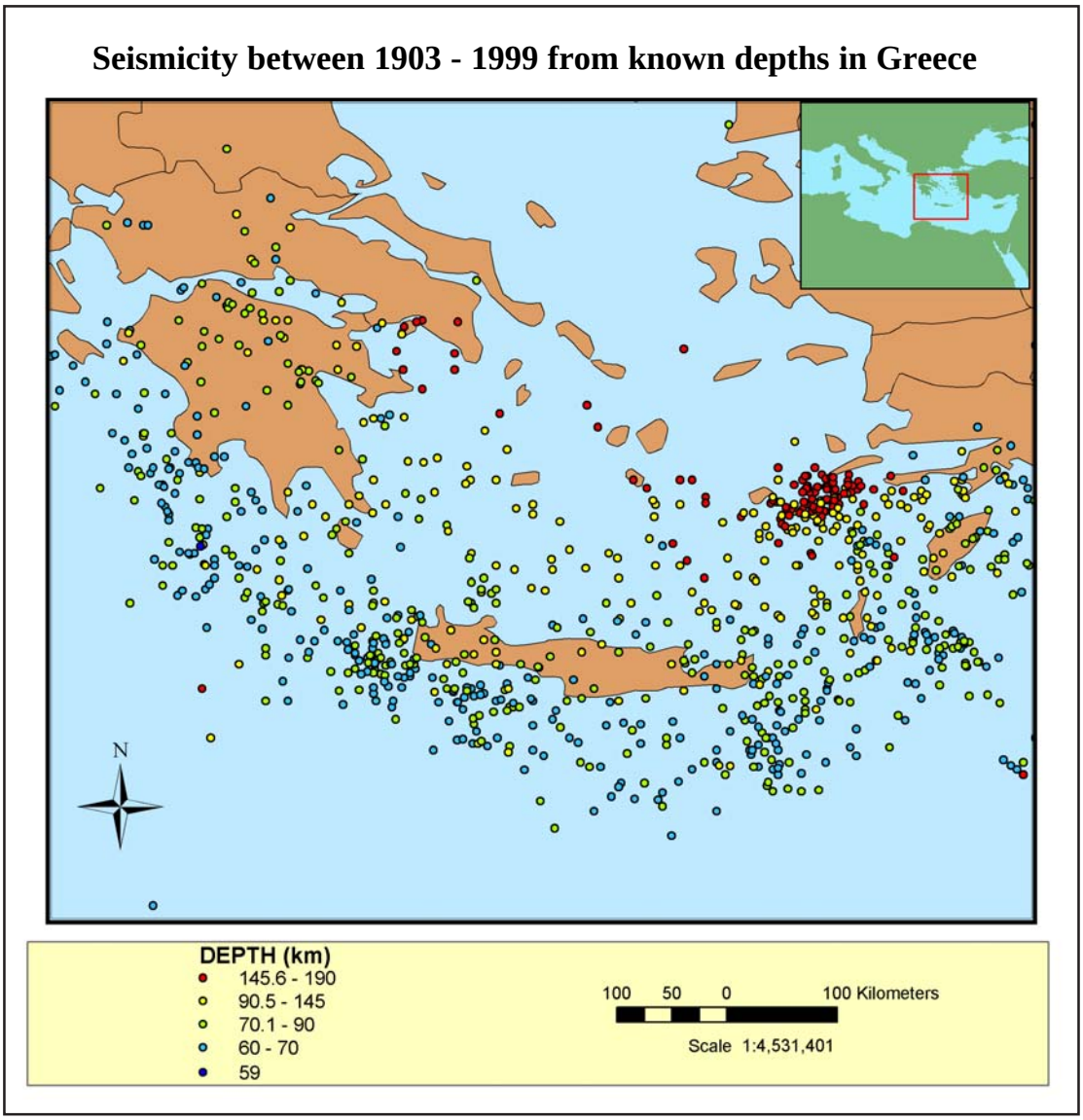

***Figure 92a**:* GIS-Map of seismicity of known earthquake foci of a variety of depths from the time span 1903-1999, showing the Bennioff zone that passes at the depth of 60-70km underneath of Kythera Island.

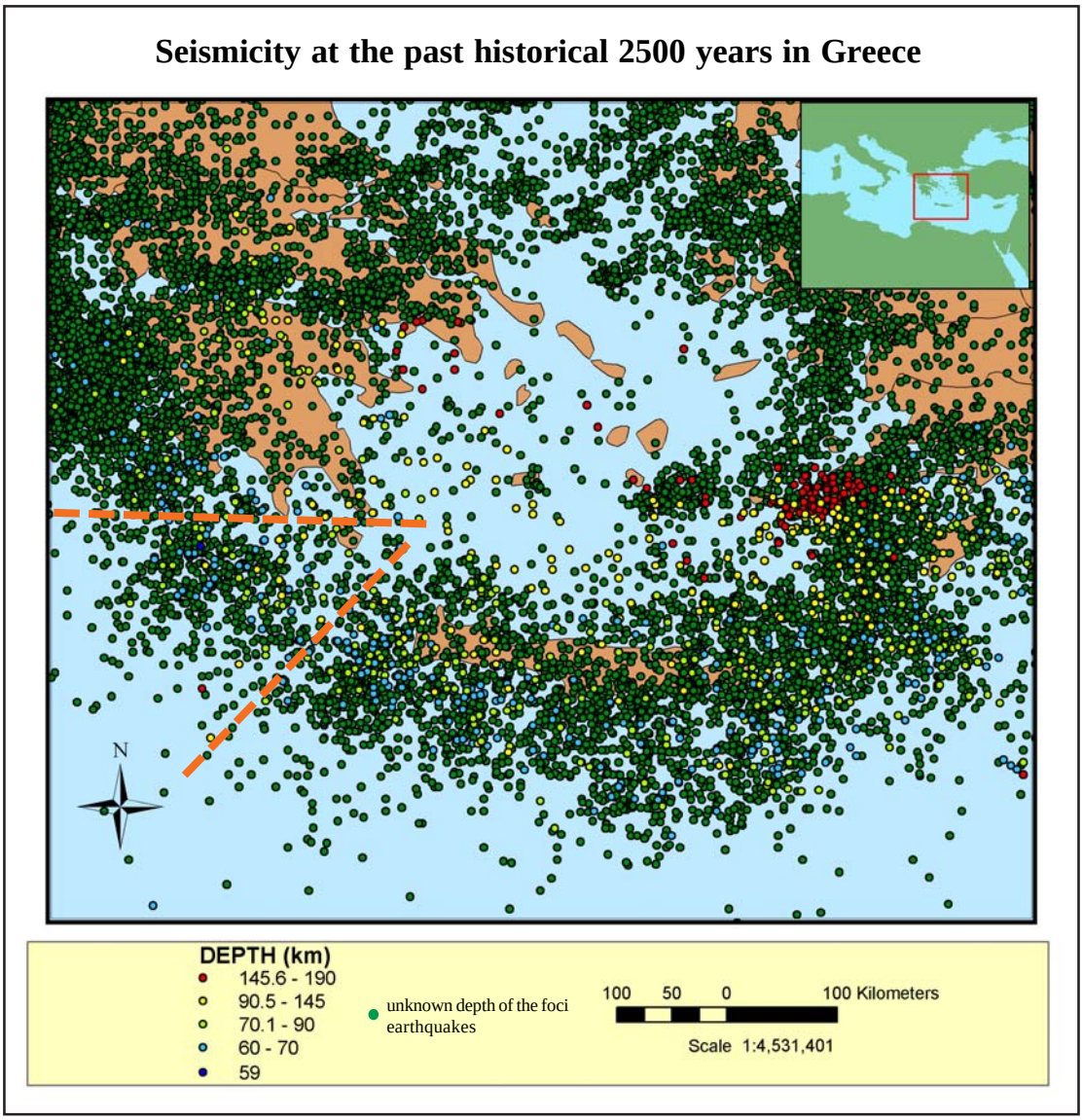

Figure 92b: GIS-Map of Historical Seismicity of earthquakes foci of known and unknown depths from the last 2500 years that implies the two possible unrevealed strike-slip faults close to Kythera straits.

diavase merika conclusions apo alla paper gia ekfraseis kai perne stoixeia apo to discussion edo, kai telione!! kai meta grapse to ABSTRACT, pos? pare apo allou.

Discussion

Introduction

The intention of this research is to discuss specific questions concerning the origin of the metamorphic nappe (PQU), which is part of the broad metamorphic core complex of the Southewestern part of the Hellenic arc, attempting to explain the associated detachment fault, and associated shear structures, that may reveal the behavior of the detachment fault. The mapping and interpretation of the results of fabric and micro-, macro-structural observations in many outcrops instruct this research to assume that paralleling the surface of the domed structure of the metamorphic core complex is a detachment fault, where crustal displacement has occurred over many kilometers. The structures occur throughout the Southewestern part of the Hellenic arc, at Kythera Island, while there is a hypothesis in which the detachment fault that occurs in Kythera Island is possible to be a prolongation of that of Cyclades area (through Milos and Naxos Islands) . However, timing is another important aspect on the forenamed hypothesis, in which it is assumed and not being proved, yet, that Kythera detachment fault is newer than this of Cyclades area.

PQU as a part of the Metamocrphic Core Complex (MMC) of Kythera Island

The basic structure of a MCC consists of a metamorphic basement terrane and an unmetamorphosed cover. Between these structures is a discontinuity, or decollement, which consists of shear and mylonitic fabric. The MCC of Kythera Island shows evidence of tectonic denudation along low- and high-angle faults with brittle over-prints onto already ductily deformed rock. Coney (1980) refers that the related structures of an MCC are asymmetrically dome like and form the highest elevation at the region. At the contrary, the topography on the Kythera Island region compare to Peloponnesus

or Crete Island, is not the highest. The latter evidence may imply that the exposed detachment fault (at the mylonitic occurrence area, Potamos) is independently or moreover unrelated to that of Crete Island. A reliable determination of the latter hypothesis would be a dating technique on fluid inclusions in quartzes veins that occur close to the detachment.

Foster et al (1993) refers that MCC usually formed in a region of thick crust which is gravitationally unstable, and occur in areas of synextensional magmatism, which is thought to have heated the upper crust and "lubricated" faults. In Kythera Island it appears the opposite scenario, where the crust occurs thinner beneath Kythira and Antikythira than beneath Crete and Peloponnesus (Makris, 1977), as well as the elevated topography of Kythira Island is almost 5 times lower than of Crete and Peloponnesus (fig. DEM constructed from SRTM). Isostasy is one of the main factors of rapid uplift, after the extensional thinning of the upper crust. Even that there are no evidence of synextensional magmatism in Kythera Island, it is believed that fluids played the role of "lubricate" the faults, at the time of the exhumation of the PQU, and diminished its rigidity.

Prior to the 1930's this complex was thought by Ktenas (1924) to be exposure of pre-Triassic "Principal crystalline system". It was not until the 1980's that the fabric was noted to have been deformed and metamorphosed in the Late Mesozoic-Cenozoic.

On this research, mylonitic fabric and associated shear bands were found on the mapping fieldtrip that indicate the presence of a detachment fault underneath of the PQU. The major fold axis of the MCC in Kythera Island is parallel to the regional extension of NW-SE, while the minor axis is perpendicular. Although, the crust of

Kythera strait is thinner than of Crete and Peloponnesus, the latter is accordant to Yin (1991) studies on the formation of domal detachment faults.

Does Kythera MMC corresponds to Cyclades area MMC

Lister et al (1984) have studied the area of Cyclades. According to the forenamed authors, Ios and Naxos Islands contain elongate domes over which a pervasive stretching lineation is warped. These islands may be metamorphic core complexes of Cordilleran type, involving middle crustal rocks drawn upward and outward from beneath the sedimentary basins now 100 km to the south, close to Crete Sea. Furthermore, they determine a non-coaxial shear zone that deformed the crystalline rocks, and now are exposed on the islands from the deeper levels of a major shallow-dipping ductile shear zone.

Considering the hypothesized differential rotations of Peloponnesus and Crete Island areas, respectively, I think that the shear zone in Kythera straits may have connected with low-angle normal faults at upper levels and be extended from Kythera Island through Cyclades to explain the exhumation of the HP-LT metamorphic rocks on Kythera with the Cyclades. Furthermore, it forms a distended paired metamorphic belt separated by an active extensional sedimentary basin, the Cretan Sea. The latter hypothesis is similar to Lister's (et al, 1984) hypothesis about Crete and Cyclades. Angelier et al. (1982) associated the dextral displacement of NW-SE of Kythera (relative to Peloponnesus) to the opening of the Sea of Crete. However, the latter authors refer that the fault patterns that occur on Kythera Island cannot quantitatively explain, under their present form, the considerable lengthening of the southwestern narrow arc segment of the Kythera straits and probably reflect some recent aspects of the deformation pattern in this key area. I think that the most recently deformation pat-

tern in this area is the bend of the submarine faults, western of Kythera Island. The latter implies the highest extension of the southwestern part of the Cretan Sea, lesser rigidity of this strait and dextral shear sense of Kythera Island of W-E direction. Until today, very significant evidences were missing to strengthen this hypothesis of maximum deformation in Kythera Island, such as the exhumed mylonitic fabric along the inferred detachment fault, S-C, S-C' fabrics and shear bands that prevail a tectonic strain setting similar to Cyclades metamorphic core complex construction.

The studied shear sense indicators that occur across the inferred detachment fault line on Kythera Island show a close spatial and temporal relation to detachment faulting, during and posteriori metamorphic core complex formation. These were overprinted later from brittle faulting. A structural and sense of shear kinematic indicators mapping took place on this research. Although a full kinematic reconstruction has not yet been created, we tried to correspond the MMC formation with the exposed detachment fault in Kythera Island, as well as to identify shear sense kinematics of the detachment.

The Palaeozoic metamorphic core complex that hosts the PQU at North part of Kythera Island is an asymmetric complex with a possible southwest-northeast-rooting master detachment fault. The PQU, that occurs in Kythera Island, is the southeasternmost metamorphic core complex (MCC) of the Tertiary extensional belt of the outer island Hellenic arc. Ductile and brittle-ductile deformations were produced by Late Miocene and mostly Tertiary extension along a detachment fault. Shear sense is consistent across the contact between the metamorphic occurrence of PQU and the limestones' units that lie on top, confirming the rapid exhumation of the MMC of Kythera Island. This research supports the hypothesis that underplating and exhu-

mation caused uplift and denudation of the detachment, as well as successive low-angle and high-angle normal faulting across the southwestern part of the Hellenic Arc. Moreover, the Kythera strait provided prerequisite conditions for the forenamed denudation of the MMC, such as lesser rigidity compare to vicinal microplates.

Middle Cycladic Lineament

The shear zones parallel to the MCL indicate a broad zone of displacement between two crustal blocks rotating in opposing directions as rollback took place at the Hellenic subduction zone (Pe-Piper et al., 2001). Furthermore, we may be able to correlate the continuity of the MCL to the two different families of shear sense indications in Kythera Island and infer the end of the forenamed MCL at the locality of the metamorphic core complex of Kythera Island that hosts two intersected lineation families, one NW-SE and one NE-SW (fig. 90).

Detachment

Taking into account of the 25-30^{o} clockwise rotation of Peloponnesus in contrast to Kythera almost zero rotation, then the major normal fault system, that now strikes NW-SE, was trending NWW-SEE during the Late Miocene or Early Pliocene; the direction of extension probably being NNE-SSW (Lyberis et al, 1982). The latter orientation of extension is in agreement with the mylonitic extensional shear of NNE-SSW at Kythera Island (Potamos area). If we assume that Kythera Island has not undergone any significant rotation as Peloponnesus, then we could estimate the kinematic direction movement of the detachment and correlate it with the Cyclades detachment fault. However, this kind of determination needs more analyses, as well as it contrads the relationship with Crete Island's detachment and gives a new perspective relationship with Cyclades.

Southwestern segment of the arc has undergone the maximum extension and deformation of the Hellenic Arc

Fundamental tectonic changes in the past two million years indicate that much of the deformation resulting from the interaction of the Eurasian, African and Anatolian-Aegean plates is taken up at the southern margin of the Aegean microplate (Piper & Perissoratis, 2003). Subduction of the African plate has slowed as a result of collision of continental crust. Rotation studies at Kythera Lower Pliocene sediments (from Hinsbergen et al., 2005) reveal both counterclockwise (ccw) and clockwise (cw) rotations in Kythera Island. In addition, the mean value of the palaeomagnetic measurements indicates a counterclockwise rotation of 5° and declination of 355.2° on middle Pliocene sediments (Steenbrick, 2001). From Meulenkamp et al. (1977), it was determined both cw and ccw rotations of 5° and 3° in Tortonian sediments, respectively. The above rotation measurements infer a synthetic differential rotation in Kythera Island. Synthetic as the intersection of these two reversal rotations, of Western and Eastern Aegean, respectively, at their perimeter of their circles, "looking" at the same direction. Taking into account that Kythera Island is between the two opposite rotations of Hellenides, we could conclude that this part of the Arc has undergone the maximum deformation and extension that occurs in the Kythera Island and being affected by this synthetic differential rotation. The latter is well being clarified from the bended submarine faults.

Transcurrent plate boundary - Evidence of strike slip faults at Kythera straits

Combination of the differential rotation with fault kinematic analysis as well as shear sense indications can led us to ascribe these evidence to strike-slip faults associated with the Pliny and Strabo trench fault system or moreover to unrevealed strike-

slip faults close to Kythera straits, as it was appeared on the GIS maps that were developed. Two linear "silent" areas (red dashed lines) were observed that do not occur so many earthquakes as at the vicinal areas. This "silent" areas occur in a direction of E-W and NE-SW direction (fig. 92b), implying unrevealed strike-slip faults or areas of very low rigidity and high strain that host, perhaps, the maximum deformation of the outer Island Hellenic Arc. The latter is accordant to Tzanis & Vallianatos hypothesis, that the southwestern area of the Hellenic Arc hosts seismic release patterns that can possibly be explained with a family of NE-SW oriented, left-lateral, strike-slip to oblique-slip faults and capable of producting earthquakes.

The question that derives from the above hypothesis is of whether it is possible to have this kind of strike-slip fault in the SW part of Hellenic Arc, where the accretionary prism of the subduction zone occurs. Hitherto work on fault plane solutions earthquakes has not revealed any evidence of strike-slip faulting at shallow crustal depths. Although, there is evidence of NE-SW strike-slip faulting at intermediate depths (Papazachos and Papazachou, 1997), it should be note that while an intermediate depth NE-SW strike-slip rupture is possible, a relatively shallow fault cannot be ruled out, as it may comprise a transucrrent structure facilitating the SW-ward motion of the Aegean plate (Tzanis & Vallianatos, 2003).

Returning to Kythera Island, in order to provide a possible tectonic model, a future transcurrent plate boundary may occur on NE-SW trending, southwestern of Kythera and Antikythera as a continuity of the MCL differential kinematics. In a convergence setting such as the Hellenic arc, lithospheric scale strike-slip faults accommodate part of the convergence between the Eurasean and Africa plates. Semi-rigid microplates move away from the convergence zone to provide space for the indenter

subducted plate (Africa). A similar example derives from the convergence setting of the Himalayas, at convergence setting between the Indo-Australian and Asian plates.

Unrevealed strike-slip zone in Kythera Straits

Southwards to the Antikythira Island, NW-trending faults are sparse, whereas NNE-trending faults become important (Kokkalas & Doutsos, 2001). In the contrary, at Kythera Island it appears an almost opposite scenario, where NW-SE and NNW-SSE trending faults become important. The following hypothesis could be derived from the previous discussed observations of this research. A NNE-trending fault pattern that consists of an unrevealed strike-slip zone is occurring, specifically at the bend of the submarine faults, north- and south-western of Kythera Island since there is a migrating change of fault pattern between Crete and Peloponnesus from the Late Miocene. Also, the previous hypothesis is strengthening by the description of Angelier et al. (1982) and Lyberis et al. (1982), who describe a complex fault zone in the Kythira-Antikythera strait associated with the opening of the Cretan Sea.

Complicated shear sense indicators and the related detachment fault in Kythera Island reveal a complex tectonic history

Kythera Island appears to host shear zones of very high inhomogeneous deformation. The deformation is simple shearing, but mostly consists of simple shearing plus a component of either shortening or extension normal to the shear zone boundaries, while it overprints previous deformation events. The latter shearing is associated with or without a rotation about an axis normal to the boundaries (e.g. bookself structures at the west side of the metamorphic occurrence at the north area of the island - Ligia area). The observation at the field was not scale-dependent. Shear zones were found under developing at any scale from the single grain (pressure shadows, δ-type

porphyroclasts, etc) to that of major mountainous areas (e.g. Riedel fractures on mountain ridges mostly of Agia moni, Agia Elesa of W-E shear sense trending).

Kythera Island shows three type of shear zones which may be broadly classified by their occurrence frequency at the field as cataclastic, transitional and mylonitic deformation, respectively. Deformation is characterized by crystal-plastic processes or otherwise mylonitic deformation, which is not very common on Kythera Island or it has not denudated yet, and posteriori overprinting brittle deformation and faulting. In contrast transitional deformation that shows cyclic overprinting of brittle and brittle-ductile, solution-transfer, and crystal-plastic processes are very common. The latter proves that Kythera island has undergone a very tremendous brittle-ductile overprinting episode during the uplift process of the metamorphic basement. Cataclastic shear zones in Kythera Island are developed by microfracturing and fragmentation, as well as involving stress-corrosion cracking, and show solution-transfer features. Transitional shear zones show cyclic overprinting of brittle, solution-transfer and crystal-plastic deformation mechanisms, as shown by the development of arrays of quartz or calcite veins (fracturing and fracture healing or less sheared extensional fractures over previous high strained tension gashes, e.g. Plataia Ammos tension gashes), subsequent solution-transfer and crystal-plastic deformation (by quartz dissolution and reprecipitation, dislocation glide, creep (L04 sample location), twinning or calcite crystals in marbles, close to Potamos area) and then overprinting by younger quartz veins (fracturing).

Commonly, some mineral types show crystal-plastic features, some will be fractured (e.g. huge veins of feldsparts at the Ligia outcrop), while other will develop solution-transfer phenomena (e.g., mica beards on quartz grains on the sample xalazflev). Not surprisingly, these transitional shear zones commonly give the impression of great

structural complexity and multiple tectonic events that took place on Kythera Island, which make difficult the decipherment of Kythera Island's tectonic history. Finally, mylonitic shear zones developed by crystal-plastic phenomena associated with dislocation, diffusional deformation mechanisms with neocrystallization, or even more deformed and sheared rocks such as the mylonites that occur mostly very close to the detachment fault are generally strongly foliated and lineated, finer-grained than their host rocks (e.g. quartzites). These data were very useful to determine distinctive and reliable kinematic indicators, inferring important evidence of the detachment fault's kinematics.

The mylonitic shear zone that occurs on Potamos area is determined as it was developed in a "brittle-ductile" shear zone. Mylonitic shear zone uplifted and cooled, while deformation continues and brittle structures overprint plastic structures. Kinematic indicators, structures developed close to shear zone boundaries and within shear zones that are asymmetric with respect to both the boundaries and any foliation developed within the zones identified a large variety of shear sense orientations, rising to prominence the complicate tectonic history of the Kythera Island. Thus many of the kinematic indicators used in mylonitic shear zone were ambiguous or difficult to interpret correctly. There may be reasons, such as local flow perturbations around less-deformed bodies or unrecognized folds that indicate the opposite sense of shear and confused the interpretations. Fortunately, vicinal shear sense kinematic indicators confirm or discard any minterpreted outcrop. For the above reasons we tried to ascertain the shear sense before making any final decision by comparing to other types of more than one kinematic indicators.

Spatial relationship of S/C and S/C′ fabric with the revealed detachment fault

Close to the detachment fault occur mostly S-C′ structures; while further occur S-C structures. I agree to Mawer (1989) theory of S-C and S-C′ structures and I think that in Kythera Island the S-C texture is confined to the least foliated and deformed parts of the shear zone, whereas shear band foliation (S-C′ structures) is confined to the most deformed and foliated parts. The latter observation determines the maximum localized shear and identifies the location of the detachment fault. As a result this could be a reliable indicator to construct a parallel apparent proportional line-boundary of the detachement fault.

Interpretation of extenstion footprints

The extension lineation is a critical symmetry indicator in these shear zones. Extension lineations are generally defined by elongated mineral grains (calcite or micas, slickenfibres), slickensides, stretched crystal aggregates or strong stretching lineation that occur mostly on big folded axes of NW-SE and are co-linear. It can be recognized that the lineations follow a folding pattern of a NW-SE fold axis or as a secondary explanation they follow two different tectonic events of extension, while shear sense of E-W orientation has affected the tectonic signature that is revealed from the structures in Kythera Island.

External tectonic influences to Kythera Island tectonic setting

The active fault pattern over the Kythera Ridge (fig. 87)shows that many of the many linear scarps and the top of the individual Mounts (Agia Moni and Agia Elessa) trend 135o (NW-SE), which is normal to the direction of maximum shortening and folding in the strain ellipse for W-E dextral shearing. These 135^{o} trends are continued southwestward, where subdued expressions of these mountains are observed until we reached the antipodal parallel orientated mountain of Agia Elessa (Agia Elessa moun-

tain ridge, Tripolis limestones). This structure, as it was explained in previous from Shuttle Radar Terrain Model of 90m resolution (1 Arc), appears to be a 15 km long anticline or horst which originated since the beginning of the exhumation process of the high pressure rocks. The northern end (Agia Moni mountain ridge, Tripolis limestones) of both parallel mountain chains terminates abruptly against the detachment fault, originated from the rapid uplift and exhumed high pressure rocks (PQU).

In addition, it was observed multiple extensional fault patterns of different trending, mainly of NNE-SSW, NE-SW and NEE-SWW. From the Shuttle Radar Terrain Model, topography reveals fault patterns, such as this of Agia Moni mountain ridge. On the above mountain ridge, is obviously the maximum shortening of NE-SW and the maximum extension of NNW-SSE. The latter pattern reveals a dextral sense of shear of an almost W-E trending (fig. 87). The latter observation is not constrained by structural field observations of shear sense, as it is located outside of the researched mapped area, and it must be regarded as hypothetical. However, this hypothetical observation was studied under aerial photos, Landsat imagery and SRTM elevation data. The latter observation was necessary for the understanding of the tectonic setting of Kythera Island. This model illustrates a number of significant consequences from shear of E-W direction, at this important segment of the Hellenic arc. The latter could be, as well as a result from exogenous tectonic influences at Aegean plate. Other microplate boundaries in the central and eastern Mediterranean may have interact and influence the movement of Aegean plate, besides the tectonic escape of Turkey plate.

The Strait of Kythera separates the area of Peloponnesus, where a clockwise paleomagnetic rotation took place, from Crete, where counter clockwise or no rotation was detected, implying a major rupture between the two areas. According to

Jongsma et al., (1987), a fault zone lies along the same small circle, around the Africa-Ionian pole, as a prolongation of the Medina Ridge, close to the southwestern part of the Hellenic arc. The continuation of the Ionian microplate boundary eastward of the Medina Ridge is obscured by the front deformation associated with the Aegean plate boundary. However, according to our observations (e.g. Plataia Ammos, tension gashes and S/C′ that reveal an E-W dextral shear sense, as well as E-W dextral shear sense of Riedel fractures on Mounts of Agia Moni and Agia Elesa) and Jongsma et al., (1987) implied hypothesis, then there is a link between both of the vicinities close to Kythera Straits. Finally, it should be note that the latter authors conclude that the average rate of convergence along the southwestern Aegean plate boundary for the past 5 Ma is 6.6 +/- 1 cm a-1.

The tectonic behavior of the Medina Wrench Zone exhibits from west to east divergent, strike-slip, and convergent sections. The initiation of the Medina Wrench caused Sicily to separate from Africa, and Greece to extend by more than 233 km in the Aegean region. The Medina wrench zone has acted as a right-lateral transform plate boundary since the Late Miocene, as demonstrated by available marine geological and geophysical data (Jongsma et al., 1987). This could be a further explanation of the dextral sense of shear kinematics behavior on Kythera Island, although that more investigation is prerequisite to establish such a theory.

Conclusions

Paralleling the surface of the domed structure of the metamorphic core complex is a detachment fault, where crustal displacement has occurred over many kilometers, after the Late Miocene extension took place. Graben formation of the unmetamorphosed upper tectonicstratigraphic units (Pindos and Tripolis limestone

units) caused as a result of the uplift and exhumation of the PQU of Kythera.

The denudation of the Phyllites-Quartzites on surface followed by syntectonical synsedimentation of breccia and neogene unconformities. Between the unmetamorphosed upper tectonic units and the PQU a detachment occurred as a result of the Late Miocene extension. En enchelon faults associated with fluids accompanied the expansion of the detachment, the construction of strong stretched lineated rocks and the precipitation of rarely occurred at the surface ore deposits, commonly of aimatite. The decollement forms of a domal structure, caused of syncompressional uplift and isostatical buoyancy forces. The precise date for the onset of extension, possibly controlled by the roll-back of the subsiding African lithosphere remains at this point as a discussion. The detachment consists of shear and mylonitic fabric. Shear sense of mylonitic fabric of top-to-the southeast (NWW-SEE) displacement implies a Late Miocene extensional field, while a dislocation creep of NEE-SWW implies Dextral shear sense of E-W direction, sinistrial shear sense of NW-SE related to the extensional sedimentary basin of Cretan Sea, top-to-the southeast or east and top-to-the southwest or west displacement

The exhumation of the high-pressure rocks was accompanied by NEE-SWW extensional graben model, which is related to the observed NEE-SWW mylonitic dislocation creep. Later brittle-ductile faulting provoked S/C′ fabric of NNW-SSE orientation and top-to-the southeast displacement that occur mostly at the northeastern coast of Kythera, while at the northwestern coast of Kythera occur S/C fabric of NNE-SSW orientation and top-to-the southwest displacement. The latter implies a NE-SW gradient shear that maximizes through northeastern direction pointing to Cyclades area.

Ductile and brittle-ductile deformations were produced by Late Miocene and

mostly Tertiary extension. Afterwards, these were overprinted by brittle faulting. Unfortunately, it has not been clarified, yet, the exact time that brittle faulting started.

Kythera Island is situated at the end of the inferred Middle Cycladic Lineament. Differential rotations of Peloponnesus and Crete localize the Kythera strait at the edge of these rotations strengthening any kind of deformation occurs. The latter may be related to the dextral shear sense of E-W, to the bending of the submarine faulting western of Kythera, to a "quiet" earthquake activity of the last 2500 years of the same direction as well as of the NE-SW, that may reveal an unexpressed transcurrent boundary.

Future Study

Future study could be the mean fission-track length that could indicate rapid cooling and consequent rapid uplift of this PQU during the last stage of crustal extension. More detailed map of the complete variety of the metamorphic grades and rocks that occur in the Kythera Island could give more reliable results about the behavior of the MMC. In addition, pliocene sediments that may related to the detachment faulting needs more field evidence to clarify the Quaternary behavior of the detachment fault.

Synthesis

The exhumation of the high-pressure/low temperature Phyllite – Quartzite during middle Miocene time was accompanied by the occurrence of the mapped detachment fault, bringing the sedimenatary units on top of the metamorphic nappe, and leading to formation of brittle, brittle-ductile and ductile structures. The tectonometamorphic evolution of this detachment fault provides information on the state of the southwestern part of the Hellenic Arc at that time.

Many suitable types of asymmetric and symmetrical structures were identified and interpreted. This research has concentrated on the most common reliable macro-, meso- and microscale kinematic indicators. The shear sense can be unambiguously interpreted by the judicious use of kinematic indicators.

Shear zones are fundamental components of all continental margin orogenic belts, irrespective of style or age. A variety of shear zones of any depth in the lithosphere was observed, such as cataclastic, transitional and mylonitic. These infer a protracted and complex tectonic history. They dominate mostly close to the detachment fault. Consequently, they imply the intensive localized deformation of a detachment fault presence. The kinematics of the detachment fault control the formation and siting of the metamorphic nappe, as well as, of the overthrusted limestones. The kinematic indicators that mostly were observed were Riedel fracture assemblages, implying cataclastic shear zone, deformed sigmoidal and en echelon vein arrays (transitional zone), S-C textures, as well as, shear-band foliation S-C′ (mylonitic zone). Finally, the studied asymmetric structures developed within these zones indicate the presence of a broad shear zone of almost NEE-SWW trending, at a lithospheric depth of approximately 30km, a direction of a symmetrical top-to-the west, top-to-the southwest,

top-to-the east and top-to-the southeast displacement and a dextral sense of shear of E-W direction.

The nonmetamorphic units are separated from the tectonostratigraphic units by fault and gauge breccia. It was found no deposition of neogene sediments on top of these breccia deposits. In contrast, a lot of neogene sediments were observed on top of the inferred detachment fault at the north area of the Kythera Island (Fanari area). The detachment zone occurs at the surface as a brecciated layer, accompanied with mylonites and high deformed rock formations.

The latter observations conclude that the detachment fault took place during the deposition of Miocene sediments and continues through the denudation of the PQU. The expose of the metamorphic nappe only at the north part of the Kythera island implies that the uplift and exhumation rate of the tectonostratigraphic units is higher at the north part of the Kythera Straits.

Lineation mapping and Landsat image interpretation shows that the metamorphic nappe forms an antiform structure. The latter confirms the hypotheses of a more rapid graben scenario, exhumation and denudation at the north part of the Kythera Island than the south. At the south part more trough fault structures are still preserved.

Predominent metamorphic components below the detachment are within an elevation span of 0-400m, while Peloponnesus and Crete present the Phyllite-Quartzite unit in almost 800m. In addition, most of the Southern parts of Peloponnesus and western parts of Crete reveal ten times higher elevation. Crete, Peloponnesus and Kythera represent the western-central part of the today's Hellenic Arc. The latter observations of the different uplift and exhumation of these localities remains enigmatic.

However, it is believed by this research that the PQU that occurs on Kythera Island represents the lower part of a broad MMC that occurs at the outer Island Hellenic Arc.

References

ΑΛΕΞΟΠΟΥΛΟΣ, Α. (1990). Γεωλογικές και υδρογεωλογικές συνθήκες της περιοχής του τοπογραφικού φύλλου "Μοχος" (Κεντροανατολική Κρήτη). Διδακτορική διατριβή, Αθήνα, σελ. 640.

ALEXOPOULOS, A., 1990. Geological and hydrogeological setting of the "Mochos" topographic area map (Eastern-central Crete). Doctoral thesis, Athens, Pages 640.

ALVAREZ, W., ENGELDER, T., LOWRIE, W., 1976. Formation of spaced cleavage and folds in brittle limestone by dissolution. Geology, Vol. 4, p. 698-701.

ANGELIER, J., THEODOROPOULOS, D., TSOFLIAS, P., 1976. Sur la neotectonique du seuil de Cythere, dans l'arc egeen externe (Grece). C.r. hebd. Seanc. Acad. Sci., Paris 283, 1273.

ANGELIER, J., 1979. Neotectonique de l'arc egeen. These de Doctorat d'Etat. Publs Soc. geol. No 3, p. 1-418.

ANGELIER, J. et al., 1982. The tectonic development of the Hellenic arc and Sea of Crete: a synthesis. – Tectonophysics 86: 159-196.

ARMIJO, R., MEYER, B., HUBERT, A., BARKA, A., 1999. Westward propagation of the North Anatolian fault into the northern Aegean: Timing and kinematics. Geology. Vol. 27, No.3, p. 267-270.

AUBOUIN, J., 1959. Contribution a l'etude geologique de la Grece septentrional: les confins de l'epire et de la Thessalie. Ann. Geol. Pays Hell., Vol. 10, Pages 403.

AVIGAD, D., GARFUNKEL, Z., 1991. Uplift and exhumation of high-pressure metamorphic rocks: the example of the Cycladic blueschist belt (Aegean

Sea), Tectonophysics, Vol. 188, Pages 357-372.

AVIGAD, D., 1993. Tectonic juxtaposition of blueschists and greenschists in Sifnos island (Aegean Sea) implications for the structure of the Cycladic blueschist belt. J. Struct. Geol., Vol. 15, Pages 1459-1469.

AVIGAD DOV., GIDON BAER, HEIMANM ARIEL, 1998, "Block rotations and continental extension in the central Aegean Sea: palaeomagnetic and structural evidence from Tinos and Mykonos (Cyclades, Greece)", Earth and Planetary Science Letters, Vol.157, Issues 1-2, Pages 23-40.

AYDIN, A. & NUR, A., 1982. Evolution of pull-apart basins and their scale independence. Tectonics, Vol. 1, p. 91-105.

BASSIAS, Y., 1984. Etude geologique du domain Parnonien (feuille d'Astros au 1:50,000, Peloponnese oriental, Grece). These 3e cycle. Mem. Sc. Terre Univ. Curie, Paris, No 84-14, Pages 264.

BASSIAS, Y., 1994. Tectono-metamorphic evolution of blueschist formations in the Peloponnesus (Parnon and Taygetos massifs, Greece): a model of nappe stacking during Tertiary orogenesis. J. Geology. Vol. 102. Pages 697-708.

BEACH, A., 1975. The geometry of en-echelon vein arrays. Tectonophysics, Vol. 28, p. 245-263.

BERNIER, P., FLEURY, J.J., 1980. La plate-forme carbonatee de Gavrovo - Tripolitza (Grece): Evolution des conditions de sedimentation au cours du Mesozoique. Geol. Medit., 7/3, Pages 247-259.

BERTHE, D., CHOUKROUNE, P., JEGOUZO, P., 1979. Orthogneiss, mylonite and non-coaxial deformation of granites: The example of the South Armorican shear zone. J. Str. Geology, Vol. 1, p. 31-42.

BIJWAARD, H., SPAKMAN, W., ENGDAHL, E.R., 1998. Closing the gap between regional and global trave time tomography. J. Geophys. Res., Vol. 103, Pages 30055-30078.

BLAKE et al., 1981. A geological reconnaissance of the Cycladic blueschist belt, Greece. Bull. Geol. Soc. Am. 92, 247-254.

BLUMENTHAL, M., 1933. Zur Kenntnis des Querprofils des zentralen und nordlichen Peloponnes. Neuen Jahrbuch fur Mineralogie, Beil. Bd. 70, Abt. B., Seit. 449-514.

BONNEAU, M., 1982. Tectonic evolution of Central Aegean Hellenides from Upper Jurassic to Miocene times. Soc. Geol. Fr., Bulletin, Vol. 24, Pages 229-242.

BONNEAU, KIENAST, J.R., 1982. Subduction, collision et schistes bleu: example de l' E´ ge´e, Grece. Bull. Soc. Geol.

BORONKAY, K. & DOUTSOS, T., 1994. Transpression and transtension within different structural levels in the central Aegean region. J. Struct. Geol. 11, p.1555-1573.

BRIX, M.R., STOCKHERT, B., SEIDEL, E., THEYE, T., THOMSON, S.N., KUSTER, M., 2002. Thermobarometric data from a fossil zircon partial annealing zone in high pressure-low temperature rocks of eastern and central Crete, Greece. Tectonophysics, Vol. 349, p. 309-326.

BURG, J.P., IVANOV, Z., RICOU, L.E., DIMOR,D. & KLAIN,L., 1990. Implications of shear-sense criteria for the tectonic evolution of the Central Rhodope massic, southern Bulgaria. Geology. Vol. 18, p. 451-454.

CAYEUX, L., 1903. Phenomenes de charriage dans la Mediterranee orientale. C.R.Acad.Sc. Paris, Vol. 136. Pages 474-476.

CELET, R, 1962. Contribution a l'etude geologique du Parnasse-Kiona et d'une partie des regions meridionales de la Grece continentale. Ann. Geol. Pays Hell., Vol. 13, Pages 425.

ΧΡΙΣΤΟΔΟΥΛΟΥ, Γ., 1967. Παρατηρήσεις επί της γεωλογίας των Κυθήρων και μικροπαλαιοντολογική ανάλυσης των νεογενών σχηματισμών της νήσου. Δελτ. Ελλ. Γεωλ. Εταιρ., 6/2, σελ. 385-399.

CHRISTODOULOU, G., 1965. Quelques observations sur la geologie de Cythere et examen micropaleontologique des formations neogenes de l'ile. Bull. Soc. geol. Grece, Vol. 6, p. 385-399.

CHRISTODOULOU, G., 1967. Geological observations of Kythera Island and micro-palaeontological analysis of neogene formation. Bull. Hellen. Geol. Assoc., 6/2, Pages 385-399.

COCARD, M. et al., 1999. New constraints on the rapid crustal motion of the Aegean region: recent results inferred from GPS measurements (1993–1998) across the West Hellenic Arc, Greece Earth and Planetary Science Letters, Volume 172, Issues 1-2, Pages 39-47.

COLEMAN, R.G. & LEE, D.E., 1963. Glaucophane-bearing metamorphic rock types of the Cazadero area, California. J. Petrology, Vol. 4, p. 260-301.

CONEY, P.J., 1980. Cordilleran metamorphic core complexes: An overview, in Crittenden, M.D., Coney, P.J., and Davis, G.A., eds., Cordilleran metamorphic core complexes: Boulder, Colorado, Geol. Soc. Am. Memoir 153, p. 7-31.

COWIE, P.A. & SCHOLZ, C.H., 1992. Physical explanation for the displacement-length relationship of faults using a post-yield fracture mechanics model. J. Str. Geol., Vol. 14, p. 1133-1148.

ΔΑΝΑΜΟΣ, Γ., ΖΑΜΠΕΤΑΚΗ-ΛΕΚΚΑ, Α., 1989. Περί μίας εμφανίσεως του κλαστικού Τριαδικού της Πίνδου στα Κύθηρα. 4ο Γεωλογικό Συνέδριο Ε.Γ.Ε., Αθήνα 1988, Δελτ. Ελλ. Γεωλ. Εταιρ., 23/2, σελ. 49-58.

DANAMOS, G., ZAMPETAKI-LEKKA, A., 1989. Study of Pindos Triassic clastic on Kythera Island. 4th Geol. Conf. Hellenic Geol. Soc. Assoc., Athens 1988, Bull. Hellenic Geol. Assoc., 23/2, Pages 49-58.

ΔΑΝΑΜΟΣ, Γ., 1992. Συμβολή στη Γεωλογία και Υδρογεωλογία της Νήσου των Κυθήρων. Διδακτορική διατριβή. Αθήνα. Σελ. 348.

DANAMOS, G., 1992. Contribution to Geology and Hydrogeology of Kythera Island. Doctoral Thesis. Athens. Pages 348.

DAVIS, G.H., 1984. Structural geology of rocks and regions. John Wiley & Sons Inc., Canada, p. 492.

DAVIS, G.H., REYNOLDS, S.J., 1996. Structural Geology of rocks and regions. 2nd Ed., USA, p. 776.

DEGNAN, P. , ROBERTSON, A., 1991. Tectonic and sedimentary evolution of the western Pindos ocean: NW Peloponnese, Greece. 5th Geol. Cong. of Geol. Soc. Greece, Thessaloniki, 1990. Bull. Geol. Soc. Greece, 25/1, Pages 263-273.

DEGNAN, P., ROBERTSON, A., 1998. Mesozoic-early Tertiary passive margin evolution of the Pindos ocean (NW Peloponnese, Greece. Sedimentary Geology, Vol. 117, Pages 33-70.

DEGNAN, P., 1992. Tectono-Sedimentary Evolution of a Passive Margin: The Pindos Zone of the NW Peloponnese, Greece. Unpublished PhD thesis, University of Edinburgh, Pages 391.

DERCOURT, J., 1964. Contribution a l'etude geologique d'un secteur du Peloponnese

septentrional. Ann. Geol. Pays Hell., Vol. 15, Athenes, p. 408.

DEWEY, J.F., 1965. Nature and origin of kink bands. Tectonophysics, Vol. 1, 459–494.

DEWEY, J.F., PITMAN, W.,C., RYAN, W.,B.,F., BONNIN J., 1973. Plate tectonics and the evolution of the Alpine system. Geological Society of America, Bulletin Vol. 84, Pages 3137-3180.

DINTER, D.A., MACFARLANE,A.M., HAMES, W., ISACHSEN, C., BOWRING, S. & ROYDEN, L., 1995. U-Pb and $^{40}Ar/^{39}Ar$ geochronology of the Symvolon granodiorite: implications for thermal and structural evolution of the Rhodope metamorphic core complex, northeastern Greece. Tectonics, Vol. 14, p.886-908.

DONATH, F. A., & PARKER, R. B., 1964. Folds and folding: Geological Society of America Bulletin. Vol. 75, Pages 45-62.

DROOGER, C.W. & MEULENKAMP, J.E., 1973. Stratigraphic constributions to geodynamics in the Mediterranean area: Crete as a case history. Bull. Soc. geol. Grece, Vol. 10, p. 193-200.

DUERMEIJER, C.E., KRIJGSMAN, W., LANGEREIS, C.G., Ten VEEN, J.H., 1998. Post-early Messinian counterclockwise rotations on Crete: implications for Late Miocene to Recent kinematics of the southern Hellenic arc. Tectonophysics, Vol. 298, Pages 177-189.

DUERMEIJER, C.E., NYST, M., MEIJER, P.TH., LANGEREIS, C.G., SPAKMAN, W., 2000. Neogene evolution of the Aegean arc: paleomagnetic and geodetic evidence for a rapid and young rotation phase. Earth and Planetary Science Letters, Vol. 179, p. 509-525.

DURNEY, D.W. & RAMSAY, J.G., 1973. Incremental strains measured by syntectonic crystal growth. In: Gravity Tectonics (edited by de Jong, K.A. & Scholten, R). Wiley, New York, p. 67-96.

ENGELDER, T., 1987. Joints and shear fractures in rock. In: Fracture Mechanics of Rock (edited by Atkinson, B.K.). Academic Press, London, p. 27-65.

ERNST, W.G., 1975. Metamorphism and plate tectonic regimes. Benchmark papers in geology, Halsted Press, New York, p. 440.

ETCHECOPAR, A., 1977. A plane kinematic model of progressive deformation in a polycrystalline aggregate. Tectonophysics, Vol. 39, p. 121-139.

FASOULAS C., 1999. The structural evolution of central Crete: insight into the tectonic evolution of the south Aegean (Greece). Journal of Geodynamics, Vol. 27, Pergamon, p. 23-43.

FAURE, M., BONNEAU, M., PONS, J., 1991. Ductile deformation and syntectonic granite emplacement during late Miocene extension of the Aegean. Bull. Soc. Geol. Fr. Vol. 162, Pages 3–12.

FLEURY, J.J., 1980. Les zones de Gavrovo-Tripolitza et du Pinde-Olonos. Evolution d' une plate-forme et d' un bassin dans leur cadre alpin. Soc. Geol. Nord., Publ. No. 4, Pages 651.

FOSTER, D.A., GLEADOW, A.J.W., REYNOLDS, S.J., FITZGERALD, P.G., 1993. The denudation of metamorphic core complexes and the reconstruction of the transition zone, west-central Arizona: Constraints from apatite fission track thermochronology. J. Geoph. Res., Vol. 98, p. 2,167-2,186.

FREYBERG, B., 1967. Die Neogen Diskordanz in Central Kythira. Praktika Akad., Athinon, Vol. 42, p. 361-381.

ΦΥΤΡΟΛΑΚΗΣ, Ν., 1980. Η γεωλογική δομή της Κρήτης. Διατριβή επί Υφηγεσία, Αθήνα, σελ. 146.

FYTROLAKIS, N., 1980. Geological structure of Crete Island. Doctoral Thesis, Athens, Pages 146.

FYTIKAS, M., INNOCENTI, F., MANETTI, P., MAZZUOLI, R., PECCERILLO, A. & VILLARI, L., 1984. Tertiary to Quaternary evolution of volcanism in the Aegean region. Geol. Soc. (London), Spec. Publ. Vol. 17, p. 687-699.

GAMOND, J.F., 1983. Displacement features associated with fault zones: a comparison between observed examples and experimental models. J. Str. Geol., Vol. 5, p. 33-45.

GAUDEMER, Y. & TAPPONIER, P., 1987. Ductile and brittle deformations in the northern Snake Range, Nevada. J. Str. Geol., Vol. 9, p. 159-180.

GAUTIER, P., 1995. Geometrie crustale et cinematique de l'extension tardi-orgenique dans le domaine centre-egeen. Universite de Rennes, Rennes, Pages 420.

GHOSH, S. K., 1968. Experiments of buckling of multilayers which permit interlayer gliding: Tectonophysics. Vol. 6. Pages 207-249.

GOLDSTEIN, A.G., 1988. Factors affecting the kinematic interpretation of asymmetric boudinage in shear zones. J. Str. Geol., Vol. 10, No. 7, p. 707-715.

GOSCOMBE, B., 1991. Intense non-coaxial shear and the development of mega-scale sheath folds in the Arunta Block, Central Australia. J. Str. Geol., Vol. 13, p. 299-318.

GOSCOMBE, B., 1998. Geology of the Chewore Inliers, Zimbabwe: constraining the tectonic evolution of the Zambezi Belt. J. African Earth Sci.

GOSCOMBE, B., 1999. The geometry of folded tectonic shear sense indicators. J. Str.

Geol., Vol. 21, Issue 1, p. 123-127.

GOSCOMBE, B.D., PASSCHIER, C.W., 2003. Asymmetric boudins as shear sense indicators - an assessment from field data. J. Str. Geol., Vol. 25, p. 575-589.

GRAY, D.,R., 1979. Microstructure of crenulation cleavages: An indication of cleavage origin: American Journal of Science, Vol. 279, p. 97-128.

HANCOCK, P.L., 1973. Shear zones and veins in the Carboniferous limestone near the observatory, Clifton, Bristol. Proc. Bristol Nat. Soc., Vol. 32, p. 297-306.

HANCOCK, P.L., 1985. Brittle microtectonics: principles and practice. J. Str. Geol. 7, p. 437-457.

HANMER, S., 1986. Asymmetrical pull-aparts and foliation fish as kinematic indicators. J. Str. Geol., Vol. 8, No. 2, p. 111-122.

HEMPTON, M.R. & DUNNE, L.A., 1984. Sedimentation in pull-apart basins: active examples in eastern Turkey. J. Geology, Vol. 92, p. 513-530.

HINSBERGEN, VAN D.J.J., SNEL, E., GARSTMAN, S.A., MARUNTEANU, M., LANGEREIS C.G., WORTEL, M.J.R., MEULENKAMP, J.E., 2004. Vertical motions in the Aegean volcanic arc: evidence for rapid subsidence preceding volcanic activity on Milos and Aegina. Marine Geology, Vol. 209, p. 329-345.

HINSBERGEN, VAN D.J.J, LANGEREIS, C.G., MEULENKAMP, J.E., 2005. Revision of the timing, magnitude and distribution of Neogene rotations in the western Aegean region. Tectonophysics, Vol. 396, Pages 1-34.

HUGUEN C., MASCLE J., CHAUMILLON E., WOODSIDE J.M., BENKHELIL J., KOPF A., VOLKONSKAIA A., 2001. Deformational styles of the eastern Mediterranean Ridge and surroundings from combined swath mapping and seismic reflection profiling. Tectonophysics, Vol. 343, Pages 21-47.

JACKSON, J., 1994. Active tectonics of the Aegean region. Annu. Rev. Earth Planet. Sci., Vol. 22, p.239-271.

JOLIVET, L., BRUN, J.-P., GAUTIER, P., LALLEMANT, S., PATRIAT, M., 1994. 3-D kinematics of extension in the Aegean from the early Miocene to the Present, insights from the ductile crust.Bull. Soc. Geol. Fr., Vol. 165, Pages 195–209.

JOLIVET, L., GOFFE, B., BOUSQUET, R., OBERHANSLI, R., MICHARD, A., 1998. Detachments in high-pressure mountain belts, Tethyan examples.

JONES, G., 1990. Tectonostratigraphy and Evolution of the Pindos Ophiolite and Associated Units. Northwest Greece. Unpublished PhD. thesis, University of Edinmburgh.

JONGSMA, D., J.M., WOODSIDE, KING, G.C.P., HINTE V.J.E., 1987. The Medina Wrench: a key to the kinematics of the central and eastern Mediterranean over the past 5 Ma. Earth and Planetary Sci Let. Vol. 82, p. 87-106.

KARAKITSIOS, V., 1979. Contribution a l'etude geologique des Hellenides: Etude de la region de Sellia (Crete moyenne-occidentale, Greece). Les relations lithostratigraphiques et structurales entre la serie des Phyllades et la serie de Tripolitza. These 3e cycle. Univ. P.M.Curie, Paris.

ΚΑΤΣΙΚΑΤΣΟΣ, Γ., 1980. Γεωλογική μελέτη περιοχής Βασιλικού-Ιθώμης, Μεσσηνίας. Διδακτορική διατριβή, Πάτρα, σελ. 196.

KAROTSIERIS, Z., 1978. Eocene's bauxite occurrence of Vitina area, Tripoli. Bull. Hellenic Geol. Assoc., Vol. 13/2, Pages 153-161.

ΚΑΡΟΤΣΙΕΡΗΣ, Z., 1981. Γεωλογικές έρευνες στην περιοχή Βυτίνας (Κεντρική Πελοπόννησος). Διδακτορική διατριβή, Αθήνα, σελ. 202.

KAROTSIERIS, Z., 1981. Geological studies of Vitina area (Central Peloponnesus). Doctoral Thesis, Athens, pages 202.

KASTENS, K.A.,1991. Rate of outward growth of the Mediterranean Ridge accretionary complex. Tectonophysics, Vol. 199, Vol. 25-50.

KATSIKATSOS, G. 1980. Geological study of Vasilikou-Ithomis area, Messenias. Doctoral thesis, Patra, Pages 196.

ΚΑΡΟΤΣΙΕΡΗΣ, Ζ., 1978. Περί μίας ηωκαινικής βωξιτοφόρου εμφανίσεως εις την περιοχήν Βυτίνας, Τριπόλεως. Δελτ. Ελλ. Γεωλ. Εταιρ., 13/2, σελ. 153-161.

KIRATZI, A.A., 1993. A study on the active crustal deformation of the North and East Anatolian Fault Zones. Tectonophysics, Vol 225, Pages 191-203.

KIRATZI A., LOUVARI E., 2003, Focal mechanisms of shallow earthquakes in the Aegean Sea and the surrounding lands determined by waveform modelling: a new database, Journal of Geodynamics, Vol. 36, Issues 1-2, Pages 251-274.

KISKYRAS, D., 1957. The mineral deposits of the Peloponnese (Greece). Peloponnesiaka Protochronia, Pages 500-511.

KISSEL, C., KONDOPOULOU, D., LAJ, C., PAPADOPOULOS, P., 1986. New paleomagnetic data from Oligocene formations of northern Aegean. Journal 13, Pages 1039–1042.

KISSEL, C., LAJ, C., SENGOR, A.M.C., POISSON, A., 1987. Paleomagnetic evidence for rotation in opposite senses of adjacent blocks in northeastern Aegea and western Anatolia. Journal 14, Pages 907–910.

KISSEL, C., LAJ, C., 1988. The Tertiary geodynamical evolution of the Aegean arc: a paleomagnetic reconstruction. Tectonophysics 146, 183-201.

KOKKALAS, S., DOUTSOS, T., 2001. Strain-dependent stress field and plate motions

in the south-east Aegean region. Journal of Geodynamics. Vol. 32, p. 311-332.

KTENAS, K., 1908. Die Uberschiebungen in der Peloponnisos. Der Ithomiberg. Sitzungs-berichte XLIV, Akad. der Wissenhaften, V. 33, Pages 1076-1080.

KTENAS, K., 1924. Formations primaires semimetamorphiques du Peloponnese central. C.R.som.S.G. France, Pages 61-63.

LAJ, C., JAMET, M., SOREL, D., VALENTE, J.P., 1982. First paleomagnetic results from Mio-Pliocene series of the Hellenic sedimentary arc. Tectonophysics, Vol. 86, p.45-67.

LEONHARD, R., (1899). Die Insel Kythera. Eine geographische Monographie. Peterm. Mitt. Erg. H.128, Gotha, seit. 47.

LE PICHON X., 1982. Landlocked oceanic basins and continental collision: the Eastern Mediterranean as a case example. In: Hsu, K. (Ed.), Mountain Building Processes. Academic Press, London, pp. 201–211.

LE PICHON X. et al., 1993, Implications des nouvelles mesures de geodesie spatiale en Grece et en Turquie sur l'extrusion laterale de l'Anatolie et de l'Egee. C.R. Acad. Sci. Paris. 316, 983-990.

LE PICHON, X. ANGELIER, J., 1981. The Aegean Sea.Philosoph. Transact. Roy. Soc. London, Ser. A 300: pages 357-372.

LE PICHON, X., CHAMOT-ROOKE, N., LALLEMANT, S., NOOMEN, R., VEIS, G., 1995. Geodetic determination of kinematics of central Greece with respect to Europe: implications for eastern Mediterranean tectonics. Journal of Geophys.Res. Vol. 100, Pages 12675-12690.

LEKKAS, S., 1978. Donnees nouvelles sur la stratigraphie et la structure de la region au SE de Tripolis. Ann. geol. Pays Hell., Vol. 29. Pages 226-264.

LISTER, G.S. & SNOKE, A.E., 1984. S-C mylonites. J. Struct. Geol., Vol. 6, p. 617-638.

LYBERIS, N., ANGELIER, J., BARRIER, E., 1982. Active deformation of a segment of arc: the strait of Kythira, Hellenic arc, Greece. Journal of Structural Geol., Vol. 3, Pages 299-311.

ΜΑΡΙΟΛΑΚΟΣ, Η., 1975. Σκέψεις και απόψεις επί ορισμένων προβλημάτων της γεωλογικής και τεκτονικής δομής της Πελοποννήσου. Ann. Geol. Pays. Hell., 27, sel. 215-313.

MAKRIS, J., 1977. Geophysical investigations of the Hellenides. Hamb. Geoph. Einz, R.A., Vol. 34. p. 1-124.

MARIOLAKOS, I., 1975. Thoughts and aspects of Peloponnesus geological and tectonic structure. Ann. Geol. Pays Hell., 27, Pages 215-313.

MARLOW, P.C., ETHERIDGE, M.A., 1977. Development of a layered crenulation cleavage in mica schists of the Kanmantoo Group near Macclesfield, South Australia: Geological Society of America Bulletin, Vol. 88, Pages 873-882.

MAWER, C.K., 1989. Kinematic indicators in shear zones. International basement tectonics association, publ. No. 8, p. 67-81.

MCKENZIE, D. P., 1970. The plate tectonics of the Mediterranean region. – Nature 226: 239-243.

McKENZIE., D., J. JACKSON, J., 1986. A block model of distributed deformation by faulting, J. Geol. Soc. Lond., Vol. 143, Pages 349-353.

MERCIER, J. L., DELIBASSIS, N., GAUTHIER, A., JARRIGE, J.J., LEMEILLE, F., PHILIP, H., SEBRIER, M. SOREL, D., 1979. La neotectonique de l'arc egeen. Rev. Geol. Dyn. Geogr. Phys., Vol. 21, p.67-92.

MEULENKAMP, J.E., THEODOROPOULOS, P., TSAPRALIS, V., 1977. Remarks on the Neogene of Kythira, Greece. Sixth Coll. Geol. Aegean Region, Vol. 1, p.355-362.

MEULENKAMP et al., 1988. On the Hellenic subduction zone and the geodynamic evolution of Crete since the late Middle Miocene. – Tectonophysics 146: 203-215.

MIYASHIRO, A., 1973. Metamorphism and metamorphic belts. William Clowes & Sons, Ltd., London, p. 492.

MORRIS, A., ANDERSON, M., 1996. First paleomagnetic results from the Cycladic Massif, Greece, and their implications for Miocene extension directions and tectonic models in the Aegean. Earth and Planetary Science Letters 142, 397-408.

NEGRIS, P., 1908. Composition de la nappe charriee du Peloponnese au mont Ithome (Messenie). C.R.Acad. Sc. Paris, Vol. 147, Pages 316-318.

NEUMANN, P., RISCH, H., ZACHER, W., FYTROLAKIS, N., 1996. Die stratigraphische und sedimentologische Entwicklung der Olonos-Pindos-Serie zwischen Koroni und Finikounda (SW-Messenien Griechenland). Neues Jahrb. Geol. Palaontol. Abh. 200, Pages 405-420.

NICKELSEN, R. P., 1972. Attributes of rock cleavage in some mudstones and limestones of the Valley and Ridge province, Pennsylvania. Pennsylvania Academy of Science Proceedings, Vol. 46, Pages 107-112.

NICHOLSON, R. & EJIOFOR, I.B., 1987. The three-dimensional morphology of arrays of echelon and sigmoidal, mineral-filled fractures: datafrom north Cornwall. J.Geol.Soc. Lond., Vol. 144, p. 79-83.

OLSON, J.E. & POLLARD, D.D., 1991. The initiation and growth of en echelon veins. J. Str. Geol., Vol. 13, No. 5, p. 595-608.

ORAL, M.B. et al., 1995. Global positioning system offers evidence of plate motion in eastern Mediterranean. EOS, Vol 76 (2), Pages 9-11.

PAPAZACHOS, C.B. et al., 2000. The geometry of the Wadati – Benioff zone and lithospheric kinematics in the Hellenic arc. Tectonophysics 319, 275-300.

PAPANIKOLAOU, D., 1986. Geology of Greece. Athens, Pages 252.

ΠΑΠΑΝΙΚΟΛΑΟΥ, Δ. & ΔΑΝΑΜΟΣ, Γ., 1991. Αντιστοίχιση της γεωτεκτονικής θέσης των Κυθήρων και των Κυκλάδων στη γεωδυναμική εξέλιξη του Ελληνικού τόξου. Δελτ. Ελ. Γεωλ. Ετ., Πρακτικά 5ου Επιστημονικού Συνεδρίου, Θεσ/κη, τόμ.XXV/1, σελ. 65-79.

PAPANIKOLAOU, D. & DANAMOS, G., 1990. Correlation of the geotectonic position of Kythira and Cyclades within the geodynamic evolution of the Hellenic arc. Bul. of the Geol. Soc. Greece, vol. XXV/1, Proceedings of the 5th Congress, Thessaloniki, p. 65-79.

PASSCHIER, C.W. & SIMPSON, C., 1986. Porphyroclast systems as kinematic indicators. J. Str. Geol., Vol. 8, No. 8, p. 831-843.

PASSCHIER, C.W. & TROUW, R.A.J., 1996. Microtectonics. Springer-Verlag, Germany, p. 366.

PEACOCK, D.C.P & SANDERSON, D.J., 1995. Strike-slip relay ramps. J. Str. Geol., Vol. 17, p. 1351-1360.

ΠΕΤΡΟΧΕΙΛΟΣ, Ι., 1966. Γεωλογικός χάρτης νήσου Κυθήρων, κλίμακας 1:50,000. ΙΓΕΥ, Αθήνα.

PETROCHELOS, J., 1966. Geological map of Kythera Island, scale 1:50,000. Institute

for Geology and Subsurface Research, IGSR. Athens.

PE-PIPER, G., D.J.W., PIPER, MATARANGAS, D., 2001. Regional implications of geochemistry and style of emplacement of Miocene I-type diorite and granite, Delos, Cyclades, Greece.

PE-PIPER, G., D.J.W., PIPER, 2002. The Igneous Rocks in Greece. The anatomy of an orogen. Gebruder Borntraeger, Berlin, p. 573.

PE-PIPER, G. et al., 2002. Regional implications of geochemistry and style of emplacement of Miocene I-type diorite and granite, Delos, Cyclades, Greece, Lithos, Volume 60, Issues 1-2, Pages 47-66.

PHILIPPSON, A., 1930. Beitrage zur Morphologie Griechenlands. Geographische Abhandlungen, R.H. 3, Stuttgart, seit. 93.

PIPER D.J.W. & PERISSORATIS C., 2003. Quaternary neotectonics of the South Aegean arc. Marine Geology, Volume 198, Pages 259-288.

PLATT, J.P. & Vissers, R.L.M., 1980. Extensional structures in anisotropic rocks. J. Str. Geol., Vol. 2, p. 397-410.

PLATT, J.P., 1986. Dynamics of orogenic wedges and uplift of high-pressure metamorphic rocks. Geol. Soc. Amer. Bull. 97, Pages 1037-1053.

RAMBERG, H., 1955. Natural and experimental boudinage and pinchand-swell structures. Journal of Geology, Vol. 63, Pages 512–526.

RAMSAY, J.G., 1967. Folding and fracturing of rocks: McGraw-Hill Book Company, New York, Pages 560.

RAMSAY, J.G. & HUBER, M.I., 1983. The techniques of modern structural geology, vol. 1, Strain analysis: Academic Press, London, Pages 307.

RAMSAY, J.G. & HUBER, M.I., 1987. The techniques of modern structural geology.

Vol. 1: Strain analysis, Academic Press, London, p. 307.

REILINGER, R.E., et al., 1997. Global positioning system measurements of present-day crustal movements in the Arabia-Africa-Eurasia plate collision zone. Journal of Geophysical Research. Vol. 102, Pages 9983-9999.

RENZ, C., 1940. Die Tektonik der griechischen Gebirge. Praktika Akadimia Athinon, Vol. 8, Pages 1-171.

RENZ, C., 1955. Die vorneogene Stratigraphie der normalen sedimentaren Formationen Griechenlands. Institute for Geology and Subsurface Research, Athens.

REY et al., 1997. The Scandinavian Caledonides and their relationship to the Variscan belt. – In: Burg, J.P. & Ford, M. (eds.): Orogeny through time. – Geol. Soc. (London), Spec. Publ. 121: 179-200.

ROBERTSON, A.H.F., CLIFT, P.D., DEGNAN, P., JONES, G., 1991. Paleoceanography of the Eastern Mediterranean Neotethys. Palaeogeography, Palaeoclimatology, Palaeoecology, Vol. 87, no 1-4, Pages 289-343.

ROBERTSON, A.H.F., 1994. Role of the tectonic facies concept in orogenic analysis and its application to Tethys in the Eastern Mediterranean region. Earth Sci. Rev. 37, Pages 139-213.

ROERING, C., 1968. The geometrical significance of natural en-echelon crack arrays. Tectonophysics, Vol. 5, p. 107-123.

RON, H., FREUND , R., GARFUNKEL, A., NUR., 1984. Block rotation by strike slip faulting: structural and palaeomagnetic evidence. J. Geophys. Res., Vol. 89, Pages 6256-6270.

ROYDEN, L.H., 1993. Evolution of retreating subduction boundaries formed during

continental collision – Tectonics 12: 629-638.

SAVOSTIN, L. A., SIBUET, J-C., ZONENSHAIN, L. P., LE PICHON, X. & ROULET, M-J. 1986. Kinematic evolution of the Tethys belt from the Atlantic Ocean to the Pamirs since the Triassic. Tectonophysics, Vol. 123, Pages 1-35.

SCHOPFER, M.P.J., ZULAUF, G., 2002. Strain-dependent rheology and the memory of plasticine. Tectonophysics, Vol. 354, Pages 85-99.

SEYFERTH, M., HENK, A., 2004. Syn-convergent exhumation and lateral extrusion in continental collision zones-insights from three-dimensional numerical models. Tectonophysics, Vol. 382, Pages 1-29.

SENGOR, A.,M.,C., 1979. The North Anatolian transform fault: its age, onset and tectonic significance. J. Geol. Soc., London, Vol. 136, pages 269-282.

SIBSON, R.H., 1989. Earthquake faulting as a structural process. J. Str. Geol., Vol. 11, p. 1-14.

SHIMUZU, A., SUMINO, H., NAGAO, K., NOTSU, K., MITROPOULOS, P., 2005. Variation in noble gas isotopic composition of gas samples from the Aegean arc, Greece. Journal of Volcanology and Geothermal Research, Vol. 140, Issue 4, p. 321-339.

SIGAL, J., 1977. Essai de zonation du Cretace mediterraneen a l' aide des foraminiferes planctoniques. Geol. Mediterraneenne, 4/2, Pages 99-108.

SIMPSON, C. & Schmid, S. M., 1983. An evaluation of criteria to determine the sense of movement in sheared rocks. Bull. geol. Soc. Am., Vol. 94, p. 1281-1288.

SMITH, J.V., 1995. True and apparent geometric variability of en-echelon vein arrays. J. Str. Geol., Vol. 17, No. 11, p. 1621-1626.

SMITH, J.V., 1996. Geometry and kinematics of convergent conjugate vein array

systems. J.Structural Geol., Vol. 18, No. 11, p. 1291-1300.

SMITH, A.G., HYNES, A.J., MENZIES, M., NISBET, E.G., PRICE, I., WELLAND, M.J.P., FERRIBRE, J., 1975. The stratigraphy of the Othris Mountains, eastern central Greece: a deformed Mesozoic continental margin succession. Eclogae Geol. Helv., Vol. 86, Pages 463-481.

SMITH, A.G., WOODCOCK, N.H., NAYLOR, M.A., 1979. The structural evolution of a Mesozoic continental margin, Othris Mountains, Greece. J. Geol. Soc. London, Vol. 136, Pages 589-603.

SONDER, L.J. & ENGLAND, P.C., 1989. Effects of a temperature dependant rheology on a large-scale continental extension. J. Geophys. Res., Vol. 94, p. 7603-7609..

SOWA, A., 1985. Die Geologie der Insel Folegandros (Kykladen, Griechenland). Erlanger Geol. Abh., Vol. 112, Pages 85–101.

SPAKMAN, W., WORTEL, M.J.R., VLAAR, N.J., 1988. The Hellenic subduction zone: a tomographic image and its geodynamic implications. Geophys. Res. Letters, Vol. 15, Pages 60-63.

SPAKMAN, W., VAN DER LEE, S., VAN DER HILST, R., 1993. Travel-time tomography of the European – Mediterranean mantle down to 1400 km. Phys. Earth Planet. Inter. 79, 3-74.

STEENBRINK, J., 2001. Orbital signatures in lacustrine sediments: the late Neogene intramontane Florina-Ptolemais_Servia Basin, northwestern Greece, Geol. Ultraiectina. Vol. 205, p.167.

SWANSON, M.T., 1992. Late Acadian-Allegenian transpressional deformation: evidence from asymmetric boudinage in the Casco Bay area, coastal Maine. J.

Str. Geol., Vol. 14, p.323-341.

ΤΑΤΑΡΗΣ, Α., 1964. Οι μεσοηωκαινικοί βωξίτες της ζώνης Τρίπολης και τα ενδοηωκαινικά τεκτονικά γεγονότα. Δελτ. Ελλ. Γεωλ. Εταιρ., 5/2, σελ. 36-58.

TATARIS, A., 1964. The inter-eocene bauxites of Tripolis zone and the inter-eocene tectonic events. Bull. Hellenic Assoc., 5/2, Pages 36-58.

ΤΑΤΑΡΗΣ, Α., ΜΑΡΑΓΚΟΥΔΑΚΗΣ, Ν., 1965. Επί της γεωλογικής δομής των Λευκών Ορέων (Δυτ. Κρήτη). Δελτ. Ελλ. Γεωλ. Εταιρ. 6/2, σελ. 319-347.

TATARIS, A., MARAGOUDAKIS, N., 1967. Geological structure of Leuka Ori (W.Crete). Bull. Hellenic Geol. Assoc., 6/2, Pages 319-347.

TAYMAZ et al., 1991. Active tectonics of the north and central Aegean. – Geophys. J. Int. 106: 695-731.

TEN VEEN, J.H., MEIJER, P.T., 1998. Late Miocene to recent tectonic evolution of Crete (Greece): geological observations and model analysis. Tectonophysics 298, 191-208.

TEN VEEN, J.H., POSTMA, G., 1999. Neogene tectonics and basin fill patterns in the Hellenic outer-arc (Crete, Greece). Basin Research, Vol. 11, Pages 223-241.

ΘΕΟΔΩΡΟΠΟΥΛΟΣ, Δ., 1973. Φυσική Γεωγραφία της νήσου των Κυθήρων. Διδακτορική Διατριβή, Αθήνα, Σελ. 94.

THEYE, T., 1988. Aufsteigende Hochdruckmetamorphose in Sedimenten der Phyllit-Quartzit-Einheit Kretas und des Peloponnes. Doctoral dissertation, rer.nat., Braunschweig, Pages 224.

THEYE, T. & SEIDEL, E., 1991. Petrology of low-grade high-pressure metapelites from the External Hellenides (Crete, Peloponnese). A case study with attention

to sodic minerals. Eur. J. Mineral., Vol. 3, p. 343-366.

THEODOROPOULOS, D., 1973. Physical Geology of Kythera Island. Doctoral Thesis. Athens, Pages 94.

THIEBAULT, F., 1982. Evolution geodynamique des Hellenides externes en Peloponnese meridional (Grece). Soc. Geol. Nord., Publ. No. 6, Pages 574.

THIEBAULT, F., TRIBOULET, C., 1984. Alpine metamorphicsm and deformation in Phyllites nappes (external Hellenides, southern Peloponnesus, Greece): geodynamic implications. J. Geology. Vol. 92. Pages 185-199.

THOMSON, S.N., STOCKHERT, B., BRIX, M.R., 1999. Miocene high-pressure metamorphic rocks of Crete: rapid exhumation by buoyant escape. In: Ring, U., Brandon, M., Lister, G.S., Willet, S. (Eds.), Exhumation Processes: Normal Faulting, Ductile Flow and Erosion. Geol. Soc. Spec. Publ., Vol. 154, p. 87-107.

TSOKAS, G.N., HANSEN, R.O., 1997. Study of the crustal thickness and the subducting lithosphere in Greece from gravity data. J. Geophys. Res ., Vol. 102, Pages 20585–20597.

TSOFLIAS, P., 1977. Les niveaux stratigraphiques inferiers de la nappe du Pinde-Olonos dans l'ile de Cythere (Grece). Com. Int. Expl. Sc. Mer Mediterranee, 24, No 7A, Pages 235-236.

TZANNIS, A. & Vallianatos, F., 2003. Distributed power-law seismicity changes and crustal deformation in the SW Hellenic Arc. Natural Hazards and Earth Systems Sci., Vol. 3, p. 179-195.

WALCOTT, C.R., 1998. The Alpine evolution of Thessaly (NW Greece) and late Tertiary Aegean kinematics. - Geologica Ultraiectina 162: 176p.

WALCOTT, C.R., WHITE, S.H., 1998. Constraints on the kinematics of post-orogenic

extension imposed by stretching lineations in the Aegean region. Tectonophysics 298, 155-175.

WESTAWAY, R., et al., 1991. Continental extension on sets of parallel faults: observational evidence and theoretical models. (Eds.), The Geometry of Normal Faults. Geol. Soc. London Spec. Publ. 56, 143–169.

YIN, A. & DUNN, J.F., 1992. Structural and stratigraphic development of the Whipple-Chemehuevi detachment fault system, southeastern California: Implications for the geometrical evolution of domal and basinal low-angle normal faults. Geol. Soc. Am. Bull., Vol. 104, p. 659-674.

ZAGER, D., 1972. Sedimentologi der Tripolitza-Karbonate im nordlichen mitel-Kreta (Griechenland). Diss. Un. Freiburg. i.Br.